Ternary Alloys

Volume 21

MSI
Science Simplified

Ternary Alloys

A Comprehensive Compendium of Evaluated Constitutional Data and Phase Diagrams

critically evaluated by MSIT®

Volume 21

Selected Al-Fe-X Ternary Systems for Industrial Applications

Editors
Frank Stein, Martin Palm

Associate Editors
Liya Dreval, Oleksandr Dovbenko, Svitlana Iljenko

Authors
Materials Science International Team, MSIT®

MSI
Science Simplified

Editors: Frank Stein,
Martin Palm
Associate Editors: Liya Dreval
Oleksandr Dovbenko
Svitlana Iljenko

ISBN 978-3-932120-51-0

Vol. 21. Selected Al-Fe-X Ternary Systems for Industrial Applications. – 2022

This volume is part of the book series:
Ternary Alloys: A Comprehensive Compendium of Evaluated Constitutional Data and Phase Diagrams/
Materials Science International Services GmbH, Stuttgart, Germany

Group ISBN for the Ternary Alloys book series: 978-3-932120-41-1

Published by
MSI, Materials Science International Services GmbH, Stuttgart (Federal Republic of Germany)
Am Wallgraben 100, D-70565 Stuttgart, Germany
Postfach 800749, D-70507, Stuttgart, Germany
http://www.msiport.com
http://www.msi-eureka.com/

Printed on acid-free paper.

Printing and binding:
WIRmachenDRUCK GmbH, Mühlbachstraße 7, 71522 Backnang

Printed in the Federal Republic of Germany

Authors: Materials Science International Team, MSIT®

This volume results from collaborative evaluation programs performed by MSI and authored by MSIT®. In this program, data and knowledge are contributed by many individuals and have accumulated over almost thirty five years, up to the present day. The content of this volume is a subset of the ongoing MSIT® Evaluation Programs. Authors of this volume are:

Nataliya Bochvar, Moscow, Russia
Anatoliy Bondar, Kyiv, Ukraine
Gabriele Cacciamani, Genova, Italy
Lesley Cornish, Johannesburg, South Africa
Oleksandr Dovbenko, Stuttgart, Germany
Liya Dreval, Stuttgart, Germany
Yong Du, Changsha, China
Kiyaasha Dyal Ukabhai, Johannesburg, South Africa
Olga Fabrichnaya, Freiberg, Germany
Lorenzo Fenocchio, Genova, Italy
Sergio Gama, Campinas, Brasil
Gautam Ghosh, Evanston, USA
Bernd Grieb, Tübingen, Germany
Kiyohito Ishida, Sendai, Japan
Hermann A. Jehn, Stuttgart, Germany
Kostyantyn Korniyenko, Kyiv, Ukraine
Mario J. Kriegel, Freiberg, Germany
Ortrud Kubaschewski†, Aachen, Germany
K.C. Hari Kumar, Chennai, India
Bernard Legendre, Paris, France
Xiaojing Li, Changsha, China
Shuhong Liu, Changsha, China
Xing Jun Liu, Sendai, Japan
Annelies Malfliet, Heverlee, Belgium
Niraja Moharana, Chennai, India
Martin Palm, Düsseldorf, Germany
Jian Peng, Wuhan, China
Pierre Perrot, Lille, France
Alexander Pisch, Grenoble, France
Qingsheng Ran, Stuttgart, Germany
Maximilian Rank, Karlsruhe, Germany
Peter Rogl, Vienna, Austria
Lazar Rokhlin, Moscow, Russia
Rainer Schmid-Fetzer, Clausthal-Zellerfeld, Germany
Frank Stein, Düsseldorf, Germany
Vasyl Tomashyk, Kyiv, Ukraine
Lyudmila Tretyachenko†, Kyiv, Ukraine
Mikhail Turchanin, Kramatorsk, Ukraine
Oksana Tymoshenko, Kyiv, Ukraine
Thomas Vaubois, Chatillon, France
Alexander Walnsch, Freiberg, Germany
Chuanbin Wang, Wuhan, China
Cui Ping Wang, Sendai, Japan
Junjun Wang, Wuhan, China
Andrew Watson, Chesterfield, UK
Liming Zhang, München, Germany

Contents

Ternary Alloys
A Comprehensive Compendium of Evaluated Constitutional Data and Phase Diagrams

Volume 21
Selected Al-Fe-X Ternary Systems for Industrial Applications

Introduction

Ternary Systems

Aluminium – Iron – Nickel

Gabriele Cacciamani, Lorenzo Fenocchio, Liya Dreval

Introduction

The first extensive investigation of the Al-Fe-Ni ternary system, performed by [1933Koe], included the determination of the liquidus surface and a series of vertical sections in the region < 50 mass% Al (≲ 75 at.% Al). Subsequently, [1938Bra, 1940Bra1, 1949Bra, 1951Bra] performed a more extensive investigation of phase equilibria in the Al-Fe-Ni system. Further experimental work on phase equilibria was carried out by [1993Pov, 1994Gho, 1994Jia, 1999Dyb, 2000Dyb, 2002Bit].

Most of the early investigations were concentrated in the Fe-Ni rich part of the system, due to the structural and magnetic properties of such alloys. It was only in the last decade of the last century that the discovery of quasicrystalline decagonal phases in the Al-rich region [1989Tsa, 1994Lem, 1996Yam, 1997Sai, 2002Hir, 2003Doe] promoted a more detailed investigation of phase equilibria at Al contents greater than 50 at.%.

The first critical assessment of the system was performed by [1980Riv] with minor amendments by [1988Ray] and an update by [1992Bud]. [1994Rag] presented isothermal sections at 950 and 1050°C in the Al-rich part of the diagram (> 50 at.% Al), an isothermal section at 1050°C in the Fe-rich part of the diagram (> 50 at.% Fe) and a vertical section between Ni_3Al and $FeNi_3$. The critical evaluation of the system, which includes the literature data up to 2003, was also performed by [2004Bud]. A more recent critical assessment of the whole system was presented by [2006Ele]. In this work, phase equilibria determined by [1938Bra, 1940Bra1, 1949Bra, 1951Bra] in the Fe-Ni rich area were considered still valid. Latest phase diagram evaluations and related updates were compiled by [2005Rag, 2006Rag, 2008Rag, 2009Rag1, 2009Rag2, 2010Rag]. Moreover, a review which mainly focused on stable and metastable quasiperiodic phases in ternary Al-based systems was presented by [2007Gru].

The first calculations of the whole phase diagram by the Calphad method were carried out by [1974Kau] at 927, 1127, 1327, and 1427°C. These calculations were mainly based on the phases obtained by [1940Bra1] after slow cooling. After that, the first recent thermodynamic assessment of the whole system was carried out by [2007Zha1].

This ternary system exhibits a continuous solid solution between NiAl and FeAl, whose equilibria are complicated by structural and magnetic ordering transformations. This allows the system to be split into two parts: the Al-rich portion, from 50 to 100 at.% Al, and the Fe-Ni rich region, from 0 to 50 at.% Al. In the border vertical section at 50 at.% Al only the solidus curve has been experimentally determined, by [2002Bit].

The phase equilibria are very different within the two aforementioned regions: in the Fe-Ni-rich area either ordered or disordered *fcc* - (γFe, Ni) and Ni_3(Fe, Al) - and *bcc* - (αδFe) and (Fe,Ni)Al - extended solid solutions are present and no ternary compound has been detected. On the contrary, in the Al-rich part, binary phases with limited ternary solubility and ternary compounds generate a complex system of two- and three-phase fields.

Phase equilibria investigations performed up to the end of the last century have been discussed in the previous update of this evaluation [2004Bud]. More recent experimental works on the system are summarized in Table 1.

Additional experimental investigations in the Fe-Ni-rich area were performed by [2004Him], with particular attention given to the $FeNi_3$-Ni_3Al vertical section. After accurate preparation and equilibration, samples were analyzed by LOM, SEM, TEM, XRD, and DSC. For T_C determination, VSM and ER were also used. Their results have been considered particularly reliable for constructing the sections reported in this update, together with results by [2007Chu1, 2008Chu]. Chumak prepared and characterized a wide series of samples in this concentration range by XRD, DTA and WDS. They reported the $FeNi_3$-Ni_3Al vertical section, the Ni_3(Fe,Al) lattice parameters and the partial isothermal sections at 900, 1000 and 1100°C.

The central part of the ternary Al-Fe-Ni composition triangle presents a continuous *B*2 FeAl-NiAl solid solution. Phase equilibria in this zone of the diagram seem relatively simple, and the last experimental investigation of the 50 at.% Al vertical section dates to [2002Bit], who determined the solidus curve by EDX and DTA. The liquidus curve in this section was never investigated experimentally, but CALPHAD calculations were performed in the thermodynamic assessment by [2009Zha].

Most of the recent experimental investigations of this system target the Al-rich corner, as a consequence of the discovery of decagonal stable and metastable phases. The most reliable investigations were performed by [2007Chu2], who determined vertical sections at different Al concentrations (60, 67, 71.5, 75, 80 at.% Al), a partial isothermal section at 850°C and liquidus projection curves. Chumak also proposed a partial reaction scheme. Samples in this work were analyzed by XRD, DTA and WDS. Another significant study in the Al-rich area was performed by

[2008Zha], who reported partial isothermal sections at 627 and 850°C, after characterizing the samples by XRD, DTA, and WDS. In this work, particular attention was given to equilibria involving the ternary $FeNiAl_9$ and Fe_3NiAl_{10} phases.

The previously mentioned complete thermodynamic assessment by [2007Zha1] was soon replaced by a new paper from the same authors, [2009Zha], which reassessed the system in the full composition range and included the results from [2007Chu2, 2008Chu]. In this new assessment, however, selected binary phases were considered to be stoichiometric, with substantial consequences on the phase equilibria involving them. For this reason, in the present evaluation, it was not possible to assume [2009Zha] as the reference work for the description of the system, despite this being the most recent and complete thermodynamic assessment presently available; in fact, it was mainly used where no other data were available or where the mentioned simplifications did not affect the phase equilibria.

For all areas of the ternary diagram, a combination of results from the above-mentioned authors was adopted in this evaluation. The reasons for each choice, together with a more in-depth discussion on phase equilibria, invariant reactions and the various isothermal and vertical sections, are presented later in the related chapters.

After 2009, no significant changes were proposed for the Al-Fe-Ni phase diagram. In fact, more recent studies were focused on determining thermodynamic or crystallographic properties of previously discovered ternary decagonal phases. The main works, in this sense, were performed by [2011Del, 2013Lep, 2014Bas, 2017Fer, 2019Lip] for crystallographic investigations by XRD, SEM and EDX and by [2010Ond, 2010Pan, 2010Rzy] for thermodynamic measurements by solution or direct reaction calorimetry. Further details and discussion on the obtained results are given later in this work, in the "*Solid Phases*" and "*Thermodynamics*" sections respectively.

Finally, in the last few years most of the research on the Al-Fe-Ni system has been focused on the determination of several properties for potential applications. The main results are presented in the "*Notes on Properties and Materials Applications*" section.

Binary Systems

The binary boundary systems Al-Ni and Fe-Ni have been accepted from the critical assessments of [2016Wan] and [2010Cac], respectively. The Al-Fe phase diagram is accepted from the binary evaluation report of [2022Ste] and presented in the chapter "*Al - Fe (Aluminium - Iron)*" of this volume.

Solid Phases

Crystallographic data and temperature ranges of stability of the Al-Fe-Ni phases are listed in Table 2. In general, Fe and Ni do not dissolve appreciably in (Al). Conversely, Al dissolves significantly in Fe and Ni, which form solid solutions extending into the ternary system.

The Al-Fe based *bcc* solid solution (αδFe) extends into the ternary system and its Ni concentration increases with increasing Al. In the binary Al-Fe system, it orders forming (Fe,Ni)Al (CsCl-type) by a second order transformation. The transformation becomes first order with increasing Ni additions.

The (Fe,Ni)Al phase forms a continuous range of solid solutions between Al-Fe, Al-Ni and toward Fe. The transformation between the ordered (Fe,Ni)Al and disordered (αδFe) solid solutions, which is second order at high temperature and in the vicinity of the Al-Fe binary subsystem, forms a miscibility gap in the ternary system. Lattice parameters and hardness measurements in the (Fe,Ni)Al field have been carried out by [2001Tan]. Site occupancies of Fe in NiAl were first investigated by [1994Dun] using atom-probe field-ion microscopy. After that, an exhaustive study of lattice parameters, site occupancies and vacancy concentration, point defects, density and hardness was carried out by [1997Pik, 2002Pik] in the (Fe,Ni)Al-region, over a wide range of compositions and temperatures. The triple defect structure was observed across the entire phase field and constitutional vacancies were observed in all of the Al-rich compositions. Thermodynamic predictions that Fe anti-sites are more stable than Ni anti-sites in the Al-poor compositions were qualitatively confirmed. The lattice parameter as a function of composition for the (Fe,Ni)Al phase was reported and is shown in Figs. 1a and 1b.

The *fcc* solid solution (γFe, Ni) extends from the Fe-Ni binary subsystem to more than 20 at.% Al. With decreasing temperature, it orders to form the $Ni_3(Fe,Al)$ structure ($AuCu_3$ type) at about 75 at.% Ni and forms a continuous solid solution with the isostructural Ni_3Al [1986Bra, 1987Mas, 1998Gom]. Fe can occupy both Al and Ni sublattices. In an alloy with 2.5 at.% Fe, 78% of Fe atoms occupy the Al sublattice, while this value drops to 54% for an alloy with 9.3 at.% Fe [1977Nic]. Inclusion of Fe beyond 7 at.% does not influence the lattice parameters of $Ni_3(Fe,Al)$ [1959Gua, 1984Och, 2005Fuk, 2006Jia]. The variation of lattice parameters of the (γFe, Ni)/$Ni_3(Fe,Al)$ phase as a function of Al concentration are reported in Fig. 1c, based on [2002Pik, 2007Chu1].

Site occupancies and substitution of Fe with Ni (about 3 at.%) in Fe_3Al were investigated *via* neutron diffractometry by [1998Sun].

The monoclinic Fe_4Al_{13} phase dissolves up to 12.0 at.% Ni at 800°C. The precipitation mechanism of this phase was investigated by [2013Tav].

$NiAl_3$ dissolves up to 2.5 at.% Fe [1996Gru1] and Ni_2Al_3 can dissolve about 2, 4 and 10 at.% Fe at room temperature, 850 and 1050°C, respectively. Both Fe_2Al_5 and $FeAl_2$ can dissolve up to 2 at.% Ni at elevated temperatures [1982Kha].

As previously mentioned, no ternary phases were reported in the Al-poor region of the system, while three stable ternary phases were revealed in the Al-rich zone. The $FeNiAl_9$ phase (Co_2Al_9-type) is formed at almost constant 82 at.% Al and between 4.4 and 11.1 at.% Fe [1943Sch, 1999Dyb, 2000Dyb]. The same phase extends from 9 to 14.5 at.% Fe when precipitating from melt-spun samples [1996Zho]. Structural refinement was performed by [2007Chu2].

The hexagonal Fe_3NiAl_{10} phase (Co_2Al_5-type) has been observed at 1050°C in the $Al_{70\text{-}72.5}Fe_{18\text{-}24.5}Ni_{10.5\text{-}4.5}$ composition range [1981Kha]; this phase was structurally characterized by [1990Ell, 2007Chu2] and confirmed by [2014Bas] in a sample at the $Al_{70}Fe_{15.5}Ni_{14.5}$ composition.

Quasiperiodic structures to which higher dimensional crystallography is applicable were first discovered in Al-Fe-Ni alloys in 1989, when several different decagonal diffraction patterns were observed by [1989Tsa] in alloys prepared by melt quenching. Since then, decagonal phases have been studied by several authors [1989Tsa, 1993Tan, 1994Lem, 1996Gru1, 1997Sai, 2000Fre, 2001Hir, 2002Yok, 2003Doe, 2004Gru, 2011Del, 2014Bas].

The best-known quasiperiodic phase of this system is τ_1 (periodicity of about 0.4 nm), which is stable between 930 and 847°C in a composition range of less than 1 at.% around the $Al_{71}Ni_{24}Fe_5$ composition [1994Gru, 1994Lem, 1996Gru1, 2000Dro, 2003Doe]. This probably corresponds to an unidentified $FeNi_3Al_{10}$ phase, previously observed by [1982Kha]. The diffraction patterns of the τ_1 phase are very similar to those of the Ni-rich decagonal phase found in the more extensively studied Al-Co-Ni alloy system [1996Gru2]. It was argued by [1996Gru1] that the stable ternary τ_1 phase is an extension of a metastable isostructural Al-Ni phase. The τ_1 structure (identified as $Al_{73}Ni_{22}Fe_5$) has been discussed by [2011Del] in terms of a combination of clusters (2 nm diameter, $P\overline{10}_2m$ symmetry group) common to several decagonal structures.

Two more metastable D-phases with slightly different diffraction properties were observed by [1993Tan, 1997Sai, 2001Qia] at higher Fe contents. They were finally identified to be τ_2 of $Al_{70.5}Fe_{10}Ni_{19.5}$ composition, based on the binary $Al_{80}Ni_{20}$, and τ_3 of $Al_{72.5}Fe_{14.5}Ni_{13}$ composition, based on the binary $Al_{86}Fe_{14}$, according to [2014Bas].

Structural models belonging to the space groups $P\overline{10}m2$ and $P\overline{10}_5/mmc$ (or $P10/mmm$, according to [1993Tan]) were found to approximately recreate the HRTEM images of quasicrystals at $Fe_{30-x}Ni_xAl_{70}$ with $10 < x < 17$ and $17 < x < 20$, respectively [1997Sai]. Disorder in these phases has been studied by synchrotron X-ray and neutron diffraction experiments [2000Fre]. [2001Hir] found that large columnar clusters of atoms with a decagonal section of about 3.2 nm in diameter exist as a basic structural unit.

According to [2004Gru] all quasicrystalline phases present in the system can be considered to be derived from corresponding metastable binary phases, stabilized by addition of a third element. However, some of these phases were also observed to survive relatively long term anneal at high temperature, posing doubts about their metastability.

Due to difficulties relating to experimental factors, such as the dependence of sample structure on the preparation procedure, and the complex interpretation of results, the reported description of the Al-Fe-Ni decagonal phases may still be considered incomplete. It is representative of a more complex situation (see also the "*Miscellaneous*" section).

Finally, the formation of amorphous Al-Fe-Ni alloys has been investigated by [2011Tav, 2013Tav] at the $Al_{80}Fe_{10}Ni_{10}$ composition.

Quasibinary Systems

No actual quasibinary section is present in the Al-Fe-Ni system.

However, FeAl-NiAl and $FeNi_3$-Ni_3Al sections, where continuous solid solutions (CsCl type and $AuCu_3$ type, respectively) appear, have been approximately considered as quasibinary by several authors.

Invariant Equilibria

Invariant equilibria have been recently investigated by [2007Chu1, 2007Chu2, 2008Chu, 2008Zha]. Subsequently, [2009Zha] performed a CALPHAD assessment of the system, considering the aforementioned works in addition to the previous literature. However, certain issues exist which must be clarified experimentally.

In the composition region with aluminium content lower than 50 at.%, phase equilibria involving the liquid phase were investigated by [1933Koe, 1949Bra, 1951Bra, 1978Mar] and, more recently, by [2007Chu2]. The extensive thermal analysis data of [1933Koe] became an object of criticism even by the early 1940s. The liquidus and solidus temperatures and the coordinates of the peritectic reactions in the Al-Fe and Al-Ni systems were in poor agreement with the later established binary phase diagrams. However, the proposed phase equilibria did not include the ordered (Fe,Ni)Al phase. [1942Dan] proposed a reinterpretation of the data by [1933Koe] to include the ordered phase, but phase equilibria involving the liquid phase were not changed.

[1949Bra] tried to reconstruct the liquidus surface in the region with aluminium content lower than 50 at.%. This reconstructed projection was based on the updated phase diagrams of the Al-Fe and Al-Ni systems, the data of [1933Koe], and the results of [1949Bra] for quenched specimens. However, the NiAl phase liquidus curve in the Al-Ni phase diagram used by [1949Bra] significantly deviates from that accepted in the present work. Therefore, the resulting isotherms of the liquid phase and the proposed monovariant L + (γFe, Ni) + (Fe,Ni)Al or L + (γFe, Ni) + (αδFe) equilibria gave higher temperatures for a given composition than those suggested by [1933Koe].

Moreover, the results of [1949Bra], as well as those of [1951Bra] regarding the equilibria involving L, (Fe,Ni)Al, and (αδFe) are not consistent with the later data of [1978Mar, 1984Hao]. The former proposed that the (Fe,Ni)Al $\rightleftharpoons$ (αδFe) transformation is of first order for alloys containing less than 50 at.% Al, *i.e.*, a two-phase boundary should exist between these phases, giving rise to a L + (αδFe) $\rightleftharpoons$ (Fe,Ni)Al + (γFe, Ni) reaction. This is not confirmed by the findings of [1978Mar, 1984Hao] according to which the (Fe,Ni)Al $\rightleftharpoons$ (αδFe) transformation is of first order up to 1050°C and becomes second order at 1150°C. This suggests that the invariant reaction between L, (αδFe), (Fe,Ni)Al, and (γFe, Ni) is also of second order, so that no two-phase (Fe,Ni)Al + (αδFe) region exists. In addition, the liquidus and solidus temperatures reported by [1978Mar] for the section with atomic ratio Ni:Al = 1:1 are significantly higher than those of [1951Bra].

We must therefore conclude that the data of [1933Koe, 1949Bra, 1951Bra] are not fully reliable and that they should not be used to estimate the invariant temperatures in the composition range with aluminum content lower than 50 at.%. On this basis, critical assessment by [2006Ele], experimental data of [2007Chu1] and calculation results of [2009Zha] were here used to draw the monovariant lines and ascertain the position of the invariant reactions. The monovariant curves were further adjusted for compatibility with the accepted binary Fe-Ni and Al-Ni systems. The coordinates of the L + $Ni_3(Fe,Al)$ $\rightleftharpoons$ (γFe, Ni) + (Fe,Ni)Al reaction were accepted according to [2007Chu1]. The temperature and compositions of the phases involved in the e_2 minimum in the L $\rightleftharpoons$ (γFe, Ni) + (Fe,Ni)Al curve were accepted from the assessment by [2009Zha]. The temperature of this minimum (~1350°C) is close to that reported by [1933Koe] (~1339°C) but the minimum itself is significantly shifted towards the Al-Ni side of the composition triangle. The temperatures of the second order maximum c_1 and of the invariant reaction C_1, as well as the location of the order-disorder transformation curve, should be considered as raw estimates, mainly derived from results by [1984Hao], since [2009Zha] did not provide any results for these transformations.

The invariant reactions in the Al-rich corner essentially derive from the reaction scheme by [2007Chu2], with adjustments to preserve consistency with the accepted binary systems. The accepted reaction scheme is therefore based on the experimental data of [2007Chu2], which substantially agree with the results of the earlier works by [1943Sch, 1942Phi, 1982Kha, 1996Gru1]. The scheme is supported by the later results of [2007Zha1, 2019Lip]. The $Fe_5Al_8 + Fe_2Al_5 \rightleftharpoons$ (Fe,Ni)Al + $FeAl_2$ reaction is tentative, and it was added in the present work.

The reaction scheme from [2009Zha], in partial agreement with [2007Chu2], contains maxima in the monovariant curves, which are possible but not experimentally supported. Moreover, the assessment by [2009Zha] does not consider the homogeneity ranges of the Fe_2Al_5 and $FeAl_2$ phases in the Al-Fe system and the solubility of Fe in $NiAl_3$ in the ternary system. This means that the calculated invariant equilibria involving these phases may not fully reflect the actual invariant reactions experimentally measured.

Another issue concerning invariant equilibria regards reactions involving $NiAl_3$. According to the Al-Ni phase diagram accepted in the present evaluation, this phase forms *via* a peritectic reaction at 850°C. According to [2007Chu2] this compound is involved in two invariant reactions, L + $Ni_2Al_3 \rightleftharpoons \tau_1 + NiAl_3$ at 864°C and L + $\tau_1 \rightleftharpoons Fe_4Al_{13} + NiAl_3$ at 860°C, 14 and 10°C higher respectively than the binary peritectic temperature. It should be noted that in the 840 - 864°C temperature range, at least four invariant reactions occur, involving four solid phases: $NiAl_3$, Ni_2Al_3, τ_1 and Fe_4Al_{13}. It follows that experimental determination of the actual sequence and the nature of equilibria in this range is complicated. However, [1996Gru1, 2007Chu2] found that $NiAl_3$ dissolves up to 2 at.% Fe at 850°C, suggesting that this phase possibly nucleates at a temperature higher than 850°C in the ternary system. In the present evaluation, it is tentatively suggested that $NiAl_3$ forms in the ternary system at 864°C, which is not in contradiction with experimental vertical sections by [2007Chu2]. This means that the L + $Ni_2Al_3 \rightleftharpoons \tau_1 + NiAl_3$ reaction proposed by [2007Chu2] is here changed to L + $Ni_2Al_3 + \tau_1 \rightleftharpoons NiAl_3$ (P_3).

Based on these considerations, the accepted reaction scheme and the coordinates of invariant reactions are reported in Fig. 2 and Table 3, respectively.

Liquidus Surface

The Al-Fe-Ni liquidus surface can be divided into two separated regions: an Al-rich corner, recently investigated by [2007Chu2, 2008Zha, 2019Lip], and an Al-poor area, recently investigated by [2005Him, 2007Chu1, 2008Chu, 2011Kas]. The liquidus surface in its entirety was recently evaluated by [2006Ele] and calculated by [2007Zha1, 2009Zha, 2011Kas].

As previously discussed in the "*Invariant Equilibria*" section, the data of [1933Koe, 1949Bra, 1951Bra] cannot be used to construct the liquidus projection in the composition range with aluminum content lower than 50 at.%. Therefore, the projection of the liquidus surface for the Al-poor area was re-drawn considering critical assessment by [2006Ele], which is based on earlier investigations, vertical sections by [2002Bit, 2007Chu2, 2008Chu] and the thermodynamic assessment by [2009Zha], in addition to the liquidus curves of the accepted binary systems (Fig. 3). It should be noted that [2009Zha] did not discuss the contradictions between different datasets for this region: they used only experimental results of the FeAl-NiAl [2002Bit] and $FeNi_3$-Ni_3Al [2008Chu] sections.

Considering all the aforementioned information, some uncertainty remains about the shape of the liquidus surface in the central part of the composition triangle. According to earlier authors there is an evident saddle point close to the Fe-NiAl section, between 60 and 70 at.% Fe, causing the presence of a significant minimum along the same section. However, according to [2009Zha], no minimum seems to be present in this area. The extrapolation of the relatively well-established isothermal lines at $x(\mathrm{Al}) > 0.5$ suggests that the minimum in the liquidus surface, if present, is less evident than suggested by [1949Bra] and other early works, but this does not help to definitely solve the uncertainty.

As a conclusion, the liquidus projection reported here for compositions less than 50 at.% Al is mainly based on [2009Zha], with minor modifications to be consistent with the accepted binary systems.

In the Al-rich part, the liquidus is mainly based on the experimental investigations by [2007Chu2] (Fig. 3b), while liquidus lines reported in the isothermal sections investigated by [1982Kha] seem less reliable. Further details about this part of the liquidus projection have been discussed in the "*Invariant Equilibria*" section.

The solvus surface of the (γFe,Ni) phase in equilibrium with Ni_3(Fe,Al) between 600 and 1000°C is reported in Fig. 4, based on electrical resistivity measurements by [2005Him].

Isothermal Sections

Early experimental investigations of the Al-Fe-Ni phase equilibria (including partial isothermal sections) were conducted by [1933Koe, 1939Wim, 1941Kiu, 1942Dan] in the Fe-Ni-rich area, and by [1942Phi, 1943Sch, 1947Ray] in the Al-rich corner.

The first studies on the whole composition range were conducted by [1938Bra] on samples slowly cooled at 10°C/h. After that, a more detailed investigation in the 0-50 at.% Al region was presented by [1949Bra, 1951Bra], who reported isothermal sections at 1350, 1250, 1150, 1050, 950, 850 and 750°C in addition to liquidus surface and vertical sections. Further isothermal sections at high temperature have been experimentally investigated in the 0-50 at.% Al region by [2005Him] at 1300, 1100 and 900°C, by [2008Chu] at 1200, 1100, 1000 and 900°C and, in the Al-rich corner, by [1982Kha] at 1050 and 950°C.

For higher temperatures (≥ 1050°C), the isothermal sections adopted here are based on the critical assessment by [2006Ele] and on the experimental investigations by [1984Hao, 2007Chu1, 2007Chu2, 2008Chu], with small adjustments to be consistent with the accepted binary systems. The resulting isothermal sections at 1350, 1250, 1150 and 1050°C accepted here are reported in Figs. 5 to 8.

At 1350°C, the second order transition between (αδFe) and (Fe,Ni)Al is missing since it has not been investigated at this temperature. This section is mainly based on experimental data from [1949Bra] (also accepted in [2006Ele] critical assessment), with modifications coming from vertical sections accepted in this work and from the binary systems. Similar considerations apply to the 1250°C isothermal section (Fig 6), where the second order transition is instead visible.

At both 1350 and 1250°C, the Al-rich corner is completely occupied by the liquid phase; it follows that these sections can be considered complete. At these temperatures, the wavy shape of the (Fe,Ni)Al + L two-phase field proposed by [1949Bra] and accepted in the critical assessment by [2006Ele] has been modified, in agreement with more recent experimental work by [2007Chu2] and the thermodynamic assessment conducted by [2009Zha].

At 1150°C, the Al-rich part of the system is missing (Fig. 7). No isothermal section was experimentally investigated in this composition range at temperatures higher than 1050°C.

The main work regarding the miscibility gap between (αδFe) and (Fe,Ni)Al was performed by [1984Hao], who found that the tricritical line and the (αδFe) + (Fe,Ni)Al + γ(Fe,Ni) three-phase field appear at an undetermined temperature between 1150 and 1050°C.

At 1050°C, the isothermal section accepted here results from that reported by [2006Ele], with modifications according to [1984Hao], for the (αδFe) + (Fe,Ni)Al miscibility gap, and to [2007Chu2] for the shape of the liquidus curve, which in [2006Ele] was based on [1982Kha] (Fig. 8). The accepted binary systems have also been considered.

For lower temperatures (< 1050°C) the situation becomes more complicated. The experimental studies in this region comprise isothermal sections at 950, 900, 850 and 750°C investigated by [1949Bra, 1951Bra, 1982Kha, 1996Gru1, 2005Him] in addition to the Al-rich sections at 850 and 627°C investigated by [2008Zha] and Al-poor sections at 1000 and 900°C investigated by [2008Chu]. In the thermodynamic assessment by [2009Zha], the isothermal sections at 950, 850 and 627°C were calculated based on all the previous data, but the results of this assessment were oversimplified since the solubilities of several binary and ternary phases were not considered, with implications on the invariant equilibria involving them.

The isothermal section at 950°C is reported in Fig. 9. This section was investigated in the Al-rich corner by [1982Kha]. It is scarcely reliable for the liquidus curve, but is in good agreement with other authors for the solid-state equilibria. In the Al-poor area, the data by [1949Bra, 1951Bra, 1984Hao] have been considered.

The 850°C isothermal section is the lowest temperature completely investigated section: it is reported in Fig. 10. The Al-rich corner of the section comes from [1982Kha] and [2007Chu2], modified to be consistent with the accepted reaction scheme. The Al-poor area of the section, on the other hand, is based on [1949Bra, 1984Hao, 2009Zha] in addition to the binary subsystems. It should be noted that this section coincides with the temperature of E_1 (decomposition of τ_1) in the ternary system and p_6 (peritectic formation of $NiAl_3$) in the Al-Ni system. For clarity, the triangle of the E_1 invariant is shown, together with the $NiAl_3$ solution phase, already present at higher temperature in the ternary.

The 750°C isothermal section reported in Fig. 11 comes from [1951Bra] and does not include the Al-rich corner since the available experimental data of [1982Kha] are too scarce to draw all phase fields reliably.

At 627°C the only experimental investigation was performed by [2008Zha] in the Al-rich area. The resulting partial isothermal section is reported in Fig. 12 (with the usual modifications to agree with the accepted binary systems). In the Al-poor region no data are available.

Finally, the phase fields reported in Fig. 13 reflect results obtained from the analysis of alloys slowly cooled at 10°C/h from 900°C (600°C in the Al-rich corner) by [1938Bra, 1940Bra1, 1940Bra2].

Temperature – Composition Sections

Early studies of temperature-composition sections were performed by [1933Koe, 1941Kiu, 1942Dan, 1951Bra, 1951Iva]. These sections seem very approximate, considering the scarce agreement between them and the liquid-solid phase equilibria accepted here. Second order transitions seem to be poorly defined in these sections and contradictions exist, especially between the data of [1933Koe, 1941Kiu, 1942Dan, 1951Bra] and that of [1984Hao, 2002Bit]. For these reasons, early sections not recently re-investigated are not reported in this assessment.

The Fe-NiAl vertical section reported by [2006Ele] was based on results by [1933Koe, 1941Kiu, 1942Dan, 1951Bra, 1951Iva]. It is used here as a starting point for the section reported in Fig. 14. With respect to [2006Ele], melting equilibria are dashed, according to the comments reported in the "*Liquidus, Solidus and Solvus Surfaces*" section, the second order (αδFe) ⇌ (Fe,Ni)Al transition is modified according to [1984Hao] and the (αδFe) + (Fe,Ni)Al two-phase field boundaries are modified according to [1984Hao, 2008Chu]. The Curie temperature (T_C) line is added in the same field, at about 700°C (experimental measurements vary between 680°C [1942Dan] and 743°C [1978Mar]). Other minor modifications were adopted to maintain coherence with the accepted binary systems.

The vertical section Ni_3Al-Fe_3Al was investigated by [1949Bra, 1987Mas, 1994Jia, 1998Gom, 2004Him, 2007Chu1, 2008Chu] but the results are appreciably different. All these works were considered in [2009Zha] thermodynamic assessment, but the authors did not indicate the weight assigned to the different data. The section reported in Fig. 15 is mainly based on results from [2004Him, 2007Chu1]. Equilibria at high temperature, close to Ni_3Al (Fig. 15b), are based on [2007Chu1] and are dashed since phase equilibria in this area are uncertain.

For the FeAl-NiAl vertical section, only the solidus curve has been determined experimentally, which was by [1949Bra] and [2002Bit]. The solidus curve accepted here comes from interpolation between the results reported in these two works. The liquidus curve has not been determined experimentally, but it was calculated in the thermodynamic assessment by [2009Zha]. In Fig. 16, the liquidus curve is dashed and a two-phase field narrower than calculated by [2009Zha] is proposed to be more consistent with the accepted (yet uncertain) liquidus surface.

More systematic investigations of the Al-Fe-Ni vertical sections were performed by [2007Chu2] in the Al-rich corner at 60, 67, 71.5, 75, 80 at.% Al. Its work, in addition to the previous literature, was considered in the thermodynamic assessment by [2009Zha] who calculated vertical sections at 50, 60 and 80 at.% Al. Once again, this assessment appears oversimplified. For this reason, the isopleths reported here come from the vertical sections by [2007Chu2], combined with accepted isothermal sections, binary systems and the accepted reaction scheme. They are reported in Figs. 17-21.

The main issue is regarding the 850 - 864°C temperature range of the aforementioned isopleths. Consistent with the accepted liquidus surface, a P-type equilibrium at 864°C is introduced instead of the U-type proposed by [2007Chu2] (see comments in the "*Liquidus, Solidus and Solvus Surfaces*" section). Moreover, in the Fe-rich part of the isopleths at 60 and 67 at.% Al, the U_4 invariant equilibrium $Fe_5Al_8 + Fe_2Al_5 \rightleftharpoons (Fe,Ni)Al + FeAl_2$ is tentatively proposed at a temperature between 1095 and 1140°C, to be consistent with accepted phase fields at higher and lower temperatures. Consequently, two- and three-phase fields were added in the vertical sections at 71.5 and 75 at.% Al to preserve agreement with the Al-Fe phase diagram and avoid any phase rule violation: no experimental point determined in the aforementioned isopleths contradicts with the adopted modifications.

Thermodynamics

The temperature and enthalpy of fusion of the decagonal $Fe_5Ni_{24}Al_{71}$ phase prepared by inductive melting of the pure metals, water cooling and subsequent annealing for 300h at 880°C have been respectively determined at 967 ± 5°C and 13.0 ± 0.4 $kJ \cdot mol^{-1}$ of atoms by [1999Hol]. The standard enthalpy of formation of the (Fe,Ni)Al phase at different compositions has been measured by Al solution calorimetry by [1993Zub] and, with very good reproducibility, by [2001Bre] and [2003Su]. Their results are reported in Table 4.

[2006Ben] determined the activity of the component elements in *B*2-AlFeNi alloys at 1127°C by Knudsen Effusion Mass Spectrometry (KEMS); the obtained results, reported in Table 5, were used to calculate the thermodynamic properties of the investigated alloys.

Formation enthalpies of $AlNi_3$-based alloys with iron additions were determined by solution and direct reaction calorimetry by [2010Rzy]. The results from the two different methods were compared and they are reported in Table 5.

The specific heat of the τ_1 decagonal phase was determined between 4.2 K and 40 K by [2010Pan] using both thermodynamic methods and inelastic neutron scattering. The obtained variation of lattice heat capacity with temperature is reported in Table 5 and Fig. 22.

Further heat capacity measurements were performed by [2010Ond] on (Fe,Ni)Al solid solutions by DSC between 100 and 600 K, after homogenization. The obtained results were fitted using the Kelley equation, as reported in Table 5.

Thermodynamic data have also been calculated by CALPHAD assessment [2009Zha, 2011Du] or by Miedema's model [2012Ada].

Notes on Materials Properties and Applications

Fe is one of the most important constituents of Ni-base superalloys. Although the *B*2-structured NiAl phase has a high melting temperature, high thermal conductivity and high resistance to oxidation, it lacks high temperature strength. This can be overcome using Fe or other minor additions such as Ga or Mo [2002Alb], and a systematic study of correlation between point defects and Fe precipitates has been undertaken [1998Ko, 2002Alb]. Moreover, the influence of iron on physical, mechanical (grain size, yield strength) and magnetic properties of NiAl was investigated by [2002Ban, 2002Mun]. More recent studies on the effect of Fe on NiAl powders were performed by [2004Cam], obtaining a significant improvement of ductility. [2006Gar] examined the possibility of enhancing NiAl workability and tensile ductility by alloying with Fe *via* induction melting and subsequent heat treatment (hot rolling). Indeed, these compounds would be of higher practical interest if their attractive high temperature behavior could be combined with good room temperature formability. This aim may be achieved by introducing a substantial amount of disorder in their crystal lattice. Several techniques have been proposed such as melt spinning, ion irradiation, mechanical alloying [1991Kos, 1995Gaf, 2001Sur] and introduction of dopants such as carbon [2002Kim] or boron [2007Col]. [2007Orb] investigated the effects of Fe addition in $NiAl_3$-Fe doped alloys, observing a major improvement in the mechanical resistance and formability as the Fe content increases.

Regarding physical properties, the presence of Fe in the NiAl phase improves fatigue behavior under cyclic accumulated strain [1991Har]. The fracture toughness and yield strength of the (Fe,Ni)Al phase ($Fe_{20}Ni_{45}Al_{35}$ composition) is improved by mechanical alloying with small additions of Y_2O_3, promoting grain refinement [1991Kos]. Fe doping induces magnetic transitions in NiAl alloys, increasing the ductility and decreasing the critical stress needed to move dislocations along the slip axis [2012Hua]. Studies on dislocation movement were also performed by [2006Wan, 2009Laz], confirming the effect of Fe in increasing the ductility and reducing the creep rate. Furthermore, using Fe as a container for mechanosynthesis of Ni-Al alloys, the required energy for mechanical alloying of Fe itself is reduced [2007Joa]. When large amounts of Fe are dissolved into an Al-Ni alloy, large magnetic effects are observed and a magnetic softening phenomenon occurs, according to [2007Liu]. Magnetic transitions at low temperatures for these kinds of alloys was also discussed by [2007Uwa], who suggested that magnetic properties can be used as indicators of solid solution softening or hardening when Fe is added to an Al-Ni alloy. Significant solution softening by Fe dissolution in NiAl alloys for magnetic reasons was also proved by first-principle calculations [2004Fu]. Vibrational properties of Fe impurities in NiAl intermetallics were investigated by nuclear inelastic scattering of synchrotron radiation and inelastic neutron scattering by [2004Par2]. Fe doped Ni_3Al alloys show increased disordering temperatures thanks to the strong Fe-induced magnetic effects [2013Lep].

The effect of Ni and Ni-containing compounds on Al-Fe alloys has been extensively investigated. Their effect on grain size and shape [2019Yas], strength and magneto-mechanical damping [2013Yas], internal friction and yield strength [2009Yas], pseudo-elasticity [2007Yas] and structural, elastic and electronic properties [2017Zhe] has been determined. Moreover, Ni atoms entering the Fe_3Al crystal lattice in Fe sites increase the plasticity of the resulting ternary alloy [2012Niu]. Al-Fe powders doped with Ni showed higher vacancy concentration than the pure powders when investigated by Mössbauer spectroscopy [2008Han]. The presence of Ni_3Al nanoparticles affects ternary *fcc* Al-Fe-Ni alloys by decreasing the vacancy accumulation, as demonstrated by results from positron annihilation spectroscopy [2006Dru]. Mössbauer spectroscopy has been used by [2010Sag] to study the dissolution of dispersed Ni_3Al intermetallic particles in matrices of *fcc* Fe-Ni-Al alloys at 340 K in displacement cascades produced by neutrons. Factors affecting the rate of dissolution of intermetallic particles have been investigated. Furthermore, the effect of Ni on the *B*2-FeAl structure was investigated by [2011Che] through molecular dynamics and by [2005Str] *via ab initio* calculations. In [2011Che], the site preference of each type of defect and the changes in lattice parameters and bulk modulus associated with the presence of defects in the FeAl matrix, were studied. Meanwhile, [2005Str] investigated the effect of Ni on the energy of vacancy formation. Ni also affects the lattice parameter and magnetic hyperfine field in $(Fe_{70}Al_{30})_{100-x}Ni_x$ alloys, according to [2010Pal]. The effect of precipitation of NiAl intermetallic particles was analyzed by [2010Sch] so that the different stages of the process could be modelled and thus the material properties could be optimized by modifying the aging time.

Nanostructured Al-Fe-Ni materials show significant kinetics of reordering even at 300°C. However, complete reordering cannot be achieved, even after a long anneal at 600°C [2002Joa]. Al-Fe-Ni alloys are good precursors for the preparation of Fe-Ni powders with high surface area and interesting catalytic properties [1981Kha]. Ternary alloys with nominal compositions $Ni_{30}Fe_5Al_{65}$ and $Ni_{15}Fe_{10}Al_{75}$ prepared by mechanical alloying were used to obtain Fe-Ni Raney-type catalysts by leaching aluminum with an alkaline aqueous solution [2000Zei]. Further synthesis and leaching studies on ternary Al-Fe-Ni alloys were performed by [2008Kim1, 2008Kim3], who completed his studies by measuring the magnetic properties of resulting alloys in [2008Kim2]. Factors controlling recrystallization of continuously cast Al-Fe-Ni alloys were determined by [2006Nii], after analyzing the microstructure, grain structure, texture and backscattered electron patterns of a heat-treated sample (also containing small percentages of Si, Zn and Zr).

Other Al-Fe-Ni alloys were investigated by [2004Sch], underlining the potential of these alloys as bases for ferritic superalloys and future applications. New promising alloys in this system can be obtained by mechanical alloying as in [2004Maz] and [2010Sha, 2011Sha]. [2010Sha, 2011Sha] also investigated the effect of plastic deformation on particle dissolution and, consequently, on the alloys properties.

Many more studies focused on the alloys of this system, given their promising behavior. $Al_{50}Fe_{10}Ni_{40}$, $Al_{25}Fe_{27.5}Ni_{47.5}$, $Al_{45}Fe_{35}Ni_{20}$, $Al_{15}Fe_{75}Ni_{10}$, $Al_{17}Fe_{33}Ni_{50}$ and $Al_{10}Fe_{50}Ni_{40}$ alloys were prepared and characterized by [2006Tsa, 2006Wan, 2007Mun, 2010Sor, 2012Ma, 2013Had] respectively. A wider series of alloys with formula $Al_{25}Fe_xNi_{75-x}$ was prepared and characterized by [2004Kau]. A more recent and complete work on these alloys was performed by [2017Wan], creating a mechanical properties database based on first principle calculations for multicomponent alloys, focusing mainly on the Al-rich corner.

New materials may be obtained through thermal explosion reactions as an alternative to combustion synthesis. The order of reaction, n, and the activation energy, *E*, of thermal explosive reactions for $Fe_{30}Ni_{50}Al_{20}$ (in mass%) have been respectively measured as n = 0.37 and *E* = 152 kJ/mol [2002He]. The maximum reaction temperature is 657°C, higher than the eutectic temperature between Al and $NiAl_3$, so that the thermal explosion consists of both liquid and solid-state reactions. Moreover, the high temperature thermal stability of an Al-Fe-Ni eutectic alloy was investigated by [2019Bia].

Al-Fe-Ni alloys present a shape memory effect in the (Fe,Ni)Al+(γFe,Ni) field [1992Kai]. Control of the Ms (Martensite start) temperature is difficult to achieve in Al-Ni alloys because of the very sensitive dependence on Al content. However, it is very easily achieved in the ternary two-phase alloy by manipulating the composition of the (Fe,Ni)Al phase through appropriate choice of annealing temperatures. Other recent studies on shape-memory Al-Fe-Ni alloys were performed by [2008Muk, 2011Zho] and [2006Oik] who analyzed the decrease of martensitic temperature as a function of Fe content. Furthermore, melt-spun ribbons of the $Ni_{55}Fe_{22.5}Al_{22.5}$ Ferromagnetic Shape-Memory Alloy (FSMA) were extensively characterized by [2011Oku], who investigated their microstructure, martensitic transformation and magnetic properties.

More recently, some alloys of this system have become of great interest thanks to their full-Heusler behavior. The Fe_2NiAl alloy was extensively investigated by [2019Gan], focusing on its mechanical, magnetic and transport properties. He also described crystal and band structure, determining the effective magnetic moment and the ferromagnetic ordering. The same alloy was also investigated by [2012Shr], who measured its optical properties and [2016Dah, 2018Wei] who performed DFT and *ab initio* calculations to determine its Curie temperature and metallicity. Moreover, the $FeNi_2Al$ alloy also showed full-Heusler behavior both experimentally [2007Zha2] and in DFT calculations [2018Wen]. Structural, electronic, dynamic and thermodynamic properties of the $FeNi_2Al$ alloy have been theoretically investigated by [2020Ben]. Further calculations on mechanical, electronic and thermal properties of such alloys were performed by [2021Liu].

Possible future applications for the alloys of this system regard the human body environment, thanks to their oxidation resistance. [2009Cas] investigated the electrochemical behavior of several Al-Fe-Ni alloys in simulated human-body conditions by potentiodynamic polarization experiments, electrochemical impedance spectroscopy and electrochemical noise measurements. Similar studies were performed by [2007Gon], who underlined the effect of different Ni concentrations and thermal treatments on the corrosion resistance of Al-Fe-Ni ternary alloys in the same conditions: the best results were obtained for 5 at.% Ni alloys heat treated at 400°C for 144 h.

The Al-Fe-Ni alloys can be reinforced by favoring the *in-situ* formation of composite materials. This can be achieved by the addition of K_2TiF_6 or KBF_4 to the alloys in liquid form, obtaining needle like crystallites of Ti composites and nanoparticles, which results in interdendritic precipitation and alloy strengthening [2009Vou]. Also, nanoscale precipitations can be used to strengthen the Al-Fe-Ni alloys: the kinetics of this process was investigated by magnetic measurements *via* VSM [2011Dum, 2012Dum]. The upper temperature limits for possible long-term applications of Al-Fe-Ni materials were defined by [2008Mun], who suggested the optimum annealing conditions to obtain alloys with thermally stable microstructures.

The main works on Al-Fe-Ni materials properties are schematically reported in Table 6.

Miscellaneous

The crystallographic features of decagonal structures and the formation rules for Al-Fe-Ni quasicrystals were presented in [1996Yam, 2002Hir] and [2001Qia], respectively. Several different decagonal diffraction patterns have been first observed by [1989Tsa] in Al-Fe-Ni alloys prepared by melt quenching in the composition range 9-16 at.% Ni, 9-21 at.% Fe, balance Al, in good agreement with the more recently proposed $Fe_{20-x}Ni_{10+x}Al_{70}$ ($0 \le x \le 10$) composition range [1993Tan, 1997Sai].

[1993Tan] and [1997Sai] found by convergent-beam electron diffraction (CBED) that $Fe_{20-x}Ni_{10+x}Al_{70}$ quasicrystals belong to the noncentrosymmetric $P\overline{10}m2$ (for $0 \le x \le 7$) and to the centrosymmetric $P10/mmm$ (for $7 \le x \le 10$) space groups. Moreover, these quasicrystals present periodicities multiple of 0.4 nm along the tenfold axis [1997Yam]. These structures probably correspond to the τ_3 ($Fe_{14.5}Ni_{13}Al_{72.5}$) and τ_2 ($Fe_{9.83}Ni_{19.34}Al_{70.83}$) phases, whose structure has been described by [2001Qia]. The τ_3 phase was observed to coexist with the Fe_3NiAl_{10} phase (denoted as $FeNiAl_5$ in the original paper). Decagonal phases reveal higher positron lifetime than crystalline compounds [1995Wue], which implies higher concentration of structural vacancies. A characteristic feature of these structures, isotypic with decagonal phases encountered in Al-Co-Ni and Al-Co-Cu systems [1994Gru], is that they consist of 2 nm clusters with pentagonal symmetry. The superstructure is due to chemical ordering in the central part of the clusters. More recently, a cluster-based composition rule for stable ternary quasicrystals of the Al-Fe-Ni system was developed by [2006Don]. Star-shaped and butterfly-shaped tiles observed in quasicrystals are well understood from observations of [2002Yok]. Diffuse synchrotron scattering of X-rays and neutrons shows disordered layers perpendicular to the unique tenfold axis [2000Fre].

The amount of transition metals in decagonal phases precipitating in the Al-Fe-Ni alloys is connected to solid solution hardening, caused by intermetallic phases dispersion [2005Set]. By mixing pure Al with the $Al_{75}Fe_{10}Ni_{15}$ and $Al_{71}Fe_{24}Ni_5$ decagonal alloys it is possible to influence type, number and properties of the forming phases in the resulting alloy [2005Set].

The latest study on decagonal phases was carried out by [2021Mly], performing a complete characterization (by LOM, XRD, HRTEM, and DSC) of a rapidly solidified $Al_{71}Ni_{24}Fe_5$ alloy.

The diffusion experiments, carried out at 1002°C in the *B*2 (NiAl) domain of the ternary system presents anomalous behavior [1976Moy], since the interactions among the various components are strongly composition dependent. This is explained [1997Kai] by NiAl having a wide composition range and exhibiting two types of structural imperfections, depending on the nature of deviation from stoichiometry. In NiAl, iron was observed to preferentially substitute aluminum atoms whatever the Al/Ni ratio [1994Dun, 2002Ban, 2007Liu]. Substitution (up to 10 at.%) of Al by Fe in NiAl causes decreasing of the lattice parameter and increasing of the Young's modulus [1991Mas]. More generally, the introduction of Fe increases the hardness of Al rich alloys, while the opposite effect is observed in Ni rich alloys [1997Pik, 2001Tan, 2007Liu]. This softening is attributed to the replacement of Ni anti-site defects with Fe defects on the Al sublattice. Moreover, the site preference of Ni in (Fe,Ni)Al ordered iron aluminide has been determined using ALCHEMI technique (Atom Location by Channeling-Enhanced Microanalysis), first in the $Fe_{50}Ni_5Al_{45}$ alloy [1997And] and then in the whole (Fe,Ni)Al domain (40 to 52 at.% Al) [2002Pik]. Ni was found to occupy Fe sites exclusively, displacing Fe to Al anti-sites [2002Ban, 2002Pik]. The influence of Ni on formation and growth characteristics of Fe based aluminide diffusion layers has been modelled [1998Akd, 1999Mek] by a quasichemical method combined with an electronic theory in the pseudopotential approximation; furthermore, the influence of Fe on lattice parameters and hardening of NiAl has been modelled [2002Liu] by first principle quantum mechanical calculations. *Ab initio* calculations on the stability of the *B*2 phase were performed by [2006Fuk], who underlined the strong *B*2 stabilizing effect of Ni. More diffusion studies in the *B*2 (Fe,Ni)Al domain were performed by [2004Div, 2006Div], who concluded that the diffusion rate of Fe is 3 to 5 times higher than that of Ni, which diffuses faster as the Fe content increases in the alloy. Controversial results on the interdiffusion processes in (Fe,Ni)Al alloys were found by [2004Her], who determined the site preferences of the different elements and vacancies during diffusion.

The site preference in various (Fe,Ni)Al solid solutions ($Fe_xNi_{50-x/2}Al_{50-x/2}$, $Fe_xNi_{50-x}Al_{50}$, and $Fe_xNi_{50}Al_{50-x}$ compositions) has also been modelled [2002Boz] *via* Monte-Carlo simulation. A phenomenological model for multicomponent diffusion in the (Fe,Ni)Al phase was presented by [1999Hel] and the calculated diffusion paths were compared with the experimental results from [1976Moy]. The OTL (ordering tie-line) approach [2000Ama] confirmed previous observations showing that, while Ni segregates preferentially to the Fe sublattice in Al depleted FeAl, Fe segregates preferentially to the Al sublattice in Al depleted NiAl. Moreover, [2006Kau] investigated the effect of site disorder on the martensitic transition and the Curie temperature in a sample at the $Ni_{55}Fe_{20}Al_{25}$ composition.

Other diffusion studies by [2003Cer1, 2003Cer2] determined the ternary interdiffusion coefficients along the $AlNi_3$-$FeNi_3$ vertical section in the 900-1260°C temperature interval by diffusion couples method. A more complete study of diffusion profiles and reaction paths as a function of ideal mixing entropy was performed by [2010Leu]. Experimental investigations of long-range ordering kinetics in $Ni_{75}Al_{25x}Fe_x$ ($0 \le x \le 15$) alloys with $L1_2$ superstructure were carried out by [2004Par1].

A more systematic study on diffusivities in Al-Fe-Ni melts was performed by [2010Zha], evaluating atomic mobilities of Al, Fe and Ni atoms by using the DICTRA software. As a conclusion of his work, an atomic mobility database for the Al-Fe-Ni system was built.

[2006Ako] found a series of anomalies of the magnetic and elastic properties in a $Fe_{65}Ni_{23}Al_{12}$ shockwave compacted powder mixture studied by X-ray diffraction, microstructure observation, temperature dependence of magnetic susceptibility, elastic modulus and internal friction determination. Factors causing such anomalies were suggested.

Finally, [2012Ada] provided a full thermodynamic description for the $(Al,Fe)Ni_3$ phase, prepared by mechanical alloying of powders. Gibbs free energy and mixing enthalpy changes were calculated by an extended Miedema's model; the intermetallic compound formation resulted to be favored over solid solution or amorphous phase formation at any composition.

References

[1933Koe] Koester, W., "Iron-Nickel-Aluminium System" (in German), *Arch. Eisenhuettenwes.*, **7**(4), 257-262 (1933), doi:10.1002/srin.193300045 (Phase Diagram, Experimental, #, 8)

[1938Bra] Bradley, A.J., Taylor, A., "An X-Ray Study of the Iron-Nickel-Aluminium Ternary Equilibrium Diagram", *Proc. Roy. Soc. (London) A*, A**166**, 353-375 (1938), doi:10.1098/rspa.1938.0098 (Phase Diagram, Experimental, #, 3)

[1939Wim] Wyman, L.L., "Constitution of Iron-Nickel-Aluminium Alloys", *Metals Handbook*, 416-417 (1939) (Assessment, Phase Diagram, Phase Relations, 3)

[1940Bra1] Bradley, A.J., Taylor, A., "An X-Ray Investigation of the Aluminium Rich Iron-Nickel-Aluminium Alloys after Slow Cooling", *J. Inst. Met.*, **66**, 53-63 (1940) (Phase Diagram, Experimental, #, 14)

[1940Bra2] Bradley, A.J., Bragg, W.L., Sykes, C., "Researches into the Structure of Alloys", *J. Iron Steel Inst., London*, **80**, 63-156 (1940) (Phase Diagram, Experimental, Crystal Structure, #, 22)

[1941Kiu] Kiuti, S., "An X-Ray Investigation on the Ternary Equilibrium in the Iron-Nickel-Aluminium System", *Sci. Rep. Tohoku Imp. Univ.*, **29**, 742-794 (1941) (Phase Diagram, Crystal Structure, Experimental, #, 30)

[1942Dan] Dannöhl, W., "The Iron-Nickel-Aluminium Phase Diagram" (in German), *Arch. Eisenhuettenwes.*, **15**(7), 321-330 (1942), doi:10.1002/srin.194200603 (Phase Diagram, #, 33)

[1942Phi] Phillips, H.W., "The Constitution of the Aluminium Rich Alloys of the Aluminium-Nickel-Iron and Aluminium-Nickel-Silicon Systems", *J. Inst. Met.*, **68**, 27-46 (1942) (Phase Diagram, Phase Relations, Experimental, #, 15)

[1943Sch] Schrader, A., Hanemann, H., "The Aluminium-Rich Region of the System Aluminium-Iron- Nickel", (in German), *Aluminium*, **25**(10), 339-342 (1943) (Phase Diagram, Experimental, #, 5)

[1947Ray] Raynor, G.V., Pfeil, P.C.L., "The Constitution of the Aluminium-Rich Aluminium-Iron-Nickel Alloys", *J. Inst. Met.*, **73**(6), 397-419 (1947) (Phase Diagram, Experimental, #, 15)

[1949Bra] Bradley, A.J., "Microscopical Studies on the Iron-Nickel- Aluminium System. Part I. α+β Alloys and Isothermal Section of the Phase Equilibrium Diagram", *J. Iron Steel Inst., (London)*, **163**(1), 19-30 (1949) (Phase Diagram, Experimental, #, 19)

[1951Bra] Bradley, A.J., "Microscopical Studies on the Iron-Nickel-Aluminium System. Part II. The Breakdown of Body-Centered Cubic Lattice", *J. Iron Steel Inst., (London)*, **168**(3), 233-244 (1951) (Phase Diagram, Crystal Structure, Experimental, #, 18)

[1951Iva] Ivanov, O.S., "Main features of the Phase Equilibrium in High-coercive Fe-Ni-Al Alloys" (in Russian), *Dokl. Akad. Nauk SSSR*, **78**, 1157 (1951) (Phase Diagram, Experimental, 7)

[1958Tay] Taylor A., Jones, R.M., "Constitution and Magnetic Properties of Iron-Rich Iron-Aluminium Alloys", *J. Phys. Chem. Solids*, **6**, 16-37 (1958), doi:10.1016/0022-3697(58)90213-0 (Crystal Structure, Experimental, Magnetic Properties, Phase Diagram, 49)

[1959Gua] Guard, R.W., Westbrook, J.H., "Alloying Behavior of Ni_3Al (γ') Phase", *Trans. Metall. Soc. AIME*, **215**, 807-814 (1959) (Phase Diagram, Experimental, 27)

[1967Ng] Ng, S.C., Brockhouse, B.N., Hallman, E.D., "Characterization of Large Alloy Single Crystals by Neutron Diffraction", *Mater. Res. Bull.*, **2**(1), 69-73 (1967), doi:10.1016/0025-5408(67)90044-X (Crystal Structure, Experimental, 8)

[1974Kau] Kaufman, L., Nesor, H., "Calculation of Superalloy Phase Diagrams. Part II", *Met. Trans. (J. of Metals, AIME)*, **5**(7), 1623-1629 (1974), doi:10.1007/BF02646334 (Phase Diagram, Calculation, #, 20)

[1976Moy] Moyer, T.D., Dayananda, M.A., "Diffusion in β_2 Fe-Ni-Al Alloys", *Metall. Trans. A,* **7A**(7), 1035-1040 (1976), doi:10.1007/BF02644070 (Phase Diagram, Diffusion, Experimental, #, 13)

[1977Nic] Nicholls, J.R., Rawlings, R.D., "A Mössbauer Effect Study of Ni_3Al with Iron Additions", *Acta Metall.*, **25**, 187-194 (1977), doi:10.1016/0001-6160(77)90122-5 (Crystal Structure, Electronic Structure, Mössbauer, 16)

[1978Mar] Marcon, G., Peffen, R., Lemaire, H., "Iron-Nickel-Aluminium Phase Diagram in AlNi Type Permanent Magnets Related Area", *IEEE Trans., Magn.*, **14**(5), 685-687 (1978), doi:10.1109/TMAG.1978.1059951 (Experimental, Magnetic Properties, Phase Diagram, Phase Relations, 16)

[1980Riv] Rivlin, V.G., Raynor, G.V., "Phase Equilibria in Iron Ternary Alloys. Part 2: Critical Evaluation of Constitution of Aluminium-Iron-Nickel System", *Int. Met. Rev.*, **25**(3), 79-93 (1980), doi:10.1179/imtr.1980.25.1.79 (Phase Diagram, Review, #, *, 38)

[1981Kha] Khaidar, M., “Equilibrium of Phases and Intermetallic Compounds of the Ni-Fe-Al System: Characterization of the Catalysts Deriving from These Compounds” (in French), *Tezisy, Dokl. Grenobl. Univ.*, 1-71 (1981) (Phase Diagram, Crystal Structure, #, 67)

[1982Ell] Ellner, M., Kattner, U., Predel, B., “Constitutional and Structural Studies in Aluminum-rich Phases of the Ni-Al and Pt-Al Systems”, *J. Less-Common Met.*, **87**(2), 305-325 (1982), doi:10.1016/0022-5088(82)90097-2 (Crystal Structure, Experimental, Phase Diagram, Phase Relations, 48)

[1982Kha] Khaidar, M., Allibert, C.H., Driole, J., “Phase Equilibria of the Fe-Ni-Al System for Al-Content above 50 at.% and Crystal Structures of Some Ternary Phases”, *Z. Metallkd.*, **73**(7), 433-438 (1982), doi:10.1515/ijmr-1982-730705 (Phase Diagram, Crystal Structure, #, *, 17)

[1984Hao] Hao, S.M., Takayama, T., Ishida, K., Nishizawa, T., “Miscibility Gap in Fe-Ni-Al and Fe-Ni-Al-Co Systems”, *Metall. Trans. A*, **15A**, 1819-1828 (1984), doi:10.1007/bf02664895 (Phase Diagram, Experimental, #, *, 18)

[1984Och] Ochiai, S., Mishima, Y., Suzuki, T., “Lattice Parameter Data of Ni (γ), Ni_3Al (γ') and Ni_3Ga (γ') Solid Solutions”, *Bull. Res. Lab. Precis. Machin. Electron., Tokyo Inst. Technol.*, **53**, 15-28 (1984) (Crystal Structure, Experimental, 66)

[1986Bra] Bramfitt, B.L., Michael, J.R., “AEM Microanalysis of Phase Equilibria in Ni_3Al Intermetallic Alloys Containing Iron”, *Mater. Res. Soc. Symp. Proc.*, **62**, 201-208 (1986), doi:10.1557/PROC-62-201 (Phase Diagram, Experimental, #, *, 20)

[1986Fun] Fung, K.K., Yang, C.Y., Zhou, Y.Q., Zhao, J.G., Zhan, W.S., Shen, B.G., “Icosahedrally Related Decagonal Quasicrystal in Rapidly Cooled Al-14 at.% Fe Alloy”, *Phys. Rev. Lett.*, **56**(19), 2060-2066 (1986), doi:10.1103/PhysRevLett.56.2060 (Crystal Structure, Experimental, 12)

[1987Mas] Masahashi, N., Kawazoe, H., Takasagi, T., Izumi, O., “Phase Relations in the Section Ni_3Al-Ni_3Fe of the Al-Fe-Ni System”, *Z. Metallkd.*, **78**(11), 788-794 (1987), doi:10.1515/ijmr-1987-781106 (Phase Diagram, Experimental, #, 18)

[1988Ray] Raynor, G.V., Rivlin, V.G., “*Phase Equilibria in Iron Ternary Alloys*”, Inst. Metals, London, 107-121 (1988) (Phase Diagram, Review, #, 32)

[1989Ell] Ellner, M., Kek, S., Predel, B., “Ni_3Al_4 - A Phase with Ordered Vacancies Isotypic to Ni_3Ga_4”, *J. Less-Common Met.*, **154**(1), 207-215 (1989), doi:10.1016/0022-5088(89)90185-9 (Experimental, Crystal Structure, 26)

[1989Tsa] Tsai, An-P., Inoue, A., Masumoto, T., “New Decagonal Al-Ni-Fe and Al-Ni-Co Alloys Prepared by Liquid Quenching”, *Mater. Trans., JIM*, **30**(2), 150-154 (1989), doi:10.2320/matertrans1989.30.150 (Crystal Structure, Experimental, 21)

[1990Ell] Ellner, M., Röhrer, T., “On the Structure of the Ternary Phase $FeNiAl_5$” (in German), *Z. Metallkd.*, **81**(11), 847-849 (1990), doi:10.1515/ijmr-1990-811111 (Phase Diagram, Crystal Structure, *, #, 23)

[1991Ell] Ellner, M., Kolatschek, K., Predel, B., “On the Partial Atomic Volume and the Partial Molar Enthalpy of Aluminum in Some Phases with Cu and Cu_3Au Structures”, *J. Less-Common Met.*, **170**(1), 171-184 (1991), doi:10.1016/0022-5088(91)90062-9 (Crystal Structure, Experimental, Thermodynamics, 57)

[1991Har] Hartfield-Wuensch, S.E., Gibala, R., “Cyclic Deformation of *B*2 Aluminides”, *Mater. Res. Soc. Symp. Proc.: High-Temp. Order. Intermet. Alloys IV*, **213**, 575-580 (1991), doi:10.1557/PROC-213-575 (Crystal Structure, Experimental, Mechanical Properties, 12)

[1991Kos] Kostrubanic, J., Koss, D.A., Locci, I.E., Nathal, M., “On Improving the Fracture Toughness of a NiAl-Based Alloy by Mechanical Alloying”, *MRS Symp. Proc.: High-Temp. Order. Intermet. Alloys IV*, **213**, 679-684 (1991), doi:10.1557/PROC-213-679 (Experimental, Physical Properties, 17)

[1991Mas] Maslenkov, S.B., Filin, S.A., Abramov, V.O., “Effect of Structural State and Alloying of Transition Metals on the Degree of Hardening of Ternary Solid Solutions Based on Nickel Monoaluminide”, *Russ. Metall.*, (1), 115-118 (1991) translated from *Izv. Akad. Nauk SSSR, Met.*, (1), 111-115 (1991) (Crystal Structure, Experimental, Mechanical Properties, 10)

[1992Bud] Budberg, P., Prince, A., “Al-Fe-Ni Ternary Phase Diagram Evaluation”, in *MSI Eureka*, Effenberg, G. (Ed.), MSI, Materials Science International Services GmbH, Stuttgart (1992), Document ID: 10.10205.1.9 (Crystal Structure, Phase Diagram, Phase Relations, Assessment, 37)

[1992Kai] Kainuma, R., Ishida, K., Nishizawa, T., “Thermoelastic Martensite and Shape Memory Effect in *B*2 Base Ni-Al-Fe Alloy with Enhanced Ductility”, *Metall. Trans. A*, **23A**(4), 1147-1153 (1992), doi:10.1007/BF02665046 (Mechanical Properties, Experimental, 24)

[1993Kat] Kattner, U.R. and Burton, B.P., “Al-Fe (Aluminum-Iron)”, in “*Phase Diagrams of Binary Iron Alloys*”, Okamoto, H. (Ed), ASM International, Materials Park, OH 44073-0002, 12-28 (1993) (Phase Diagram, Review, 99)

[1993Kha] Khadkikar, P.S., Locci, I.E., Vedula, K., Michal, G.M., "Transformation to Ni_5Al_3 in a 63.0 at.% Ni-Al Alloy", *Metall. Trans. A,* **24A**(1), 83-94 (1993), doi:10.1007/BF02669606 (Phase Diagram, Crystal Structure, Experimental, 28)

[1993Pov] Povarova, K.B., Filin, S.A., Maslenkov, S.B., "Phase Equilibria in the Ni-Al-Me (Me = Co, Fe, Mn, Cu) Systems in Vicinity of β-Phase at 900 and 1100°C", *Russ. Metall. (Engl. Transl.)*, (1), 156-169 (1993), translated from: *Izv. Akad. Nauk SSSR, Met.*, (1), 191-205 (1993). (Crystal Structure, Experimental, Phase Diagram, 19)

[1993Tan] Tanaka, M., Tsuda, K., Terauchi, M., Fujiwara, A., Tsai, A., Inoue, A., "Electron Diffraction and Electron Microscope Study on Decagonal Quasicrystals on Al-Ni-Fe Alloys", *J. Non-Cryst. Solids*, **153-154**, 98-102 (1993), doi:10.1016/0022-3093(93)90322-O (Crystal Structure, Experimental, 7)

[1993Zub] Zubkov, A.A., Emel'yanenko, L.P., Ul'yanov, V.I., "Enthalpy of Formation of β-Phase in Iron-Alloyed Nickel-Aluminum System", *Russ. Metall. (Engl. Transl.)*, (3), 35-38 (1993), translated from *Izv. Akad. Nauk SSSR, Met.*, (3), 39-42 (1993) (Experimental, Thermodynamics, 17)

[1994Bur] Burkhardt, U., Grin, J., Ellner, M., Peters, K., "Structure Refinement of the Iron-Aluminium Phase with the Approximate Composition Fe_2Al_5", *Acta Crystallogr., Sect. B*, **B50**, 313-316 (1994), doi:10.1107/S0108768193013989 (Crystal Structure, Experimental, *, 9)

[1994Dun] Duncan, A.J., Kaufman, M.J., Liu, C.T., Miller, M.K., "Site Occupation of Iron in Intermetallic NiAl", *Appl. Surface Sci.*, **76-77**(1-4), 155-159 (1994), doi:10.1016/0169-4332(94)90336-0 (Crystal Structure, Experimental, 17)

[1994Gho] Ghosh, G., Olson, G.B., Kinkus, T.J., Fine, M.E., "Phase Separation in Fe-Ni-Al and Fe-Ni-Al-Cr Alloys", in "*Solid Phas. Transform.*" Proc. Int. Conf. Solid-Solid Phase Transform. Inorg. Mater., 359-364 (1994) (Calculation, Thermodynamics, Experimental, #, 13)

[1994Gru] Grushko, B., Urban, K., "A Comparative Study of Decagonal Quasicrystalline Phase", *Philos. Mag. B*, **70B**(5), 1063-1075 (1994), doi:10.1080/01418639408240273 (Crystal Structure, Phase Relations, Experimental, 26)

[1994Jia] Jia, C.C., Ishida, K., Nishizawa, T., "Partition of Alloying Elements between γ (A1), γ\` (*L*1$_2$) and β (*B*2) Phases in Ni-Al Base Systems", *Metall. Mater. Trans. A*, **25A**, 473-485 (1994), doi:10.1007/BF02651589 (Crystal Structure, Experimental, Phase Diagram, #, 25)

[1994Lem] Lemmerz, U., Grushko, B., Freiburg, C., Jansen, M., "Study of Decagonal Quasicrystalline Phase Formation in the Al-Ni-Fe Alloy System", *Philos. Mag. Lett.*, **69**(3), 141-146 (1994), doi:10.1080/09500839408241583 (Crystal Structure, Experimental, 9)

[1994Rag] Raghavan, V., "The Al-Fe-Ni System", *J. Phase Equilib.*, **15**(4), 411-413 (1994), doi:10.1007/BF02647565 (Phase Diagram, Review, 14)

[1995Gaf] Gaffet, E., "Structural Investigation of Mechanically Alloyed $(NiAl)_{1-x}(M)_x$ (M = Fe, Zr) Nanocrystalline and Amorphous Phases", *NanoStruct. Mater.*, **5**(4), 393-409 (1995), doi:10.1016/0965-9773(95)00251-9 (Crystal Structure, Mechanical Properties, Experimental, 58)

[1995Wue] Wuerschum, R., Troev, T., Grushko, B., "Structural Free Volumes and Systematics of Positron Lifetimes in Quasicrystalline Decagonal and Adjacent Crystalline Phases of Al-Ni-Co, Al-Cu-Co, and Al-Ni-Fe Alloys", *Phys. Rev. B*, **52B**(9), 6411-6416 (1995), doi:10.1103/PhysRevB.52.6411 (Crystal Structure, Experimental, Phase Diagram, 37)

[1996Gru1] Grushko, B., Lemmerz, U., Fischer, K., Freiburg, C., "The Low-Temperature Instability of the Decagonal Phase in Al-Fe-Ni", *Phys. Status Solidi A*, **155A**, 17-30 (1996), doi:10.1002/pssa.2211550103 (Experimental, Phase Diagram, 29)

[1996Gru2] Grushko, B., Holland-Moritz, D., "High-Ni Al-Ni-Co Decagonal Phase", *Scr. Mater.*, **35**(10), 1141-1146 (1996), doi:10.1016/1359-6462(96)00281-3 (Experimental, Crystal Structure, 19)

[1996Pau] Paufler, P., Faber, J., Zahn, G., "X-Ray Single Crystal Diffraction Investigation on $Ni_{1+x}Al_{1-x}$", *Acta Crystallogr., Sect. A : Found. Crystallogr.*, **A52**, C319 (1996) (Crystal Structure, Experimental, Abstract, 3)

[1996Vik] Viklund, P., Häußermann, U., Lidin, S., "$NiAl_3$: a Structure Type of its Own?", *Acta Crystallogr., Sect. A: Found. Crystallogr.*, **A52**, C321 (1996), doi:10.1107/S0108767396086655 (Crystal Structure, Experimental, Abstract, 0)

[1996Yam] Yamamoto, A., "Crystallography of Quasiperiodic Crystals", *Acta Crystallogr., Sect. A: Found. Crystallogr.*, **A52**, 509-560 (1996), doi:10.1107/S0108767396000967 (Calculation, Crystal Structure, Review, 211)

[1996Zho] Zhongtao, Z., Yinyan, L., Qihua, Z., Zhengxin, L., Ruzhang, M., "Mössbauer Study of Precipitates in Rapidly Solidified Al-Fe-Ni Alloys", *Z. Metallkd.*, **87**(1), 40-44 (1996), doi:10.1515/ijmr-1996-870107 (Experimental, Electronic Structure, Mössbauer, Phase Configurations, 12)

[1997And] Anderson, I.M., "Alchemi Study of Site Distributions of 3*d*-Transition Metals in *B*2-Ordered Iron Aluminides", *Acta Mater.*, **45**(9), 3897-3909 (1997), doi:10.1016/S1359-6454(97)00042-6 (Calculation, Crystal Structure, Experimental, Theory, 26)

[1997Kai] Kainuma, R., Ikenoya, H., Ohnuma, I., Ishida, K., "Pseudo-Interface Formation and Diffusion Behaviour in the *B*2 Phase Region of NiAl-Base Diffusion Couples", *Def. Diffus. Forum*, **143-147**, 425-430 (1997), doi:10.4028/www.scientific.net/DDF.143-147.425 (Crystal Structure, Experimental, Phase Diagram, Physical Properties, 10)

[1997Pik] Pike, L.M., Chang, Y.A., Liu, C.T., "Solid-Solution Hardening and Softening by Fe Additions to NiAl", *Intermetallics*, **5**, 601-608 (1997), doi:10.1016/S0966-9795(97)00040-X (Crystal Structure, Mechanical Properties, Experimental, 18)

[1997Poh] Pohla, C., Ryder, P.L., "Crystalline and Quasicrystalline Phases in Rapidly Solidified Al-Ni Alloys", *Acta Mater.*, **45**, 2155-2166 (1997), doi:10.1016/S1359-6454(96)00317-5 (Crystal Structure, Experimental, 48)

[1997Sai] Saiton, K., Tsuda, K., Tanaka, M., "Structural Models for Decagonal Quasicrystals with Pentagonal Atom-Cluster Columns", *Philos. Mag. A*, **76A**(1), 135-150 (1997), doi:10.1080/01418619708209966 (Crystal Structure, Experimental, 14)

[1997Yam] Yamamoto, A., Weber, S., "Superstructure and Color Symmetry in Quasicrystals", *Phys. Rev. Lett.*, **79**(5), 861-864 (1997), doi:10.1103/PhysRevLett.79.861 (Crystal Structure, Experimental, 20)

[1998Akd] Akdeniz, M.V., Mekhrabon, A.O., "The Effect of Substitutional Impurities on the Evolution of Fe-Al Diffusion Layer", *Acta Mater.*, **46**(4), 1185-1192 (1998), doi:10.1016/S1359-6454(97)00318-2 (Calculation, Thermodynamics, 55)

[1998Gom] Goman'kov, V.I., Tret'yakova, S.M., Monastyrskaya, E.V., Fykin, L.E., "Structural Diagrams of Quasi Binary Alloys Ni_3Fe-Ni_3Al, Ni_3Mn-Ni_3Al, and Ni_3Mn-Ni_3Ga", *Russ. Metall.*, (6), 125-131 (1998), translated from *Izv. Akad. Nauk SSSR, Met.*, (6), 104-108 (1998) (Experimental, Phase Diagram, Phase Relations, #, 15)

[1998Ko] Ko, H.-S., Park, H.-S., Hong, K.-T., Lee, K.-S., Kaufman, M.J., "The Effects of the Point Defects on Precipitation in NiAlFe Alloys", *Scr. Mater.*, **39**(9), 1267-1272 (1998), doi:10.1016/S1359-6462(98)00297-8 (Experimental, Phase Diagram, 12)

[1998Sun] Sun, Z.Q., Yang, W.Y., Shen, L.Z., Huang, Y.D., Zhang, B.S., Yang, J.L., "Neutron Diffraction Study on Site Occupation of Substitution Elements at Sub Lattices in Fe-Al Intermetallics", *Mater. Sci. Eng. A*, **258A**, 69-74 (1998), doi:10.1016/S0921-5093(98)00919-8 (Crystal Structure, Experimental, Magnetic Properties, Mechanical Properties, 19)

[1999Dyb] Dybkov, V.I., "Physicochemical and Structural Investigations of Materials. Phase Formation at an Interface between Aluminium and an Iron-Nickel Alloy", *Powder Metall. Met. Ceram.*, **38**(11-12), 590-596 (1999), doi:10.1007/BF02676192, Translated from *Poroshkovaya Metallurgiya*, Nos. 11-12(410), 67-74 (1999) (Experimental, Mechanical Properties, Phase Diagram, #, 10)

[1999Hel] Helander, T., Agren, J., "Diffusion in the *B*2-*B.C.C.* Phase of the Al-Fe-Ni System - Application of a Phenomenological Model", *Acta Mater.*, **47**(11), 3291-3300 (1999), doi:10.1016/S1359-6454(99)00174-3 (Assessment, Calculation, Thermodynamics, Diffusion, #, 20)

[1999Hol] Holland-Moritz, D., Lu, I.-R., Wilde, G., Schroers, J., Grushko, B., "Melting Entropy of Al-Based Quasicrystals", *J. Non-Cryst. Solids*, **250-252**, 829-832 (1999), doi:10.1016/S0022-3093(99)00187-8 (Experimental, Thermodynamics, 17)

[1999Mek] Mekhrabov, A.O., Akdeniz, M.V., "Effect of Ternary Alloying Elements Addition on Atomic Ordering Characteristics of Fe-Al Intermetallics", *Acta Mater.*, **47**(7), 2067-2075 (1999), doi:10.1016/S1359-6454(99)00087-7 (Calculation, Theory, Thermodynamics, 63)

[2000Ama] Amancherla, S., Banerjee, R., Banerjee, S., Fraser, H. L., "Ordering in Ternary *B*2 Alloys", *Inter. J. Ref. Met. Hard Mater.*, **18**(4-5), 245-252 (2000), doi:10.1016/S0263-4368(00)00023-8 (Calculation, Experimental, Magnetic Properties, Phase Diagram, Thermodynamics, 23)

[2000Dro] Drobek, T., Heckl, W.M., "Scanning Probe Microscopy Studies of the Surface of Decagonal Quasicrystals in Ambient Conditions", *Mater. Sci. Eng. A*, **294A-296A**, 878-881 (2000), doi:10.1016/S0921-5093(00)01038-8 (Crystal Structure, Experimental, 16)

[2000Dyb] Dybkov, V.I., "Interaction of Iron-Nickel Alloys with Liquid Aluminium Part II. Formation of Intermetallics", *J. Mater. Sci.*, **35**, 1729-1736 (2000), doi:10.1023/A:1004724401682 (Experimental, Phase Diagram, #, 9)

[2000Fre] Frey, F., "Disorder Diffuse Scattering of Decagonal Quasicrystals", *Mater. Sci. Eng. A*, **294A-296A**, 178-185 (2000), doi:10.1016/S0921-5093(00)01234-X (Crystal Structure, Experimental, 15)

[2000Zei] Zeifert, B.H., Salmones, J., Hernandez, J.A., Reynoso, R., Nava, N., Reguera, E., Cabanas-Moreno, J.G., Aguilar-Rios, G., "X-Ray Diffraction and Mössbauer Characterization of Raney Fe-Ni Catalysts", *J. Radioanal. Nucl. Chem.,* **245**(3), 637-639 (2000), doi:10.1023/a:1006798302775 (Crystal Structure, Electronic Structure, Mössbauer, 10)

[2001Bre] Breuer, J., Gruen, A., Sommer, F., Mittemeijer, E.J., "Enthalpy of Formation of $B2$-$Fe_{1-x}Al_x$ and $B2$-$(Ni,Fe)_{1-x}Al_x$", *Metall. Mater. Trans. B*, **32B**, 913-918 (2001), doi:10.1007/s11663-001-0077-8 (Experimental, Thermodynamics, 18)

[2001Hir] Hiraga, K., Ohsuna, T, "The Structure of an Al-Ni-Fe Decagonal Quasicrystal Studied by High-Angle Annular Detector Dark-Field Transmission Electron Microscopy", *Mater. Trans., JIM*, **42**, 894-896 (2001), doi:10.2320/matertrans.42.894 (Crystal Structure, Experimental, Phase Diagram, 31)

[2001Qia] Qiang, J.-B., Wang, D.-H., Bao, C.-M., Wang, Y.-M., Xu, W.-P., Song, M.-L., Dong, Ch., "Formation Rule for Al-Based Ternary Quasi-Crystals: Example of Al-Ni-Fe Decagonal Phase", *J. Mater. Res.*, **16**(9), 2653-2660 (2001), doi:10.1557/JMR.2001.0364 (Crystal Structure, Experimental, Phase Diagram, Phase Relations, 31)

[2001Sur] Suryanarayana, C., "Mechanical Alloying and Milling", *Prog. Mater. Sci.*, **46**(1-2), 1-184 (2001), doi:10.1016/S0079-6425(99)00010-9 (Crystal Structure, Experimental, Kinetics, Phase Diagram, Review, Thermodynamics, 932)

[2001Tan] Tan, Y., Shinoda, T., Mishima, Y., Suzuki, T., "Stoichiometry Splitting of β Phase in Ni-Al-Mn, Ni-Al-Co and Ni-Al-Fe Ternary Systems", *Mater. Trans., JIM*, **42**(3), 464-470 (2001), doi:10.2320/matertrans.42.464 (Crystal Structure, Experimental, Mechanical Properties, Phase Diagram, Phase Relations, 16)

[2002Alb] Albiter, A., Bedolla, E., Perez, R., "Microstructure Characterization of the NiAl Intermetallic Compound with Fe, Ga and Mo Additions Obtained by Mechanical Alloying", *Mater. Sci. Eng. A*, **328A**, 80-86 (2002), doi:10.1016/S0921-5093(01)01664-1 (Crystal Structure, Mechanical Properties, Experimental, 14)

[2002Ban] Banerjee, R., Amancherla, S., Banerjee, S., Fraser, H.L., "Modeling of Site Occupancies in *B*2 FeAl and NiAl Alloys with Ternary Additions", *Acta Mater.*, **50**, 633-641 (2002), doi:10.1016/S1359-6454(01)00371-8 (Calculation, Crystal Structure, Experimental, Phase Diagram, 21)

[2002Bit] Bitterlich, H., Loeser, W., Schultz, L., "Reassessment of Al-Ni and Ni-Fe-Al Solidus Temperatures", *J. Phase Equilib.*, **23**(4), 301-304 (2002), doi:10.1361/105497102770331541 (Experimental, Phase Diagram, 18)

[2002Boz] Bozzolo, G. H., Khalil, J., Noebe, R. D., "Modeling of the Site Preference in Ternary *B*2-Ordered Ni-Al-Fe Alloys", *Comput. Mater. Sci.*, **24**(4), 457-480 (2002), doi:10.1016/S0927-0256(02)00153-2 (Calculation, Crystal Structure, 22)

[2002He] He, X., Han, J., Zhang, X., "Kinetic Parameters of the Thermal Explosion Reaction of Ni-Al-Fe System", *Key Eng. Mater.*, **217**, 51-54 (2002), doi:10.4028/www.scientific.net/KEM.217.51 (Experimental, Kinetics, 7)

[2002Hir] Hiraga, K., "The Structure of Quasicrystals Studied by Atomic-Scale Observations of Transmission Electron Microscopy", *Adv. Imag. Electr. Phys.*, **122**, 1-86 (2002), doi:10.1016/S1076-5670(02)80051-9 (Review, Crystal Structure, 85)

[2002Joa] Joardar, J., Pabi, S.K., Fecht, H.-J., Murty, B.C., "Stability of Nanocrystalline Disordered NiAl Synthesized by Mechanical Alloying", *Philos. Mag. Lett.*, **82**(9), 469-475 (2002), doi:10.1080/09500830210145336 (Experimental, Phase Relations, Kinetics, 16)

[2002Kim] Kim, S.H., Kim, M.C., Lee, J.H., Oh, M.H., Wee, D.M., "Microstructure Control in Two-Phase ($B2$ + $L1_2$) Ni-Al-Fe Alloys by Addition of Carbon", *Mater. Sci. Eng. A*, **329A-331A**, 668-674 (2002), doi:10.1016/S0921-5093(01)01603-3 (Experimental, Phase Diagram, Mechanical Properties, 20)

[2002Liu] Liu, C.T., Fu, C.L., Pike, L.M., Easton, D.S., "Magnetism-Induced Solid Solution Effects in Intermetallic", *Acta Mater.*, **50**, 3203-3210 (2002), doi:10.1016/S1359-6454(02)00136-2 (Calculation, Crystal Structure, Experimental, Mechanical Properties, 21)

[2002Mun] Munroe, P.R., George, M., Baker, I., Kennedy, F.E., "Microstructure, Mechanical Properties and Wear of Ni-Al-Fe Alloys", *Mater. Sci. Eng. A*, **325A**, 1-8 (2002), doi:10.1016/S0921-5093(01)01403-4 (Experimental, Mechanical Properties, Phase Diagram, 35)

[2002Pik] Pike, L.M., Anderson, I.M., Liu, C.T., Chang, Y.A., "Site Occupancies, Point Defect Concentrations, and Solid Solution Hardening in *B*2 (Ni, Fe)Al", *Acta Mater.*, **50**(15), 3859-3879 (2002), doi:10.1016/S1359-6454(02)00192-1 (Calculation, Crystal Structure, Experimental, Mechanical Properties, 38)

[2002Yok] Yokosawa, T., Saitoh, K., Tanaka, M., Tsai, A.P., "Structural Variations in Local Areas of an $Al_{70}Ni_{15}Fe_{15}$ Decagonal Quasicrystal and the Interpretation by the 1-nm Column-Pair Scheme", *J. Alloys Compd.*, **342**, 169-173 (2002), doi:10.1016/S0925-8388(02)00166-4 (Crystal Structure, Experimental, 10)

[2003Cer1] Cermak, J., Rothova, V., "Concentration Dependence of Ternary Interdiffusion Coefficients in Ni_3Al/Ni_3Al-X Couples with X=Cr, Fe, Nb and Ti", *Acta Mater.*, **51**(15), 4411-4421 (2003), doi:10.1016/S1359-6454(03)00276-3 (Electronic Structure, Experimental, Kinetics, Transport Phenomena, 15)

[2003Cer2] Cermak, J., Gazda, A., Rothova, V., "Interdiffusion in Ternary Ni_3Al/Ni_3Al-X Diffusion Couples with X = Cr, Fe, Nb and Ti", *Intermetallics*, **11**(9), 939-946 (2003), doi:10.1016/S0966-9795(03)00118-3 (Experimental, Kinetics, Transport Phenomena, 24)

[2003Doe] Doeblinger, M., Wittmann, R., Grushko, B., "Initial Stages of the Decomposition of the Decagonal Phase in the System Al-Ni-Fe", *J. Alloys Compd.*, **360**, 162-167 (2003), doi:10.1016/S0925-8388(03)00342-6 (Crystal Structure, Experimental, 17)

[2003Dsa] D´Santhoshini, B.A., Kaul, S.N., "Site Preference of Ternary Fe Addition in $Ni_{75}Al_{25}$", *J. Phys.: Condens. Matter*, **15**(29), 4903-4918 (2003), doi:10.1088/0953-8984/15/29/302 (Crystal Structure, Experimental, Phase Relations, 21)

[2003Su] Su, H.N., Nash, P., Liu, Z.K., "Enthalpies of Formation of Alloys in the Al-Ni-Fe System", *High Temperature Corrosion and Materials Chemistry,* Pennington (NJ): Electrochem. Soc., **4**, (2003) (Thermodynamics)

[2004Bud] Budberg, P., Prince, A., Cacciamani, G., Ferro, R., Grushko, B., Perrot, P., Schmid-Fetzer, R., "Al-Fe-Ni Ternary Phase Diagram Evaluation", in *MSI Eureka*, Effenberg, G. (Ed.), MSI, Materials Science International Services GmbH, Stuttgart (2004), Document ID: 10.10205.2.8 (Crystal Structure, Phase Diagram, Phase Relations, Assessment, 133)

[2004Cam] Cammarota, G.P., Casagrande, A., "Effect of Ternary Additions of Iron on Microstructure and Microhardness of the Intermetallic NiAl in Reactive Sintering", *J. Alloys Compd.*, **381**(1-2), 208-214 (2004), doi:10.1016/j.jallcom.2004.04.077 (Crystal Structure, Experimental, Mechanical Properties, Morphology, 17)

[2004Div] Divinski, S., Kang, Y.-S., Loeser, W., Herzig, Ch., "Ni and Fe Tracer Diffusion in the *B*2-Ordered $Ni_{40}Fe_{10}Al_{50}$ Ternary Alloy", *Intermetallics*, **12**(5), 511-518 (2004), doi:10.1016/j.intermet.2004.01.003 (Crystal Structure, Experimental, Kinetics, Transport Phenomena, 28)

[2004Fu] Fu, C.L., Liu, C.T., Wang, X.-L., Krcmar, M., Fernandez-Baca, J.A., "Magnetism-induced Solid Solution Softening in NiAl with Co, Fe, Mn, and Cr Solute Atoms: Theory and Experiment", *Intermetallics*, **12**(7-9), 911-919 (2004), doi:10.1016/j.intermet.2004.02.008 (Calculation, Crystal Structure, Electronic Structure, Experimental, Magnetic Properties, Mechanical Properties, 16)

[2004Gru] Grushko, B., Velikanova, T.Ya., "Stable and Metastable Quasicrystals in Al-Based Alloy System with Transition Metals", *J. Alloys Compd.*, **367**(1-2), 58-63 (2004), doi:10.1016/j.jallcom.2003.08.012 (Crystal Structure, Phase Diagram, Phase Relations, Review, 44)

[2004Her] Herzig, C., Divinski, S., "Essentials in Diffusion Behavior of Nickel- and Titanium-aluminides", *Intermetallics*, **12**(7-9), 993 (2004), doi:10.1016/j.intermet.2004.03.005 (Calculation, Crystal Structure, Kinetics, Transport Phenomena, 54)

[2004Him] Himuro, Y., Tanaka, Y., Kamiya, N., Ohnuma, I., Kainuma, R., Ishida, K., "Stability of Ordered $L1_2$ Phase in Ni_3Fe-Ni_3X (X:Si and Al) Pseudobinary Alloys", *Intermetallics*, **12**(6), 635-643 (2004), doi:10.1016/j.intermet.2004.03.008 (Crystal Structure, Electrical Properties, Experimental, Magnetic Properties, Morphology, Phase Diagram, Phase Relations, 19)

[2004Kau] Kaul, S.N., D´Santhoshini, B.A., "Magnetic Properties of $Ni_{75-x}Fe_xAl_{25}$ Alloys: Effect of Site Disorder", *J. Magn. Magn. Mater.*, **272-276**(1), 489-490 (2004), doi:10.1016/j.jmmm.2003.11.198 (Crystal Structure, Magnetic Properties, Review, 7)

[2004Maz] Maziarz, W., Dutkiewicz, J., Senderski, J., "Processing of Nanocrystalline FeAlX (X = Ni, Mn) Intermetallics Using a Mechanical Alloying and Hot Pressing Techniques", *J. Mater. Sci.*, **39**(16/17), 5425-5429 (2004), doi:10.1023/B:JMSC.0000039259.16153.fb (Experimental, Mechanical Properties, Morphology, Nanomaterials, Phase Relations, 7)

[2004Par1] Partyka, E., Kozubski, R., Pierron-Bohnes, V., "Atomic-jump Kinetics in Intermetallics with Varying Superstructure Stability - A Resistometric Study", *J. Alloys Compd.*, **378**(1-2), 308-311 (2004), doi:10.1016/j.jallcom.2003.10.079 (Crystal Structure, Experimental, Kinetics, Morphology, Phase Relations, 14)

[2004Par2] Parlinski, K., Jochym, P.T., Leupold, O., Chumakov, A.I., Rüffer, R., Schober, H., Jianu, A., Dutkiewicz, J., Maziarz, W., "Local Modes of Fe and Co Atoms in NiAl Intermetallics", *Phys. Rev. B: Condens. Matter*, **70**(22), 224304 (2004), doi:10.1103/PhysRevB.70.224304 (Calculation, Crystal Structure, Electronic Structure, 20)

[2004Sch] Schneider, A., Sauthoff, G., "Iron Aluminium Alloys with Strengthening Carbides and Intermetallic Phases for High-Temperature Applications", *Steel Res. Int.*, **75**(1), 55-61 (2004), doi:10.1002/srin.200405927 (Mechanical Properties, Review, 74)

[2005Fuk] Fuks, D., Dorfman, S., Liubich, V., Kutsenko, L., Mehrer, H., "Site Preference Occupation of Ni and V in Fe_3Al-based Alloys", *Mater. Sci. Forum*, **480-481**, 81-88 (2005), doi:10.4028/www.scientific.net/MSF.480-481.81 (Calculation, Crystal Structure, 26)

[2005Him] Himuro, Y., Tanaka, Y., Ohnuma, I., Kainuma, R., Ishida, K., "Phase Equilibria and γ`-$L1_2$ Phase Stability in the Ni-rich Portion of Ni-Fe-Si and Ni-Fe-Al Systems", *Intermetallics*, **13**(6), 620-630 (2005), doi:10.1016/j.intermet.2004.10.009 (Electrical Properties, Experimental, Phase Diagram, Phase Relations, 19)

[2005Rag] Raghavan, V., "Al-Fe-Ni (Aluminum-Iron-Nickel)", *J. Phase Equilib. Diffus.*, **26**(1), 70-71 (2005), doi:10.1007/s11669-005-0064-x (Phase Diagram, Phase Relations, Review, 18)

[2005Set] Setyawan, A.D., Louzguine, D.V., Sasamori, K., Kimura, H.M., Ranganathan, S., Inoue, A., "Phase Composition and Transformation Behavior of Readily Solidified Al-Ni-Fe Alloys in α-Al-Decagonal Phase Region", *J. Alloys Compd.*, **399**(1-2), 132-138 (2005), doi:10.1016/j.jallcom.2005.03.020 (Experimental, Mechanical Properties, Phase Relations, 25)

[2005Str] Strutz, A., Fuks, D., Kiv, A., "The Influence of Doping by Transition Metal Elements on the Vacancy Formation Energy in Fe-Al *B*2 Phase", *J. Phase Equilib. Diffus.*, **26**(5), 529-533 (2005), doi:10.1007/s11669-005-0046-z (Crystal Structure, Experimental, Morphology, Phase Relations, Thermodynamics, 30)

[2006Ako] Akopov, F.Kh., Gabuniya, V.M., Mamniashvili, G.I., Martkoplishvili, G.S., Oniashvili, G.Sh., Peikrishvili, A.V., Chikhradze, N.M., Chkhartishvili, I.V., "Shock-Wave Compacting of a Fe-Ni-Al Powder Mixture and Its Study", *Phys. Met. Metallogr. (Engl. Transl.)*, **102**(5), 541-544 (2006), Translated from *Fiz. Metal. Metallov.*, **102**(5), 578-581 (2006) (Crystal Structure, Experimental, Mechanical Properties, Morphology, 8)

[2006Ben] Bencze, L., Markus, T., Dash, S., Raj, D.D., Kath, D., Oates, W.A., Loser, W., Hilpert, K., "Thermodynamic Properties of *B*2-AlFeNi Alloys. Part I: Investigation by Knudsen Effusion Mass Spectrometry", *Metall. Mater. Trans. A*, **37**(11), 3171-3181 (2006), doi:10.1007/BF02586151 (Experimental, Thermodynamics, 20)

[2006Div] Divinski, S., Hisker, F., Löser, W., Södervall, U., Herzig, C., "Ni Radiotracer Diffusion in *B*2 Ordered NiFeAl Alloys", *Intermetallics*, **14**(4), 308-314 (2006) (Crystal Structure, Experimental, Kinetics, Phase Diagram, Phase Relations, Transport Phenomena, 26)

[2006Don] Dong, C., Qiang, J.B., Wang, Y.M., Jiang, N., Wu, J., Thiel, P., "Cluster-based Composition Rule for Stable Ternary Quasicrystals in Al-(Cu, Pd, Ni)-TM Systems", *Philos. Mag.*, **86**(3-5), 263-274 (2006), doi:10.1080/14786430500281308 (Crystal Structure, Phase Relations, Review, 41)

[2006Dru] Druzhkov, A.P., Perminov, D.A., Arbuzov, V.L., "Effects of Intermetallic Nanoparticles on the Evolution of Vacancy Defects in Electron-Irradiated Fe-Ni-Al Material", *J. Phys.: Condens. Matter*, **18**(2), 365-377 (2006) (Crystal Structure, Experimental, Morphology, Nanomaterials, 44)

[2006Ele] Eleno, L., Frisk, K., Schneider, A., "Assessment of the Fe-Ni-Al System", *Intermetallics*, **14**, 1276-1290 (2006), doi:10.1016/j.intermet.2005.11.021 (Assessment, Crystal Structure, Kinetics, Phase Diagram, Phase Relations, Review, Thermodynamics, *, #, 136)

[2006Fuk] Fuks, D., Strutz, A., Kiv, A., "Influence of Alloying on the Thermodynamic Stability of FeAl *B*2 Phase", *Intermetallics*, **14**, 1245-1251 (2006) (Calculation, Electronic Structure, Mechanical Properties, Thermodynamics, 34)

[2006Gar] Garcia-Galan, S., Aramburo-Perez, G., Gonzalez-Rivera, C., Herrera, R., Juarez-Islas, J.A., "The Effect of Hot Rolling on Room Temperature Ductility of a NiAl Intermetallic Compound", *Mater. Sci. Forum*, **509**, 69-74 (2006) (Experimental, Mechanical Properties, Morphology, Phase Diagram, Phase Relations, 7)

[2006Hu] Hu, R., Nash, P., "Review: Experimental Enthalpies of Formation of Compounds in Al-Ni-X Systems", *J. Mater. Sci.*, **41**(3), 631-641 (2006), doi:10.1007/s10853-006-6479-x (Experimental, Review, Thermodynamics, 101)

[2006Jia] Jianga, C., Gleeson, B., “Site Preference of Transition Metal Elements in Ni_3Al”, *Scr. Mater.*, **55**(5), 433-436 (2006), doi:10.1016/j.scriptamat.2006.05.016 (Calculation, Crystal Structure, Thermodynamics, 37)

[2006Kau] Kaul, S.N., Annie D´Santhoshini, B., Abhyankar, A.C., Barquin, L.F., Henry, P., “Thermoelastic Martensitic Transformation in Ferromagnetic Ni-Fe-Al Alloys: Effect of Site Disorder”, *Appl. Phys. Lett.*, **89**(9), 093119-093119-3 (2006), doi:10.1063/1.2337271 (Crystal Structure, Electrical Properties, Experimental, Magnetic Properties, Phase Relations, 17)

[2006Nii] Niikura, A., Kawahara, A., Kimura, G., Doko, T., “Recrystallization Behaviour in Twin-Roll Continuous Cast Al-Fe-Ni Alloy”, *Mater. Sci. Forum*, **519-521**, 1635-1640 (2006) (Experimental, Mechanical Properties, Morphology, 15)

[2006Oik] Oikawa, K., Tanaka, Y., Sutou, Y., Omori, T., Luo, F., Kainuma, R., Ishida, K., “Effects of Aging and Co Addition on Martensitic and Magnetic Transitions in Ni-Al-Fe β-based Shape Memory Alloys”, *ISIJ Int.*, **46**(9), 1287-1291 (2006) (Crystal Structure, Magnetic Properties, Morphology, Phase Diagram, Phase Relations, 29)

[2006Rag] Raghavan, V., “Al-Fe-Ni (Aluminum-Iron-Nickel)”, *J. Phase Equilib. Diffus.*, **27**(5), 489-490 (2006), doi:10.1007/BF02736451 (Crystal Structure, Phase Diagram, Phase Relations, Review, 14)

[2006Tsa] Tsau, C.-H., Yeh, J.-W., Jang, J.S.-C., “Mechanical Behaviors of Chromium- or Niobium-Modified $Ni_{47.5}Al_{25}Fe_{27.5}$ Alloy at Elevated Temperature”, *Metall. Mater. Trans. A*, **37**(1), 175-184 (2006) (Crystal Structure, Experimental, Mechanical Properties, Morphology, 10)

[2006Wan] Wang, Y.L., Jones, I.P., Smallman, R.E., “The Effects of Iron on the Creep Properties of NiAl”, *Intermetallics*, **14**(7), 800-810 (2006) (Experimental, Mechanical Properties, Phase Diagram, Phase Relations, 41)

[2007Abe] Abe, H., Yamamoto, K., Matsuoka, S., Matsuo, Y., “Atomic Short-range Order in an $Al_{72}Ni_{18}Fe_{10}$ Decagonal Quasicrystal Studied by Anomalous X-ray Scattering”, *J. Phys.: Condens. Matter*, **19**(46), 466201 (2007), doi:10.1088/0953-8984/19/46/466201 (Calculation, Crystal Structure, Electronic Structure, Experimental, Theory, 26)

[2007Chu1] Chumak, I., Richter, K.W., Fries, S.G., Ipser, H., “Experimental Phase Diagram Investigations in the Ni- Rich Part of Al-Fe-Ni and Comparison with Calculated Phase Equilibria”, *J. Phase Equilib. Diffus.*, **28**(5), 417-421 (2007), doi:10.1007/s11669-007-9157-z (Crystal Structure, Experimental, Phase Diagram, Phase Relations, *, #, 15)

[2007Chu2] Chumak, I., Richter, K.W., Ipser, H., “The Fe-Ni-Al Phase Diagram in the Al-Rich (>50 at.% Al) Corner”, *Intermetallics*, **15**(11), 1416-1424 (2007), doi:10.1016/j.intermet.2007.04.012 (Crystal Structure, Experimental, Phase Diagram, Phase Relations, *, #, 23)

[2007Col] Colas, D., Fraczkiewicz, A., Louchet, F., “Nickel-Induced Strengthening of Boron-Doped FeAl (*B*2) Alloys”, *Intermetallics*, **15**(1), 85-92 (2007) (Crystal Structure, Experimental, Mechanical Properties, Morphology, 59)

[2007Gon] Gonzalez-Rodriguez, J.G., Gonzalez-Castaneda, M., Cuellar-Hernández, M., Dominguez-Patino, G., Rosas, G., “Effect of Ni on the Corrosion Behavior of Fe-Al Intermetallics in Simulated Human Body Fluid”, *J. Solid State Electrochem.*, **12**(6), 707-713 (2007), doi:10.1007/s10008-007-0413-2 (Electrochemistry, Experimental, Interface Phenomena, Kinetics, Morphology, 24)

[2007Gru] Grushko, B., Velikanova, T., “Formation of Quasiperiodic and Related Periodic Intermetallics in Alloy Systems of Aluminum with Transition Metals”, *Calphad*, **31**(2), 217-232 (2007), doi:10.1016/j.calphad.2006.12.002 (Crystal Structure, Experimental, Phase Diagram, Phase Relations, 71)

[2007Joa] Joardar, J., Pabi, S.K., Murty, B.S., “Milling Criteria for the Synthesis of Nanocrystalline NiAl by Mechanical Alloying”, *J. Alloys Compd.*, **429**(1-2), 204-210 (2007) (Crystal Structure, Experimental, Nanomaterials, 43)

[2007Liu] Liu, C.T., Fu, C.L., Chisholm, M.F., Thompson, J.R., Krcmar, M., Wang, X.-L., “Magnetism and Solid Solution Effects in NiAl (40% Al) Alloys”, *Prog. Mater. Sci.*, **52**(2-3), 352-370 (2007) (Calculation, Crystal Structure, Experimental, Magnetic Properties, Mechanical Properties, 39)

[2007Mun] Munoz-Morris, M.A., Morris, D.G., “Microstructure and Mechanical Behaviour of a Fe-Ni-Al Alloy”, *Mater. Sci. Eng. A*, **444**(1-2), 236-241 (2007), doi:10.1016/j.msea.2006.08.082 (Experimental, Mechanical Properties, Morphology, Phase Relations, 15)

[2007Orb] Orban, R.L., Lucaci, M., “Ni_3Al-Fe-Cr Alloy Processed by Combined Mechanical Alloying - Reactive Synthesis”, *Mater. Sci. Forum*, **534-536**, 1581-1584 (2007), doi:10.4028/www.scientific.net/MSF.534-536.1 (Experimental, Mechanical Properties, Morphology, Phase Relations, 5)

[2007Ste] Stein, F., Palm, M., “Re-Determination of Transition Temperatures in the Fe-Al System by Differential Thermal Analysis”, *Int. J. Mater. Res.* (*Z. Metallkd.*), **98**(7), 580-588 (2007), doi:10.3139/146.101512 (Experimental, Phase Diagram, Phase Relations, *, 59)

[2007Uwa] Uwakweh, O.N.C., Liu, C.T., “Mössbauer Effect Measurement Evidence for Magnetic Transition in Ordered Fe-Doped NiAl”, *Intermetallics*, **15**(2), 98-102 (2007) (Crystal Structure, Electronic Structure, Experimental, Magnetic Properties, Morphology, Physical Properties, 13)

[2007Yas] Yasuda, H.Y., Kase, T., Minamiguchi, S., Yokoyama, A., Umakoshi, Y., Bronsveld, P.M., de Hosson, J.Th.M., “Effect of Third Elements on Pseudoelastic Behavior in Fe$_3$Al Single Crystals”, *Mater. Sci. Forum*, **561-565**, 391-394 (2007), doi:10.4028/www.scientific.net/MSF.561-565.3 (Crystal Structure, Experimental, Mechanical Properties, Morphology, Phase Relations, 11)

[2007Zha1] Zhang, L., Du, Y., “Thermodynamic Description of the Al-Fe-Ni System over the Whole Composition and Temperature Ranges: Modeling Coupled with Key Experiment”, *Calphad*, **31**, 529-540 (2007), doi:10.1016/j.calphad.2007.03.003 (Calculation, Experimental, Phase Diagram, Phase Relations, Thermodynamics, 67)

[2007Zha2] Zhang, W., Qian, Z., Tang, J., Zhao, L., Sui, Y., Wang, H., Li, Y., Su, W., Zhang, M., Liu, Z., Liu, G., Wu, G., “Superparamagnetic Behaviour in Melt-spun Ni$_2$FeAl Ribbons”, *J. Phys.: Condens. Matter*, **19**(9), 096214 (2007), doi:10.1088/0953-8984/19/9/096214 (Experimental, Magnetic Properties, Phase Relations, 22)

[2008Chu] Chumak, I., Richter, K.W., Ipser, H., “Isothermal Sections in the (Fe, Ni)-Rich Part of the Fe-Ni-Al Phase Diagram”, *J. Phase Equilib. Diffus.*, **29**(4), 300-304 (2008), doi:10.1007/s11669-008-9319-7 (Experimental, Morphology, Phase Diagram, Phase Relations, *, 11)

[2008Gil] Gille, P., Bauer, B., “Single Crystal Growth of Al$_{13}$Co$_4$ and Al$_{13}$Fe$_4$ from Al-Rich Solutions by the Czochralski Method”, *Cryst. Res. Technol.*, **43**(11), 1161-1167 (2008), doi:10.1002/crat.200800340 (Crystal Structure, Experimental, Morphology, Phase Relations, Theory, 17)

[2008Han] Hanc, A., Frackowiak, J.E., Pajak, L., Dercz, G., “Point Defect Structure and ^{57}Fe Hyperfine Parameters of Fe-Al Powders Doped with Ni, Cu and Cr Additions”, *Chem. Met. Alloys*, **1**(2), 128-132 (2008), doi:10.30970/cma1.0042 (Crystal Structure, Experimental, Phase Relations, 12)

[2008Kim1] Kim, H.-G., Myung, W.-N., Sumiyama, K., Suzuki, K., “Chemical Leaching of Non-Equilibrium Al(Ni-Fe) Alloy Powders Produced by Rod Milling”, *J. Alloys Compd.*, **456**, 72-78 (2008) (Crystal Structure, Experimental, Morphology, Phase Relations, 22)

[2008Kim2] Kim, H.-G., Sumiyama, K., Suzuki, K., “Formation and Chemical Leaching of Non-Equilibrium Al$_{0.6}$(Fe$_{75}$Ni$_{25}$)$_{0.4}$ Alloy Powders by Rod Milling”, *J. Alloys Compd.*, **465**(1-2), 113-118 (2008), doi:10.1016/j.jallcom.2007.10.077 (Crystal Structure, Experimental, Magnetic Properties, Morphology, 26)

[2008Kim3] Kim, H.-G., Sumiyama, K., Suzuki, K., “Magnetic Properties of a Non-Equilibrium Al(Fe-Ni) Alloy Powder by Rod-Milling and Chemical Leaching”, *J. Magn. Magn. Mater.*, **320**(12), 1822-1826 (2008), doi:10.1016/j.jmmm.2008.02.109 (Crystal Structure, Experimental, Kinetics, Magnetic Properties, Morphology, Phase Relations, 23)

[2008Muk] Mukhopadhyay, P.K., Kaul, S.N., “Dynamic Elastic Properties and Magnetic Susceptibility across the Austenite-martensite Transformation in Site-disordered Ferromagnetic Ni-Fe-Al Alloy”, *Appl. Phys. Lett.*, **92**(10), 101924 (2008), doi:10.1063/1.2896649 (Crystal Structure, Experimental, Magnetic Properties, Mechanical Properties, Phase Relations, 12)

[2008Mun] Munoz-Morris, M., Calderon, N., Morris, D., “Coarsening Kinetics of Metastable Nanoprecipitates in a Fe-Ni-Al Alloy”, *J. Mater. Sci.*, **43**(10), 3674-3682 (2008), doi:10.1007/s10853-008-2589-y (Experimental, Kinetics, Morphology, Nanomaterials, Phase Diagram, Phase Relations, 20)

[2008Rag] Raghavan, V., “Al-Fe-Ni (Aluminum-Iron-Nickel)”, *J. Phase Equilib. Diffus.*, **29**(2), 180-184 (2008), doi:10.1007/s11669-008-9258-3 (Phase Diagram, Phase Relations, Review, 12)

[2008Zha] Zhang, L., Du, Y., Xu, H., Tang, C., Chen, H., Zhang, W., “Phase Equilibria of the Al-Fe-Ni System at 850°C and 627°C”, *J. Alloys Compd.*, **454**, 129-135 (2008), doi:10.1016/j.jallcom.2006.12.042 (Crystal Structure, Experimental, Morphology, Phase Diagram, Phase Relations, *, #, 38)

[2009Cas] Castaneda, I.E., Gonzalez-Rodriguez, J.G., Colin, J., Neri-Flores, M.A., “Electrochemical Behavior of Ni-Al-Fe Alloys in Simulated Human Body Solution”, *J. Solid State Electrochem.*, **14**(7), 1145-1152 (2009), doi:10.1007/s10008-009-0941-z (Electrochemistry, Experimental, Kinetics, Morphology, 25)

[2009Laz] Lazar, P., Podloucky, R., “Ductility and Magnetism: An *ab-initio* Study of NiAl-Fe and NiAl-Mn Alloys”, *Intermetallics*, **17**(9), 675-679 (2009), doi:10.1016/j.intermet.2009.01.012 (Calculation, Electronic Structure, Magnetic Properties, Mechanical Properties, Phase Relations)

[2009Rag1] Raghavan, V., “Al-Fe-Ni (Aluminum-Iron-Nickel)”, *J. Phase Equilib. Diffus.*, **30**(1), 85-88 (2009), doi:10.1007/s11669-008-9452-3 (Crystal Structure, Phase Diagram, Phase Relations, Review, 17)

[2009Rag2] Raghavan, V., “Al-Fe-Ni (Aluminum-Iron-Nickel)”, *J. Phase Equilib. Diffus.*, **30**(4), 375-377 (2009) (Phase Diagram, Phase Relations, Review, 18)

[2009Vou] Vourlias, G., Pistofidis, N., Pavlidou, E., Stergioudis, G., “Reinforcement of Al-Fe-Ni Alloys with the *in situ* Formation of Composite Materials”, *J. Alloys Compd.*, **483**(1-2), 178-181 (2009), doi:10.1016/j.jallcom.2008.07.173 (Crystal Structure, Experimental, Morphology, Nanomaterials, Phase Relations, 9)

[2009Yas] Yasuda, H.Y., Fukushima, K., Koizumi, Yu., Minamino, Yo., Umakoshi, Yu., “Magneto-mechanical and Pseudoelastic Damping of Fe-Al Based Single Crystals”, *ISIJ Int.*, **49**(10), 1630-1635 (2009), doi:10.2355/isijinternational.49.1630 (Crystal Structure, Experimental, Kinetics, Magnetic Properties, Physical Properties, 21)

[2009Zha] Zhang, L., Wang, J., Du, Y., Hu, R., Nash, P., Lu, X.-G., Jiang, C., “Thermodynamic Properties of the Al-Fe-Ni System Acquired *via* a Hybrid Approach Combining Calorimetry, First-principles and CALPHAD”, *Acta Mater.*, **57**(18), 5324-5341 (2009), doi:10.1016/j.actamat.2009.07.031 (Calculation, Electronic Structure, Experimental, Phase Diagram, Thermodynamics, *, #, 73)

[2010Cac] Cacciamani, G., Dinsdale, A., Palumbo, M., Pasturel, A., “The Fe-Ni System: Thermodynamic Modelling Assisted by Atomistic Calculations”, *Intermetallics*, **18**(6), 1148-1162 (2010), doi:10.1016/j.intermet.2010.02.026 (Assessment, Calculation, Phase Diagram, Phase Relations, Thermodynamics, 151)

[2010Chu] Chumak, I., Richter, K.W., Ehrenberg, H., “Redetermination of Iron Dialuminide, $FeAl_2$”, *Acta Crystallogr., Sect. C*, **C66**, i87-i88 (2010), doi:10.1107/S0108270110033202 (Experimental, Crystal Structure, 10)

[2010Leu] Leute, V., “The Influence of the Ideal Mixing Entropy on Concentration Profiles and Diffusion Paths in Ternary Systems”, *J. Phys. Chem. Solids*, **71**(12), 1768-1773 (2010), doi:10.1016/j.jpcs.2010.08.018 (Calculation, Kinetics, Phase Relations, Thermodynamics, Transport Phenomena, 17)

[2010Ond] Onderka, B., Sypien, A., Wierzbicka-Miernik, A., Czeppe, T., Zabdyr, L. A., “Specific Heat Capacities of Some Ternary Aluminides”, *J. Phase Equilib. Diffus.*, **32**(1), 39-41 (2010), doi:10.1007/s11669-010-9822-5 (Experimental, Morphology, Thermodynamics, 4)

[2010Pal] Palacio, D., Vallderruten, J., Zamora, L., Perez Alcazar, G., Tabares, J., “Effect of Ni on the Lattice Parameter and the Magnetic Hyperfine Field in $(Fe_{70}Al_{30})_{100-x}Ni_x$ Alloys”, *Hyperfine Interact.*, **195**(1), 241-247 (2010), doi:10.1007/s10751-009-0125-3 (Crystal Structure, Electronic Structure, Experimental, Magnetic Properties, Phase Relations, 17)

[2010Pan] Panova, G., Zemlyanov, M., Parshin, P., Shikov, A., Brand, R., “Low-energy Lattice Excitations in the Decagonal Al-Ni-Fe and Icosahedral Al-Cu-Fe Quasicrystals and the (Al,Si)-Cu-Fe Cubic Phase”, *Phys. Solid State*, **52**(4), 771-775 (2010), doi:10.1134/S1063783410040165, Translated from *Fiz. Tverdogo Tela*, **52**(4), 718-722 (2010) (Crystal Structure, Electronic Structure, Experimental, Thermodynamics, 22)

[2010Pop] Popcevic, P., Smontara, A., Ivkov, J., Wencka, M., Komelj, M., Jeglic, P., Vrtnik, S., Bobnar, M., Jaglicic, Z., Bauer, B., Gille, P., Borrmann, H., Burkhardt, U., Grin, Yu., Dolinsek, J., “Anisotropic Physical Properties of the $Al_{13}Fe_4$ Complex Intermetallic and its Ternary Derivative $Al_{13}(Fe,Ni)_4$”, *Phys. Rev. B: Condens. Matter*, **81**(18), 184203 (2010), doi:10.1103/PhysRevB.81.184203 (Crystal Structure, Electrical Properties, Experimental, Magnetic Properties, Morphology, Physical Properties, Thermodynamics, Transport Phenomena, 42)

[2010Rag] Raghavan, V., “Al-Fe-Ni (Aluminum-Iron-Nickel)”, *J. Phase Equilib. Diffus.*, **31**(5), 455-458 (2010), doi:10.1007/s11669-010-9745-1 (Crystal Structure, Phase Diagram, Phase Relations, Review, 19)

[2010Rzy] Rzyman, K., Gachon, J.-C., “Formation Enthalpy of $AlNi_3$-Based Alloys with Iron Additions by Calorimetric Solution and Direct Reaction Methods”, *Arch. Metall. Mater.*, **55**(4), 1021-1028 (2010), doi:10.2478/v10172-010-0004-6 (Experimental, Kinetics, Phase Relations, Thermodynamics, 24)

[2010Sag] Sagaradze, V.V., Shabashov, V.A., Litvinov, A.V., Koloskov, V.M., Parkhomenko, V.D., “Radiation-Induced Dissolution of Ni_3M Intermetallic Particles (M = Ti, Al, Zr) in Displacement Cascades in Fe-Ni-M Alloys Irradiated by Neutrons at 340 K”, *Phys. Met. Metallogr.*, **109**(5), 475-482 (2010), doi:10.1134/S0031918X1005008X, Translated from *Fiz. Met. Metalloved.*, **109**(5), 511-519 (2010) (Crystal Structure, Electronic Structure, Experimental, Kinetics, Mechanical Properties, Phase Relations, 22)

[2010Sch] Schober, M., Lerchbacher, Ch., Eidenberger, E., Staron, P., Clemens, H., Leitner, H., "Precipitation Behavior of Intermetallic NiAl Particles in Fe-6 at.%Al-4 at.%Ni Analyzed by SANS and 3DAP", *Intermetallics*, **18**(8), 1553-1559 (2010), doi:10.1016/j.intermet.2010.04.007 (Crystal Structure, Experimental, Kinetics, Mechanical Properties, Phase Relations, 40)

[2010Sha] Shabashov, V.A., Sagaradze, V.V., Litvinov, A.V., Kozlov, K.A., "Effect of the Rate of Cold Plastic Deformation on the Kinetics of Mechanical Alloying of the Fe-35Ni-5Al Alloy", *Phys. Met. Metallogr.*, **109**(5), 483-491 (2010), doi:10.1134/S0031918X10050091, Translated from *Fiz. Met. Metalloved*, **109**(5), 520-528 (2010) (Crystal Structure, Electronic Structure, Experimental, Kinetics, Magnetic Properties, Mechanical Properties, Morphology, 22)

[2010Sor] Soriano-Vargas, O., Saucedo-Munoz, M.L., Lopez-Hirata, V.M., Paniagua-Mercado, A.Ma., "Coarsening of β′ Precipitates in an Isothermally-Aged Fe_{75}-Ni_{10}-Al_{15} Alloy", *Mater. Trans.*, **51**(3), 442-446 (2010), doi:10.2320/matertrans.M2009332 (Crystal Structure, Experimental, Kinetics, Morphology, 17)

[2010Ste] Stein, F., Vogel, S.C., Eumann, M., Palm, M., "Determination of the Crystal Structure of the ε Phase in the Fe-Al System by High-Temperature Neutron Diffraction", *Intermetallics*, **18**(1), 150-156 (2010), doi:10.1016/j.intermet.2009.07.006 (Crystal Structure, Experimental, Morphology, Phase Relations, 40)

[2010Zha] Zhang, L., Du, Y., Steinbach, I., Chen, Q., Huang, B., "Diffusivities of an Al-Fe-Ni Melt and Their Effects on the Microstructure During Solidification", *Acta Mater.*, **58**(10), 3664-3675 (2010), doi:10.1016/j.actamat.2010.03.002 (Calculation, Interface Phenomena, Morphology, Phase Relations, Transport Phenomena, 60)

[2011Che] Chen, P.-H., Tang, T., Long, Y., "Effects of 3d Transition Metal Elements in the *B*2-FeAl Structure", *Metall. Mater. Trans. A*, **43**(2), 757-762 (2011), doi:10.1007/s11661-011-0893-7 (Calculation, Crystal Structure, Mechanical Properties, 24)

[2011Del] Deloudi, S., Fleischer, F., Steurer, W., "Unifying Cluster-based Structure Models of Decagonal Al-Co-Ni, Al-Co-Cu and Al-Fe-Ni", *Acta Crystallogr., Sect. B*, **67**(1), 1-17 (2011), doi:10.1107/S0108768110040942 (Calculation, Crystal Structure, Electronic Structure, 31)

[2011Du] Du, Y., Liu, S., Zhang, L., Xu, H., Zhao, D., Wang, A., Zhou, L., "An Overview on Phase Equilibria and Thermodynamic Modeling in Multicomponent Al Alloys: Focusing on the Al-Cu-Fe-Mg-Mn-Ni-Si-Zn System", *Calphad*, **35**(3), 427-445 (2011), doi:10.1016/j.calphad.2011.06.007 (Calculation, Phase Diagram, Review, Thermodynamics, 143)

[2011Dum] Duman, N., Mekhrabov, A.O., Akdeniz, M.V., "Kinetics of Nanoscale Precipitation in Ni-Fe-Al Alloys: A Magnetic Monitoring Approach", *J. Alloys Compd.*, **509**(24), 6781-6786 (2011), doi:10.1016/j.jallcom.2011.03.167 (Experimental, Kinetics, Magnetic Properties, Morphology, Nanomaterials, Phase Relations, 22)

[2011Kas] Kastlunger, G., "First-principles Study of the Fe-rich $Fe_xNi_yAl_{1-x-y}$ Alloy System", *Diploma Thesis, Universität Wien*, 1-109 (2011) (Calculation, Crystal Structure, Electronic Structure, Phase Diagram, Phase Relations, Thermodynamics, 77)

[2011Oku] Okumura, H., Uemura, K., "Effects of Rotation Speed on Microstructure and Transition Temperatures in Ni-Fe-Al Melt-spun Ribbons", *Intermetallics*, **19**(12), 1996-2001 (2011), doi:10.1016/j.intermet.2011.06.015 (Crystal Structure, Experimental, Mechanical Properties, Morphology, Phase Relations, 39)

[2011Sha] Shabashov, V.A., Sagaradze, V.V., Litvinov, A.V., "The Effect of the Cold Plastic Deformation Rate on Intermetallics Dissolution Intensity in Austenitic Fe-Ni-Me (Me = Ti, Al, Zr, Si) Alloys", *Mater. Sci. Eng. A*, **528**(21), 6393-6400 (2011) (Experimental, Phase Relations, 26)

[2011Tav] Tavoosi, M., Karimzadeh, F., Enayati, M. H., Joo, S.-H., Kim, H. S., "Amorphous Phase Formation in $Al_{80}Fe_{10}M_{10}$ (M = Ni, Ti, and V) Ternary Systems by Mechanical Alloying", *J. Mater. Sci.*, **46**(23), 7633-7638 (2011), doi:10.1007/s10853-011-5741-z (Amorphous, Calculation, Experimental, Phase Relations, Thermodynamics, 21)

[2011Zho] Zhou, Z.C., Gu, S.Y., Wen, C.E., "Phase Transformation in Oil-quenched Ni-21.2Al-20Fe Alloy", *J. Alloys Compd.*, **509**(5), 1644-1647 (2011), doi:10.1016/j.jallcom.2010.11.096 (Experimental, Phase Relations, Physical Properties, 16)

[2012Ada] Adabavazeh, Z., Karimzadeh, F., Enayati, M.H., "Thermodynamic Analysis of $(Ni, Fe)_3Al$ Formation by Mechanical Alloying", *J. Chem. Thermodyn.*, **54**, 406-411 (2012), doi:10.1016/j.jct.2012.05.027 (Amorphous, Experimental, Nanomaterials, Phase Relations, Thermodynamics, 25)

[2012Dum] Duman, N., Mekhrabov, A.O., Akdeniz, M.V., "Microalloying Effects on the Microstructure and Kinetics of Nanoscale Precipitation in Ni-Al-Fe Alloy", *Intermetallics*, **23**, 217-227 (2012), doi:10.1016/j.intermet.2012.01.002 (Crystal Structure, Experimental, Kinetics, Magnetic Properties, Mechanical Properties, Morphology, Nanomaterials, Phase Relations, 40)

[2012Hua] Huang, J., Sun, J., Xing, H., Wen, Y.F., “Magnetism-induced Ductility in NiAl Intermetallic Alloys with Fe Additions: Theory and Experiment”, *J. Alloys Compd.*, **519**, 101-105 (2012), doi:10.1016/j.jallcom.2011.12.101 (Crystal Structure, Experimental, Magnetic Properties, Mechanical Properties, Phase Relations, 34)

[2012Ma] Ma, J., Yang, J., Zhang, X., Bi, Q., Fu, L., Kang, Yo., Liu, W., “Combustion Synthesis and Characterization of Bulk Nanostructured $Ni_{50}Al_{17}Fe_{33}$ Alloy”, *Int. J. Mater. Res. (Z. Metallkd.)*, **103**(07), 866-869 (2012), doi:10.3139/146.110709 (Experimental, Mechanical Properties, Morphology, Nanomaterials, 22)

[2012Niu] Niu, X., Wang, L., “Effect of Transition-metal Substitution on Electronic and Mechanical Properties of Fe_3Al: First-principles Calculations”, *Comput. Mater. Sci.*, **53**(1), 128-132 (2012), doi:10.1016/j.commatsci.2011.09.015 (Calculation, Crystal Structure, Electronic Structure, Mechanical Properties, Thermodynamics, 31)

[2012Shr] Shreder, E. I., Svyazhin, A. D., Fomina, K. A., “Optical Properties of Fe_2NiAl and Fe_2MnAl Heusler Alloys”, *Phys. Met. Metallogr.*, **113**(2), 146-152 (2012), doi:10.1134/S0031918X12020135, Translated from *Fiz. Met. Metalloved.*, **113**(2), 155-161 (2012) (Calculation, Crystal Structure, Electronic Structure, Experimental, Optical Properties, 20)

[2012Yil] Yildirim, M., Vedat, A.M., Mekhrabov, A.O., “Effect of Ternary Alloying Elements Addition on the Order-Disorder Transformation Temperatures of *B*2-Type Ordered Fe-Al-X Intermetallics”, *Metall. Mater. Trans. A*, **43**(6), 1809-1816 (2012), doi:10.1007/s11661-011-1059-3 (Crystal Structure, Experimental, Morphology, Phase Relations, 35)

[2013Had] Hadef, F., Otmani, A., Djekoun, A., Greneche, J. M., “Investigation of Mechanosynthesized $Fe_{50}Ni_{40}Al_{10}$ Powders”, *J. Magn. Magn. Mater.*, **343**, 214-220 (2013), doi:10.1016/j.jmmm.2013.04.074 (Crystal Structure, Experimental, Kinetics, Morphology, 80)

[2013Lep] Lepikhin, S.V., Stepanova, N.N., “Investigation of the Ni_3Al-Fe Alloys by Resistivity Measurements and Differential Thermal Analysis”, *Russ. J. Non-Ferrous Metals*, **54**(6), 475-479 (2013), doi:10.3103/S1067821213060151, Translated from *Izv. VUZ. Tsvetn. Metall.*, (5), 53-58 (2013) (Electrical Properties, Experimental, Morphology, Phase Relations, Physical Properties, Review, 15)

[2013Tav] Tavoosi, M., Karimzadeh, F., Enayati, M. H., “Formation and Characterization of Amorphous-nanocrystalline $Al_{80}Fe_{10}M_{10}$ [M = Fe, Nb, Ti, Ni, $(Ni_{0.5}Ti_{0.5})$] Alloys”, *J. Alloys Compd.*, **551**, 584-590 (2013), doi:10.1016/j.jallcom.2012.11.038 (Amorphous, Experimental, Morphology, Nanomaterials, Phase Relations, 30)

[2013Yas] Yasuda, H.Y., Fukushima, K., Kouzai, K., Edahiro, T., “Effect of Ni Doping on Strength and Damping Capacity of Fe-Al Alloys”, *ISIJ Int.*, **53**(4), 704-708 (2013), doi:10.2355/isijinternational.53.704 (Crystal Structure, Experimental, Interface Phenomena, Kinetics, Magnetic Properties, Mechanical Properties, Morphology, Phase Diagram, 15)

[2014Bas] Bashev, V.F., Sukhova, O.V., Ustinova, K.V., “Phase Constitution of Al-Ni-Fe Alloys in a Compositional Range of Decagonal Quasicrystals Formation”, *Build. Mater. Sci. Machinebuild. Starodub Readings*, (74), 3-7 (2014) (Crystal Structure, Experimental, Morphology, 11)

[2016Dah] Dahmane, F., Mogulkoc, Y., Doumi, B., Tadjer, A., Khenata, R., Bin Omran, S., Rai, D. P., Murtaza, G., Varshney, D., “Structural, Electronic and Magnetic Properties of Fe_2-Based Full Heusler Alloys: A First Principle Study”, *J. Magn. Magn. Mater.*, **407**, 167-174 (2016), doi:10.1016/j.jmmm.2016.01.074 (Calculation, Crystal Structure, Electronic Structure, Magnetic Properties, Thermodynamics, 47)

[2016Li] Li, X., Scherf, A., Heilmaier, M., Stein, F., “The Al-Rich Part of the Fe-Al Phase Diagram”, *J. Phase Equilib. Diffus.*, **37**, 162-173 (2016), doi:10.1007/s11669-015-0446-7 (Crystal Structure, Experimental, Phase Diagram, Phase Relations, 38)

[2016Wan] Wang, Y., Cacciamani, G., “Thermodynamic Modeling of the Al-Cr-Ni System over the Entire Composition and Temperature Range”, *J. Alloys Compd.*, **688**, 422-435 (2016), doi:10.1016/j.jallcom.2016.07.130 (Calculation, Phase Diagram, Phase Relations, Thermodynamics)

[2017Fer] Ferreira-Palma, C., Contreras-Piedras, E., Cayetano-Castro, N., Saucedo-Munoz, M.L., Lopez-Hirata, V.M., González-Velázquez, J.L., Dorantes-Rosales, H.J., “Effect of Temperature and Composition on NiAl Precipitation and Morphology in Fe-Ni-Al Alloys”, *Metall. Mater. Trans. A*, **48**(11), 5285-5293 (2017), doi:10.1007/s11661-017-4309-1 (Experimental, Interface Phenomena, Mechanical Properties, Morphology, Phase Relations, 52)

[2017Wan] Wang, J., Du, Y., Tao, X., Ouyang, Y., Zhang, L., Chen, Q., Engström, A., "First-Principles Generated Mechanical Property Database for Multi-Component Al Alloys: Focusing on Al-Rich Corner", *J. Min. Metall. B*, **53**(1), 1-7 (2017) (Calculation, Crystal Structure, Mechanical Properties, Thermodynamics, 45)

[2017Zhe] Zheng, Y., Wang, F., Ai, T., Li, C., "Structural, Elastic and Electronic Properties of *B*2-Type Modified by Ternary Additions FeAl-Based Intermetallics: First-Principles Study", *J. Alloys Compd.*, **710**, 581-588 (2017), doi:10.1016/j.jallcom.2017.03.308 (Calculation, Crystal Structure, Electronic Structure, Mechanical Properties, Thermodynamics, 40)

[2018Wei] Wei, X.P., Zhou, Y.H., "First-principles and Monte Carlo Studies of the Fe_2NiZ Compounds on Exchange Interactions and Curie Temperatures", *Intermetallics*, **94**, 283-289 (2018), doi:10.1016/j.intermet.2017.10.006 (Calculation, Crystal Structure, Electronic Structure, Magnetic Properties, Phase Relations, Thermodynamics, 45)

[2018Wen] Wen, Z., Hou, H., Tian, J., Zhao, Y., Li, H., Han, P., "First-principles Investigation of Martensitic Transformation and Magnetic Properties of Ni_2XAl (X= Cr, Fe, Co) Heusler Compounds", *Intermetallics*, **92**, 15-19 (2018), doi:10.1016/j.intermet.2017.09.007 (Calculation, Crystal Structure, Electronic Structure, Magnetic Properties, Thermodynamics, 29)

[2019Bia] Bian, Z., Dai, S., Wu, L., Chen, Z., Wang, M., Chen, D., Wang, H., "Thermal Stability of Al-Fe-Ni Alloy at High Temperatures", *J. Mater. Res. Technol.*, **8**(3), 2538-2548 (2019), doi:10.1016/j.jmrt.2019.01.028 (Experimental, Mechanical Properties, Morphology, 47)

[2019Gan] Ganai, Z.S., Yousuf, S., Batoo, K.M., Khan, M., Gupta, D.C., "Half-metallicity and Onsite Hubbard Interaction on *d*-electronic States: A Case Study of Fe_2NiZ (Z = Al, Ga, Si, Ge) Heusler Systems", *Philos. Mag.*, **99**(12), 1551-1562 (2019), doi:10.1080/14786435.2019.1587184 (Calculation, Crystal Structure, Electronic Structure, Magnetic Properties, Physical Properties, Thermodynamics, 29)

[2019Lip] Lippmann, S., Kemsies, R.H., Schick, M., Milkereit, B., Kessler, O., Rettenmayr, M., Hack, K., "Synthesis of Pure Intermetallic Phases on the Example of the Ternary Phase τ_1 in the System Al-Fe-Ni", *Intermetallics*, **105**, 107-112 (2019), doi:10.1016/j.intermet.2018.11.016 (Experimental, Morphology, Phase Diagram, Phase Relations, Thermodynamics, 36)

[2019Ran] Rank, M., Franke, P., Seifert, H.J., "Thermodynamic Investigations in the Al-Fe System: Thermodynamic Modeling Using Calphad", *Int. J. Mater. Res.*, **110**(5), 406-421 (2019), doi:10.3139/146.111765 (Calculation, Crystal Structure, Phase Diagram, Thermodynamics, 108)

[2019Yas] Yasuda, H.Y., Edahiro, T., Takeoka, N., Yoshimoto, T., Mizuno, M., Cho, K., "Effects of NiAl Precipitate Microstructure, Loading Axis and Temperature on Deformation Behavior of Fe-Al-Ni Single Crystals", *Intermetallics*, **115**, 106627 (2019), doi:10.1016/j.intermet.2019.106627 (Calculation, Crystal Structure, Electronic Structure, Experimental, Mechanical Properties, Morphology, Phase Relations, 47)

[2020Ben] Benhizia, N.E., Zaoui, Y., Amari, S., Beldi, L., Bouhafs, B., "Theoretical Study of Structural, Electronic, Dynamic and Thermodynamic Properties of Ni_2FeAl and Ni_2CoAl Alloys", *Comput. Condens. Matter*, **24**, e00480 (2020), doi:10.1016/j.cocom.2020.e00480 (Calculation, Crystal Structure, Electronic Structure, Magnetic Properties, Thermodynamics, 44)

[2021Liu] Liu, Y., Zhang, L., Cui, S., Li, W., "Effects of Transition Metal (Cr, Mn, Mo, Ni, Ti, and V) Doping on the Mechanical, Electronic and Thermal Properties of Fe_3Al", *Vacuum*, **185**, 110030 (2021), doi:10.1016/j.vacuum.2020.110030 (Calculation, Crystal Structure, Electronic Structure, Mechanical Properties, Transport Phenomena)

[2021Mly] Mlynarek, K., Czeppe, T., Babilas, R., "Structural Characterization of Rapidly Solidified $Al_{71}Ni_{24}Fe_5$ Alloy", *Arch. Foundry Eng.*, **21**(3), 90-95 (2021), doi:10.24425/afe.2021.138670 (Crystal Structure, Experimental, Morphology, 28)

[2022Ste] Stein, F., "Al-Fe Binary Phase Diagram Evaluation", in *MSI Eureka*, Watson, A. (Ed.), MSI, Materials Science International Services GmbH, Stuttgart (2022), Document ID: 20.10236.2.7 (2022), doi:10.7121/msi-eureka-20.10236.2.7 (Crystal Structure, Phase Diagram, Phase Relations, Assessment, 311)

Table 1: Recent Investigations of the Al-Fe-Ni System

Reference	Experimental Technique	Temperature/ Composition/Phase Range Studied
[2002Bit]	Electron probe microanalysis (EPMA), energy-dispersive X-ray spectroscopy (EDX), high-temperature differential thermal analysis (DTA)	Ni_xAl_{100-x} ($45 < x < 47$) and $Fe_yNi_{50-y}Al_{50}$ ($0 < y < 50$), 1259-1681°C. Solidus determination
[2002Pik]	X-Rays diffraction (XRD), Vickers hardness measurements, transmission electron microscope (TEM), EDX, channeling enhanced microanalysis	40 to 52 at.% Al, samples quenched from 700°C and 1000°C. Atomic site occupancy in the (Fe,Ni)Al domain
[2002Yok]	Scanning transmission electron microscopy	$Fe_{15}Ni_{15}Al_{70}$, prepared with a single roller melt-spinning apparatus (τ_3 phase). Crystal structure of decagonal phase
[2003Dsa]	XRD, SEM, EDX, inductively coupled plasma optical emission spectroscopy	As-cast, annealed, and rapidly quenched $Fe_xNi_{75}Al_{25-x}$ (x = 0, 5, 10, 20) samples. Site preference occupancy for Fe in Ni_3Al.
[2004Him]	Light optical microscopy (LOM), TEM, EPMA, XRD, differential scanning calorimetry (DSC), vibrating sample magnetometry, electrical resistivity measurements	$FeNi_3$-Ni_3Al section at 2.5-20 at.% Al, (γFe, Ni) and Ni_3(Fe,Al) boundaries, Curie temperature
[2004Par1]	Isochronal quasi-residual resistometry	Long-range ordering kinetics in $Fe_xNi_{75}Al_{25-x}$ (x = 2, 3, 5, 10, 15) (at.%)
[2005Fuk]	Calculations using linear-muffin-tin-orbital method for the coherent potential approximation	Site preference occupancy for Ni in Fe_3Al
[2005Him]	LOM, EDX, EPMA, TEM, electrical resistivity measurements	Partial isothermal sections at 900°C, 1100°C and 1300°C. Phase boundaries between (γFe, Ni), Ni_3(Fe,Al), (Fe,Ni)Al. Solvus temperatures for (Fe,Ni)Al. Vertical section at 30 at.% Ni.
[2006Ben]	Knudsen-effusion mass spectrometry	$Fe_xNi_{50-x}Al_{50}$ (x = 8, 16, 25, 34, 42), $Fe_xNi_{55-x}Al_{45}$ (x = 9, 18, 27.5, 37, 46), alloys with atomic ratio of Fe:Ni = 1/1 at 30, 35, 40, 52 at.% Al between 907°C and 1235°C. Activities of components and excess thermodynamic properties
[2006Kau]	Magnetization measurements, electrical resistivity measurements, neutron diffraction	$Fe_5Ni_{70}Al_{25}$, $Fe_{10}Ni_{65}Al_{25}$, $Fe_{20}Ni_{50}Al_{25}$ (at.%). Thermoelastic martensitic transformation and site disorder
[2006Oik]	DSC, TEM-EDX, SEM-EDX	Tie-lines between (γFe, Ni) and (Fe,Ni)Al at 1200°C
[2007Abe]	XRD, anomalous X-ray scattering experiments, Monte Carlo simulations	$Fe_{10}Ni_{18}Al_{72}$ (τ_2) (at.%). Short-range order in decagonal quasicrystal
[2007Chu1]	XRD, DTA, EPMA, wavelength dispersive spectroscopy (WDS)	$FeNi_3$-Ni_3Al section, lattice parameters of Ni_3(Fe,Al) at 450°C, partial isothermal section at 1000°C
[2007Chu2]	XRD, DTA, EPMA, WDS	Partial isothermal section at 850°C and isopleths at 60, 67, 75, 80 at.% Al. Temperatures of invariant reactions, partial liquidus surface. Crystal structure of $FeNiAl_9$ and Fe_3NiAl_{10}.
[2007Zha1]	DTA Thermodynamic assessment using the CALPHAD method	Phase transformations temperatures Isothermal and vertical sections, temperatures of invariant reactions, liquidus surface, thermodynamic properties

Reference	Experimental Technique	Temperature/ Composition/Phase Range Studied
[2008Chu]	XRD, EPMA, WDS	Partial isothermal sections at 900°C, 1000°C, 1100°C
[2008Zha]	XRD, SEM-EDX, EPMA	Partial isothermal section at 850°C, 627°C
[2009Zha]	High-temperature reaction calorimeter First-principles calculations Thermodynamic assessment using the CALPHAD method	Fe_3NiAl_{10}, $FeNiAl_9$. Enthalpy of formation. Fe_3NiAl_{10}, $FeNiAl_9$, $Ni_3(Fe,Al)$. Enthalpy of formation. Isothermal and vertical sections, temperatures of invariant reactions, liquidus surface, thermodynamic properties
[2010Ond]	DSC	$Fe_{10}Ni_{50}Al_{40}$, $Fe_{30}Ni_{30}Al_{40}$, $Fe_{50}Ni_{10}Al_{40}$ (at.%). Specific heat at 27-327°C
[2010Pan]	Pulse adiabatic calorimetry	$Fe_{4.7}Ni_{24.0}Al_{71.3}$ (at.%) (τ_1). Specific heat at 4.2-40 K
[2010Rzy]	Solution calorimetry, direct reaction calorimetry	(γFe, Ni), $Ni_3(Fe,Al)$. Formation enthalpy
[2011Del]	XRD	$Ni_5Fe_{22}Al_{73}$ (at.%) (τ_1), single crystals
[2012Yil]	EDS, SEM, XRD, DSC	$Fe_{50}Ni_{0.01}Al_{49.9}$ (at.%). Temperature of order-disorder transformation
[2013Lep]	Electrical resistivity measurements, DTA	$Fe_{75}Ni_xAl_{25-x}$ ($x = 3, 5, 7$), $Fe_{73}Ni_xAl_{27-x}$ ($x = 1, 2$), $Fe_{71}Ni_xAl_{29-x}$ ($x = 4, 8$) in at.%. Temperatures of phases transformations involving (γFe, Ni), $Ni_3(Fe,Al)$, (Fe,Ni)Al.
[2014Bas]	LOM, XRD, SEM, EDS	$Fe_{15.5}Ni_{14.5}Al_{70}$, $Fe_5Ni_{24}Al_{71}$ (at.%) slowly cooled samples. Phase relations involving Fe_3NiAl_{10}, τ_1
[2017Fer]	Diffusion couples, XRD, SEM, EDS, Vickers hardness measurements	49.99-78.12 at.% Fe, 22.46-9.13 at.% Ni, 27.55-12.75 at.% Al. Phase relations involving (Fe,Ni)Al
[2019Lip]	SEM, EDS, XRD, DSC	$Fe_8Ni_{12}Al_{82}$, $Fe_{2.5}Ni_{13.5}Al_{84}$ (mass%). Liquidus and solidus temperatures. Specific heat capacity of $FeNiAl_9$

Table 2: Crystallographic Data of Solid Phases

Phase/ Temperature Range (°C)	Pearson Symbol/ Space Group/ Prototype	Lattice Parameters (pm)	References/Comments
(Al) < 660.452	$cF4$ $Fm\overline{3}m$ Cu	$a = 404.96$	pure Al at 25°C [Mas2] solubility for Fe (the Al-Fe system): 0.023 at.% [2019Ran] solubility for Ni (the Al-Ni system): 0.3 at.% [2016Wan]
($\alpha\delta$Fe) < 1540	$cI2$ $Fm\overline{3}m$ W		Strukturbericht designation: $A2$ solubility for Al (the Al-Fe system): 45.0 at.% [1993Kat, 2007Ste] solubility for Ni (the Fe-Ni system): 6.4 at.% [2010Cac] ferromagnetic below 770°C
αFe < 912		$a = 286.65$	at 25°C [Mas2]
δFe 1538 - 1394		$a = 293.15$	[Mas2]

Phase/ Temperature Range (°C)	Pearson Symbol/ Space Group/ Prototype	Lattice Parameters (pm)	References/Comments
(γFe, Ni) < 1514	*cF*4 $Fm\bar{3}m$ Cu		solubility for Al (the Al-Fe system): 1.35 at.% [1993Kat] solubility for Al (the Al-Ni system): 21 at.% [2016Wan] complete mutual solubility between Ni and Fe [2010Cac] ferromagnetic below 605°C [2010Cac]
γFe 1394 - 912		a = 364.67	pure Fe at 915°C [V-C2, Mas2]
(Ni) < 1455		a = 352.40	pure Ni nickel at 25°C [V-C2, Mas2]
Fe_3Al < 545	*cF*16 $Fm\bar{3}m$ BiF_3		sometimes named α_1 or γ_1 phase Strukturbericht designation: $D0_3$ ~24 to ~34 at.% Al at 400°C [1993Kat]
		a = 579.30	at 23.1 at.% Al, water-quenched from 250°C [1958Tay]
		a = 578.86	at 35.0 at.% Al, water-quenched from 250°C [1958Tay]
		a = 579.98	at 25 at.% Al and 3 at.% Ni [1998Sun] Extends less than 10 at.% Ni into the ternary [1940Bra2]
Fe_5Al_8 1231 - 1095	*cI*52 $I\bar{4}3m$ Cu_5Zn_8		Sometimes named Fe_2Al_3 Strukturbericht designation: $D8_2$ 56.0 to 64.5 at.% Al [2016Li]
		a = 897.57 ± 0.02	at 1120°C and 59.4 at.% Al [2010Ste]
$FeAl_2$ < 1146	*aP*19 $P\bar{1}$ $FeAl_2$		Sometimes named ζ phase 64.7 to 66.7 at.% Al
		a = 487.45 b = 645.45 c = 873.61 α = 87.930° β = 74.396° γ = 83.062°	at 66.4 at.% Al [2010Chu] dissolves 2.5 at.% Ni at 1050°C [1982Kha]
Fe_2Al_5 1159 - ~331	*oC*24 *Cmcm* Fe_2Al_5		Sometimes named η phase 68.4 to 72.5 at.% Al
		a = 765.59 ± 0.08 b = 641.54 ± 0.06 c = 421.84 ± 0.04	at 71.5 at.% Al [1994Bur] dissolves 2 at.% Ni at 1050°C [1982Kha, 1993Pov]
Fe_4Al_{13} < 1150	*mC*102 *C*2/*m* Fe_4Al_{13}		Referred to as $FeAl_3$ in old literature before ~1995 Sometimes named θ phase 74.5 to 76.9 at.% Al
		a = 1548.8 ± 0.1 b = 808.66 ± 0.05 c = 1247.69 ± 0.08 β =(107.669±0.004)°	single crystal grown by Czochralski technique [2008Gil, 2010Pop] dissolves up to 12 at.% Ni at 800°C [1996Gru1]
$NiAl_3$ < 850	*oP*16 *Pnma* $NiAl_3$	a = 661.3 ± 0.1 b = 736.7 ± 0.1 c = 481.1 ± 0.1	[1996Vik] dissolves 4 at.% Fe [1982Kha]

Phase/ Temperature Range (°C)	Pearson Symbol/ Space Group/ Prototype	Lattice Parameters (pm)	References/Comments
Ni_2Al_3	$hP5$		59.2 to 64.0 at.% Al [2016Wan]
< 1127	$P\bar{3}m1$	a = 404.2 ± 0.1	at 57 at.% Al [1982Ell]
	Ni_2Al_3	c = 491.5 ± 0.1	
		a = 405.3 ± 0.1	at 63 at.% Al [1982Ell]
		c = 490.2 ± 0.1	
			dissolves up to 10 at.% Fe at 1050°C [1982Kha]
Ni_3Al_4	$cI112$	a = 1140.7 ± 0.1	at 56 at.% Al [1989Ell]
< 702	$Ia\bar{3}d$		Ordered variant of the defect CsCl structure
	Ni_3Ga_4		
Ni_5Al_3	$oC16$	a = 753	at 37.5 at.% Al [1993Kha]
< 641	$Cmmm$	b = 661	
	Pt_5Ag_3	c = 376	
(Fe,Ni)Al	$cP2$		Sometimes named β phase
< 1680	$Pm\bar{3}m$		Strukturbericht designation: $B2$
	CsCl		23.5 to ~53 at.% Al (the Al-Fe system) [2007Ste]
			29 to 41 at.% Al (the Al-Ni system) [2016Wan]
FeAl < 1318		a = 289.53-290.90	at 36.2 to 50.0 at.% Al, water-quenched from 250°C [1958Tay]
NiAl		a = 288.72 ± 0.02	at 50 at.% Al [1996Pau]
< 1680		a = 287.98 ± 0.02	at 46 at.% Al [1996Pau]
			Variation of the lattice parameters for different ternary compositions is shown Figs. 1a and 1b
$Ni_3(Fe,Al)$	$cP4$		Sometimes named γ phase
< 1369	$Pm\bar{3}m$		Strukturbericht designation: $L1_2$
	$AuCu_3$		Complete solid solution between Ni_3Al and $FeNi_3$ at T < 500°C
Ni_3Al		a = 356.95 ± 0.03	at 25 at.% Al (the Al-Ni system) [1991Ell]
< 1369		a = 356.80 ± 0.02 to 357.64 ± 0.01	at 24-27 at.% Al (the Al-Ni system) [1991Ell]
			23 to 28 at.% Al at 1000°C (the Al-Ni system) [2016Wan]
			dissolves up to 15 at.% Fe at 1000°C [1986Bra]
$FeNi_3$ < 514		a = 355.25 ± 0.01	at 75 at.% Ni (the Fe-Ni system) [1967Ng]
			55.5-83 at.% Ni (the Fe-Ni system) 353°C [2010Cac]
*$FeNiAl_9$	m*	a = 624.06 ± 0.01	Single crystals extracted from the $Fe_{6.3}Ni_{11.7}Al_{82}$ (at.%) alloy [2007Chu2]
< 809	$P2_1/c$	b = 629.93 ± 0.01	
	Co_2Al_9	c = 859.92 ± 0.01	
		β =(95.129 ± 0.001)°	7.3-12.7 at.% Ni, 10.4-4.7 at.% Fe at 620°C [1943Sch], confirmed by [1999Dyb, 2000Dyb]
*Fe_3NiAl_{10}	h*	a = 770.937 ± 0.005	Single crystals extracted from the $Fe_{18.5}Ni_{10}Al_{71.5}$ (at.%) alloy [2007Chu2]
<~ 1116	$P6_3/mmc$	c = 767.947 ± 0.008	
	Co_2Al_5		
		a = 767.81 ± 0.01 to 771.31 ± 0.01	23-15.7 at.% Fe, 5.6-12.9 at.% Ni, 71.4-71.4 at.% Al (at.%) [1982Kha]
		c = 771.31 ± 0.01 to 764.32 ± 0.01	18-23.8 at.% Fe, 10-4.6 at.% Ni, 70-71.7 at.% Al (at.%) at 1050°C [1982Kha]

Phase/ Temperature Range (°C)	Pearson Symbol/ Space Group/ Prototype	Lattice Parameters (pm)	References/Comments
*τ_1, ($Al_{71}Ni_{24}Fe_5$) ~850 - 930	- $P\overline{10}_2m$ -	 $a_D \approx 378$ $c_D \approx 411$ $a_D = 373.3$ $c_D = 407.3$	Decagonal phase with small solubility range $Fe_{4.9}Ni_{23.4}Al_{71.7}$-$Fe_5Ni_{24}Al_{71}$ (at.%) [1994Lem, 1996Gru1, 2008Chu]. Denoted as q by [2008Chu]. [1994Lem] Diameter of the decagonal section ~3200 pm [2001Hir] Metastable in the Al-Ni binary system at 24-30 at.% Ni [1997Poh]
τ_2 (m)	- $P10_5/mmc$ -	 $a_D = 712$ $c_D = 409$	Metastable in the ternary system Space group is according to [1997Sai] $Fe_{9.83}Ni_{19.34}Al_{70.83}$ at.% [2001Qia] Exists at 13-10 at.% Fe, 17-20 at.% Ni, 70 at.% Al [1993Tan, 1997Sai, 2001Qia] Metastable in the Al-Fe binary at 86 at.% Al [1986Fun]
τ_3 (m)	- $P\overline{10}m2$ -	 $a_D = 713.4$ $c_D = 818$	Metastable in the ternary system Space group is according to [1993Tan, 1997Sai] $Fe_{14.5}Ni_{13}Al_{72.5}$ at.% [2001Qia] Exists at 13-20 at.% Fe, 17-10 at.% Ni, 70 at.% Al [1993Tan, 1997Sai, 2001Qia]

Table 3: Invariant Equilibria

Reaction	T (°C)	Type	Phase	Composition (at.%)		
				Al	Fe	Ni
(Fe,Ni)Al $\rightleftharpoons$ (αδFe)	~ 1520	c_1, critical	–	–	–	–
L, (αδFe), (Fe,Ni)Al, (γFe, Ni)	1400-1500	C_1, critical	–	–	–	–
L + Ni_3(Fe,Al) $\rightleftharpoons$ (γFe, Ni) + (Fe,Ni)Al	1366	U_1	L Ni_3(Fe,Al) (γFe, Ni) (Fe,Ni)Al	22 24.5 20 28	5 0.5 4 0.5	73 75 76 71.5
L $\rightleftharpoons$ (γFe, Ni) + (Fe,Ni)Al*	~1350	e_2, min	L	~20	~12	~68
L + Fe_5Al_8 $\rightleftharpoons$ (Fe,Ni)Al + Fe_2Al_5	1137	U_2	L	70	22	8
L + (Fe,Ni)Al + Fe_2Al_5 $\rightleftharpoons$ Fe_3NiAl_{10}	1121	P_1	L	72	17	11
L + Fe_2Al_5 $\rightleftharpoons$ Fe_4Al_{13} + Fe_3NiAl_{10}	~1116	U_3	L	74.5	17.5	8
Fe_5Al_8 + Fe_2Al_5 $\rightleftharpoons$ (Fe,Ni)Al + $FeAl_2$	> 1095	U_4	–	–	–	–
L + (Fe,Ni)Al $\rightleftharpoons$ Ni_2Al_3 + Fe_3NiAl_{10}	1069	U_5	L	73	10	17
L + Fe_3NiAl_{10} $\rightleftharpoons$ Fe_4Al_{13} + Ni_2Al_3	1030	U_6	L	75	8	17
L + Fe_4Al_{13} + Ni_2Al_3 $\rightleftharpoons$ τ_1	930	P_2	L	79	4	17
L + τ_1 + Ni_2Al_3 $\rightleftharpoons$ $NiAl_3$	864	P_3	L	82	2.8	15.2
L + τ_1 $\rightleftharpoons$ Fe_4Al_{13} + $NiAl_3$	860	U_7	L	83	3	14
τ_1 $\rightleftharpoons$ Fe_4Al_{13} + Ni_2Al_3 + $NiAl_3$	~850	E_1	τ_1 Fe_4Al_{13} Ni_2Al_3 $NiAl_3$	71.7 75 61 75	4.9 14 2 2	23.4 11 37 23

Reaction	T (°C)	Type	Phase	Composition (at.%)		
				Al	Fe	Ni
L + Fe_4Al_{13} + $NiAl_3$ $\rightleftharpoons$ $FeNiAl_9$	809	P_4	L	~87	~2	~11
L + Fe_4Al_{13} $\rightleftharpoons$ (Al) + $FeNiAl_9$	650	U_8	L	~98	~1	~1
L $\rightleftharpoons$ (Al) + $NiAl_3$ + $FeNiAl_9$	638	E_2	L	~96.5	~0.3	~3.2

* according to the thermodynamic assessment of [2009Zha]

Table 4: Thermodynamic Data of Reaction or Transformation

Reaction or Transformation	T (°C)	Quantity per Reaction (J, mol, K)	Comments
xFe(α)+y(Ni)+zAl(liq) $\rightarrow Fe_xNi_yAl_z$((Fe,Ni)Al)	800	$\Delta_f H = -42780 \pm 280$	$x = 0.42$, $y = 0.08$, $z = 0.50$
		$\Delta_f H = -48730 \pm 220$	$x = 0.34$, $y = 0.16$, $z = 0.50$
		$\Delta_f H = -54420 \pm 240$	$x = 0.25$, $y = 0.25$, $z = 0.50$
		$\Delta_f H = -60860 \pm 230$	$x = 0.16$, $y = 0.34$, $z = 0.50$
		$\Delta_f H = -65740 \pm 270$	$x = 0.08$, $y = 0.42$, $z = 0.50$
		$\Delta_f H = -39870 \pm 230$	$x = 0.46$, $y = 0.09$, $z = 0.45$
		$\Delta_f H = -45740 \pm 050$	$x = 0.37$, $y = 0.18$, $z = 0.45$
		$\Delta_f H = -51920 \pm 140$	$x = 0.275$, $y = 0.275$, $z = 0.45$
		$\Delta_f H = -58070 \pm 110$	$x = 0.18$, $y = 0.37$, $z = 0.45$
		$\Delta_f H = -63110 \pm 060$	$x = 0.09$, $y = 0.46$, $z = 0.45$
		$\Delta_f H = -65380 \pm 100$	$x = 0.0$, $y = 0.55$, $z = 0.45$
		$\Delta_f H = -30920 \pm 240$	$x = 0.59$, $y = 0.06$, $z = 0.35$
		$\Delta_f H = -35460 \pm 310$	$x = 0.53$, $y = 0.12$, $z = 0.35$
		$\Delta_f H = -51520 \pm 290$	$x = 0.145$, $y = 0.505$, $z = 0.35$
			Al solution calorimetry [2001Bre]
xFe(α)+y(Ni)+zAl(liq) $\rightarrow Fe_xNi_yAl_z$((Fe,Ni)Al)	25	$\Delta_f H = -58000 \pm 3000$	$x = 0.0$, $y = 0.50$, $z = 0.50$
		$\Delta_f H = -56800 \pm 2300$	$x = 0.02$, $y = 0.50$, $z = 0.48$
		$\Delta_f H = -54100 \pm 2100$	$x = 0.05$, $y = 0.50$, $z = 0.45$
		$\Delta_f H = -48400 \pm 2400$	$x = 0.10$, $y = 0.40$, $z = 0.50$
			Al solution calorimetry [1993Zub]
xFe(α) + 0.75 (Ni) + (0.25–x) Al(liq) $\rightarrow Ni_{0.75}(Fe_xAl_{(0.25-x)})$	850	$\Delta_f H = -42300 \pm 1600$	$x = 0.00$
		$\Delta_f H = -41800 \pm 1600$	$x = 0.02$
		$\Delta_f H = -40400 \pm 1500$	$x = 0.04$
		$\Delta_f H = -37100 \pm 2200$	$x = 0.06$
		$\Delta_f H = -26600 \pm 2500$	$x = 0.085x = 0.11$
		$\Delta_f H = -20300 \pm 2500$	Al solution calorimetry [2010Rzy]
xFe(α) + 0.75 (Ni) + (0.25–x) Al(liq) $\rightarrow Ni_{0.75}(Fe_xAl_{(0.25-x)})$	27	$\Delta_f H = -39400 \pm 600$	$x = 0.00$
		$\Delta_f H = -39700 \pm 1100$	$x = 0.02$
		$\Delta_f H = -38100 \pm 1100$	$x = 0.04$
		$\Delta_f H = -34200 \pm 600$	$x = 0.065$
		$\Delta_f H = -28800 \pm 600$	$x = 0.09$
		$\Delta_f H = -23300 \pm 600$	$x = 0.12$
		$\Delta_f H = -17100 \pm 1200$	$x = 0.15$
		$\Delta_f H = -12700 \pm 800$	$x = 0.18$
		$\Delta_f H = -8100 \pm 1500$	$x = 0.215$
		$\Delta_f H = -4200 \pm 600$	$x = 0.25$
			Direct synthesis at 859°C [2010Rzy]

Reaction or Transformation	T (°C)	Quantity per Reaction (J, mol, K)	Comments
xFe(α) + y(Ni) + z(Al) → $Fe_xNi_yAl_z$ (*)	25	$\Delta_fH = -25800 \pm 1400$	$x = 0.09, y = 0.09, z = 0.82$
		$\Delta_fH = -36700 \pm 1600$	$x = 0.14, y = 0.14, z = 0.72$
		$\Delta_fH = -29800 \pm 1900$	$x = 0.40, y = 0.10, z = 0.50$
		$\Delta_fH = -44500 \pm 900$	$x = 0.25, y = 0.25, z = 0.50$
		$\Delta_fH = -47700 \pm 1200$	$x = 0.10, y = 0.40, z = 0.50$
		$\Delta_fH = -28300 \pm 2600$	$x = 0.50, y = 0.10, z = 0.40$
		$\Delta_fH = -32800 \pm 2700$	$x = 0.40, y = 0.20, z = 0.40$
		$\Delta_fH = -35400 \pm 3100$	$x = 0.30, y = 0.30, z = 0.40$
		$\Delta_fH = -42800 \pm 1900$	$x = 0.20, y = 0.40, z = 0.40$
		$\Delta_fH = -48800 \pm 1500$	$x = 0.10, y = 0.50, z = 0.40$
		$\Delta_fH = -24700 \pm 1100$	$x = 0.57, y = 0.10, z = 0.33$
		$\Delta_fH = -32300 \pm 1800$	$x = 0.50, y = 0.17, z = 0.33$
		$\Delta_fH = -39400 \pm 1300$	$x = 0.33, y = 0.33, z = 0.33$
		$\Delta_fH = -41200 \pm 1200$	$x = 0.22, y = 0.45, z = 0.33$
		$\Delta_fH = -41500 \pm 1200$	$x = 0.17, y = 0.50, z = 0.33$
		$\Delta_fH = -43800 \pm 1300$	$x = 0.10, y = 0.57, z = 0.33$
		$\Delta_fH = -34200 \pm 1100$	$x = 0.30, y = 0.40, z = 0.30$
		$\Delta_fH = -27900 \pm 1400$	$x = 0.50, y = 0.25, z = 0.25$
		$\Delta_fH = -30600 \pm 1800$	$x = 0.25, y = 0.50, z = 0.25$
		$\Delta_fH = -28300 \pm 1200$	$x = 0.07, y = 0.75, z = 0.18$
			Direct synthesis [2003Su] quoted in [2006Hu]

(*) Resulting phase not indicated

Table 5: Thermodynamic Properties of Single Phases

Phase	Temperature Range (°C)	Property, per mole of atoms (J, mol, K)	Comments
τ_1	(–268.95) - (–267.65)	$Cp = 0.80 \cdot T + +0.006(5) \cdot T^{3}$	Θ_D = 670 K [2010Pan]
(Fe,Ni)Al at $(Fe_x,Ni_{(0.6-x)})Al_{0.4}$	(–173) - (+327)	(J, g, K), not (J, mol, K) $Cp = 0.805 + 1.055 \cdot 10^{-5} \cdot T - 4.548 \cdot T^{-0.5} - 10.4 \cdot T^{-1} - 6.39 \cdot 10^{4} \cdot T^{-3} + 596.3 \cdot T^{-2}$	$x = 0.5$
		$Cp = 0.789 - 3.811 \cdot 10^{-5} \cdot T - 3.239 \cdot T^{-0.5} - 22.7 \cdot T^{-1} - 2.444 \cdot 10^{3} \cdot T^{-3} + 233.7 \cdot T^{-2}$	$x = 0.3$
		$Cp = 0.817 - 1.178 \cdot 10^{-4} \cdot T - 4.396 \cdot T^{-0.5} - 9.154 \cdot T^{-1} - 4.931 \cdot 10^{4} \cdot T^{-3} + 433.2 \cdot T^{-2}$	$x = 0.1$ [2010Ond]
(Fe,Ni)Al at $Fe_xNi_yAl_z$	1127	$a_{Fe} = (3.63 \pm 0.65) \cdot 10^{-1}$ $a_{Ni} = (8.2 \pm 2.5) \cdot 10^{-4}$ $a_{Al} = (6.79 \pm 0.85) \cdot 10^{-2}$	$x = 0.46, y = 0.09, z = 0.45$
		$a_{Fe} = (3.78 \pm 0.13) \cdot 10^{-1}$ $a_{Ni} = (1.82 \pm 0.29) \cdot 10^{-3}$ $a_{Al} = (4.08 \pm 0.88) \cdot 10^{-2}$	$x = 0.37, y = 0.18, z = 0.45$
		$a_{Fe} = (4.81 \pm 0.17) \cdot 10^{-1}$ $a_{Ni} = (5.03 \pm 0.32) \cdot 10^{-3}$ $a_{Al} = (2.76 \pm 0.10) \cdot 10^{-2}$	$x = 0.275, y = 0.275, z = 0.45$

Phase	Temperature Range (°C)	Property, per mole of atoms (J, mol, K)	Comments
(Fe,Ni)Al at $Fe_xNi_yAl_z$ (continued)	1127	$a_{Fe} = (5.38 \pm 0.26) \cdot 10^{-1}$ $a_{Ni} = (1.186 \pm 0.093) \cdot 10^{-2}$ $a_{Al} = (1.414 \pm 0.026) \cdot 10^{-2}$	$x = 0.18$, $y = 0.37$, $z = 0.45$
		$a_{Fe} = (3.66 \pm 0.35) \cdot 10^{-1}$ $a_{Ni} = (3.64 \pm 0.34) \cdot 10^{-2}$ $a_{Al} = (3.72 \pm 0.26) \cdot 10^{-3}$	$x = 0.09$, $y = 0.46$, $z = 0.45$
		$a_{Fe} = (1.48 \pm 0.25) \cdot 10^{-1}$ $a_{Ni} = (5.0 \pm 1.1) \cdot 10^{-4}$ $a_{Al} = (1.75 \pm 0.22) \cdot 10^{-1}$	$x = 0.42$, $y = 0.08$, $z = 0.45$
		$a_{Fe} = (1.562 \pm 0.053) \cdot 10^{-1}$ $a_{Ni} = (8.2 \pm 1.9) \cdot 10^{-4}$ $a_{Al} = (1.069 \pm 0.027) \cdot 10^{-1}$	$x = 0.34$, $y = 0.16$, $z = 0.50$
		$a_{Fe} = (2.11 \pm 0.14) \cdot 10^{-1}$ $a_{Ni} = (1.197 \pm 0.034) \cdot 10^{-3}$ $a_{Al} = (7.5 \pm 1.7) \cdot 10^{-2}$	$x = 0.25$, $y = 0.25$, $z = 0.50$
		$a_{Fe} = (2.56 \pm 0.14) \cdot 10^{-1}$ $a_{Ni} = (2.69 \pm 0.44) \cdot 10^{-3}$ $a_{Al} = (4.18 \pm 0.74) \cdot 10^{-2}$	$x = 0.16$, $y = 0.34$, $z = 0.50$
		$a_{Fe} = (2.244 \pm 0.064) \cdot 10^{-1}$ $a_{Ni} = (5.34 \pm 0.11) \cdot 10^{-3}$ $a_{Al} = (2.52 \pm 0.23) \cdot 10^{-2}$	$x = 0.08$, $y = 0.42$, $z = 0.50$
		$a_{Fe} = (1.01 \pm 0.15)$** $a_{Ni} = (7.4 \pm 1.4) \cdot 10^{-2}$ $a_{Al} = (2.26 \pm 0.15) \cdot 10^{-3}$	probably $x = 0.35$, $y = 0.35$, $z = 0.30$, reported as $x = 0.25$, $y = 0.25$, $z = 0.30$ [2006Ben]
		$a_{Fe} = (9.4 \pm 1.3) \cdot 10^{-1}$ $a_{Ni} = (3.52 \pm 0.66) \cdot 10^{-2}$ $a_{Al} = (4.996 \pm 0.064) \cdot 10^{-3}$	$x = 0.325$, $y = 0.325$, $z = 0.35$
		$a_{Fe} = (7.36 \pm 0.45) \cdot 10^{-1}$ $a_{Ni} = (1.58 \pm 0.17) \cdot 10^{-2}$ $a_{Al} = (9.5 \pm 1.4) \cdot 10^{-3}$	$x = 0.30$, $y = 0.30$, $z = 0.40$
		$a_{Fe} = (1.154 \pm 0.080) \cdot 10^{-1}$ $a_{Ni} = (5.98 \pm 0.23) \cdot 10^{-4}$ $a_{Al} = (1.167 \pm 0.018) \cdot 10^{-1}$	$x = 0.24$, $y = 0.24$, $z = 0.52$ [2006Ben]

** = measured value, it should be < 1

Table 6: Investigations of the Al-Fe-Ni Materials Properties

Reference	Method / Experimental Technique	Type of Property
[1981Kha]	LOM, EDX, XRD	Catalyst properties of Fe-Ni powders
[1991Har]	Extrusion, mechanical tests	Mechanical properties of $Al_{30}Fe_{20}Ni_{50}$ alloy
[1991Kos]	LOM, mechanical tests	Mechanical properties of NiAl-based alloy with Fe addictions

Reference	Method / Experimental Technique	Type of Property
[1992Kai]	XRD, SEM, mechanical tests	Thermoelastic properties of Al-Fe-Ni alloys in the *B*2 domain
[1995Gaf]	XRD, EDX	Structural investigation of Fe-(AlNi) nanocrystalline and amorphous alloys
[1998Ko]	VSM, TEM, DSC	Defect effect on precipitation and properties of Fe-Ni-Al alloys
[2000Zei]	XRD, Mössbauer spectroscopy	Characterization of Al-Fe-Ni catalytic alloys prepared by mechanical alloying
[2001Sur]	Mechanical tests	Mechanical properties of mechanically alloyed Al-Fe-Ni alloys
[2002Alb]	XRD, TEM	Effect of Fe mechanical alloying to NiAl intermetallic compound
[2002Ban]	TEM, EDS, ALCHEMI	Properties of Fe addictioned Ni-Al alloys
[2002He]	DTA	Kinetics of thermal explosion reaction in Al-Fe-Ni system
[2002Joa]	XRD, DSC	Thermal stability of mechanically alloyed Al-Fe-Ni alloys
[2002Mun]	TEM, mechanical and wear tests	Microstructure, mechanical properties and wear of Al-Fe-Ni alloys
[2004Cam]	EDX, SEM, XRD, mechanical tests	Microhardness and Microstructure of Fe addictioned NiAl intermetallic compound
[2004Fu]	XRD, first principles calculations, neutron diffraction, mechanical tests	Mechanical and magnetic properties of NiAl intermetallic with Fe addictions
[2004Kau]	XRF, magnetometer	Magnetic properties of $Ni_{75-x}Fe_xAl_{25}$ as cast, annealed and quenched alloys
[2004Maz]	XRD, SEM, TEM, mechanical tests	Density and microhardness of $Fe_{40}Al_{40}Fe_{20}$
[2004Par2]	Nuclear inelastic scattering of synchrotron radiation, neutron inelastic scattering	Vibrational properties of Fe in NiAl intermetallics
[2004Sch]	SEM, mechanical tests	Mechanical behavior of Fe-Ni-Al alloys
[2005Str]	*Ab initio* calculations	Effect of Ni doping on FeAl vacancy formation energy
[2006Dru]	TEM, ACAR spectra	Effect of nanoparticles on irradiated Fe-Ni-Al material
[2006Gar]	SEM, STEM, EDX, XRD, mechanical tests	Effect of hot rolling on room temperature ductility of NiAl intermetallic compound
[2006Nii]	SEM, EBS, TEM, mechanical tests	Recrystallization behavior in twin-roll continuous cast Al-Fe-Ni alloy
[2006Oik]	DSC, TEM, VSM	Martensitic and magnetic transitions in *B*2 Ni-Al-Fe alloys
[2006Tsa]	ICP-AES, SEM, EDS, mechanical tests	Mechanical behavior of Cr or Nb modified $Al_{25}Fe_{27.5}Ni_{47.5}$ alloy
[2006Wan]	SEM, EDX, mechanical tests	Fe effect on NiAl creep properties
[2007Col]	TEM, mechanical tests	Mechanical properties of B-doped Fe-Ni-Al *B*2 alloys
[2007Gon]	SEM, electrochemical tests	Corrosion behavior of Ni-doped FeAl alloys in human body environment
[2007Joa]	XRD, DSC	Milling criteria for NiAl alloys mechanosynthesis
[2007Liu]	First principles calculations, EELS, TEM, SQUID, ALCHEMI method	Magnetism and solid solution effect on Fe-addictioned NiAl alloys
[2007Mun]	SEM, TEM, EDX, mechanical tests	Microstructure and mechanical behavior of $Al_{45}Fe_{35}Ni_{20}$ alloy

Reference	Method / Experimental Technique	Type of Property
[2007Orb]	XRD, SEM, mechanical tests	Ni_3Al properties after Fe addition by mechanical alloying or reactive synthesis
[2007Uwa]	Mössbauer spectroscopy, magnetic measurements	Mössbauer effect on Fe-doped NiAl intermetallics
[2007Yas]	Mechanical tests	Effect of Ni on pseudo-elasticity of Fe_3Al single crystals
[2007Zha2]	XRD, PPMS magnetometer	Superparamagnetic behavior of melt spun Fe_2NiAl ribbons
[2008Han]	Mössbauer spectroscopy	Point defect structure of Ni-doped Al-Fe powders
[2008Kim1]	XRD, DSC, SEM, TEM, VSM	Chemical leaching of $Al_{0.6}(Ni_{0.5}Fe_{0.5})_{0.4}$ alloy
[2008Kim2]	XRD, DSC, SEM, TEM, VSM	Chemical leaching of Al(Ni-Fe) powders
[2008Kim3]	XRD, DSC, TEM, VSM, SQUID	Magnetic Properties of Al(Ni-Fe) powders
[2008Muk]	VSM, mechanical tests	Dynamic-Elastic properties and Magnetic susceptibility of $Al_{25}Fe_{20}Ni_{55}$ alloy
[2008Mun]	SEM, EDS, TEM, mechanical tests	Coarsening kinetics of metastable nanoprecipitates in Al-Fe-Ni alloys
[2009Cas]	SEM, electrochemical tests	Electrochemical properties of Al-Fe-Ni alloys in human body environment
[2009Laz]	*Ab initio* DFT calculations	Magnetism-related ductility (magnetic and slip properties) of NiAl-Fe alloys
[2009Yas]	Mechanical tests, magnetic measurements	Magneto-mechanical damping of Ni-doped Al-Fe alloys
[2010Pal]	XRD, Mössbauer spectroscopy	Effect of Ni on $Fe_{70}Al_{30}$ alloys lattice parameter and magnetic hyperfine field.
[2010Sag]	Mössbauer spectroscopy	Dissolution of dispersed Ni_3Al intermetallic particles in matrices of *fcc* Fe–Ni–Al alloys
[2010Sch]	Three-Dimensional Atom Probe (3DAP), Small Angle Neutron Scattering (SANS)	Precipitation behavior of NiAl intermetallics in Al-Fe-Ni alloy
[2010Sha]	Mechanical tests, Mössbauer spectroscopy	Deformation induced particles dissolution in $Al_{60}Fe_{35}Ni_5$ alloy
[2010Sor]	XRD, SEM, mechanical tests	Hardness of *B*2 $Al_{15}Fe_{75}Ni_{10}$ alloy after aging and coarsening
[2011Che]	Total energies first principles calculations	Effect of Ni on the *B*2-FeAl structure
[2011Dum]	TEM, VSM	$Ni_{50}Fe_xAl_{50-x}$ ($x = 20, 25, 30$) alloys magnetic properties and precipitation kinetics
[2011Oku]	XRD, TEM, Magnetic measurements	Microstructure, magnetic properties and martensitic transformation of $Ni_{55}Fe_{22.5}Al_{22.5}$ FSMA alloy
[2011Sha]	Mechanical tests, Mössbauer spectroscopy	Deformation induced particles dissolution in Fe-Ni-Al alloys
[2011Zho]	XRD, DSC, Mechanical tests,	Phase transformation in oil quenched Al-Fe-Ni shape-memory alloy
[2012Dum]	XRD, TEM, VSM	Kinetics and microstructure of microalloyed Al-Fe-Ni alloys
[2012Hua]	Mechano-elastic tests, *ab initio* calculations (DFT), TEM	Magnetism induced ductility in Fe-addictioned NiAl intermetallic
[2012Ma]	XRD, mechanical tests, FESEM	$Ni_{50}Al_{17}Fe_{33}$ alloy microstructure and mechanical properties
[2012Niu]	First principles calculations	Electronic and mechanical properties of Ni-doped Fe_3Al intermetallic compound
[2013Had]	XRD, Mössbauer spectroscopy	Mechanically alloyed $Fe_{50}Ni_{40}Al_{10}$ structural and microstructural properties

Reference	Method / Experimental Technique	Type of Property
[2013Lep]	Resistivity measurements, DTA	Ni_3Al-Fe alloys phase transformation and disordering temperatures
[2013Yas]	Mechanical tests, TEM, SAED patterns	Ni effect on strength and damping capacity of Al-Fe alloys
[2016Dah]	First principles calculations	Magnetic properties of Fe_2NiAl
[2017Wan]	Frist principles calculations	Mechanical properties of Al-Fe-Ni alloys
[2017Zhe]	DFT calculations	Structural, elastic and electronic properties of Ni-addictioned *B*2 FeAl intermetallics
[2018Wei]	First principles and Monte Carlo calculations	Exchange interactions and Curie Temperatures of Fe_2NiAl
[2018Wen]	First principles calculations	Martensitic transformation temperature and magnetic properties of Ni_2FeAl
[2019Bia]	XRD, DSC, SEM, ICP-AES, Hardness measurements	High temperature thermal stability of Al-Fe-Ni eutectic alloy
[2019Gan]	DFT calculations	Band structure, Spin magnetic moment, State density, Band gap, Seebeck Coefficient, Thermal and electrical conductivities
[2019Yas]	APB energy calculations, TEM, mechanical tests	Effect of NiAl precipitation on Al-Fe-Ni single crystals
[2020Ben]	DFT calculations	Structural, electronic, dynamic and thermodynamic properties of $FeNi_2Al$ alloy
[2021Liu]	First principles calculations	Mechanical, electronic and thermal properties of $FeNi_2Al$

Fig. 1a: Al-Fe-Ni. Lattice parameter of β-phase, (Fe,Ni)Al as a function of composition at constant Al contents

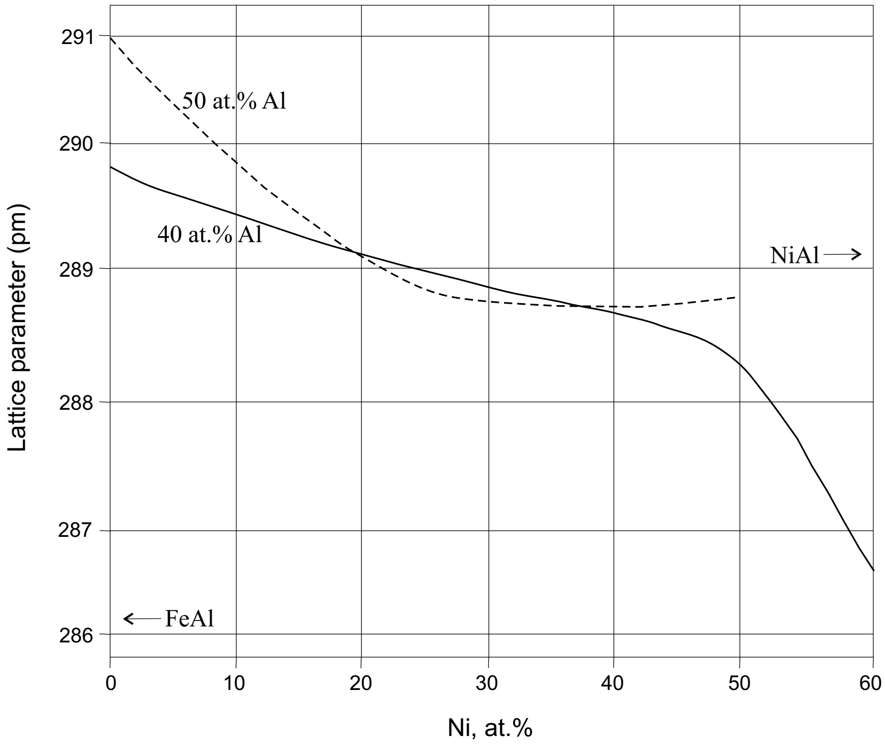

Fig. 1b: Al-Fe-Ni. Lattice parameter of β-phase, (Fe,Ni)Al as a function of composition at constant Fe:Ni ratio (0 - for NiAl, ∞ - FeAl)

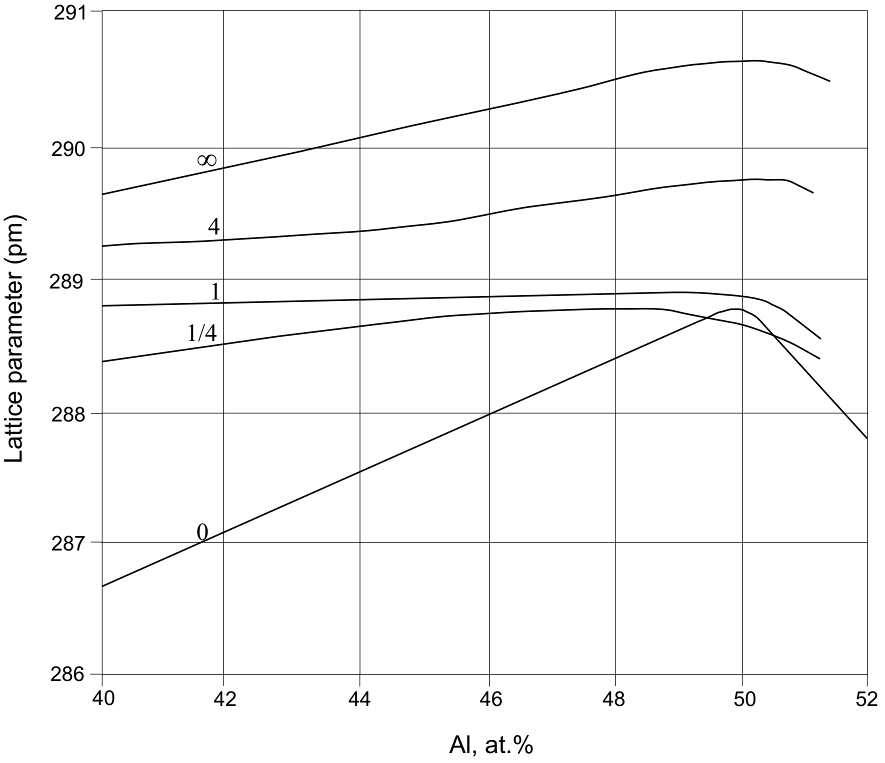

Fig. 1c: Al-Fe-Ni. Lattice parameter of the (γFe, Ni)/Ni_3(Fe,Al) phase as a function of Al concentration

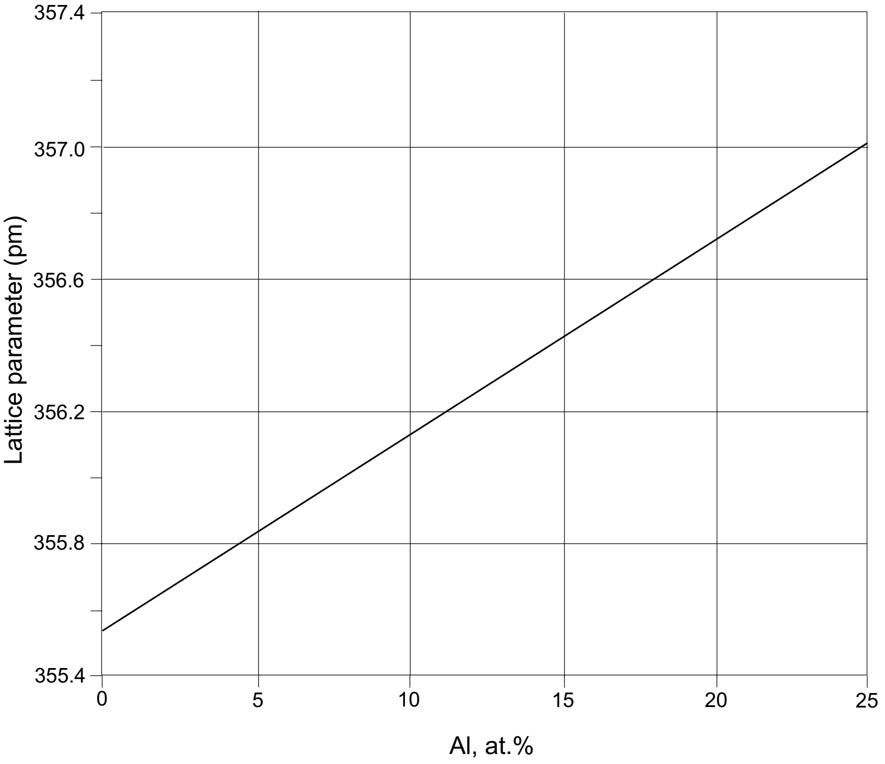

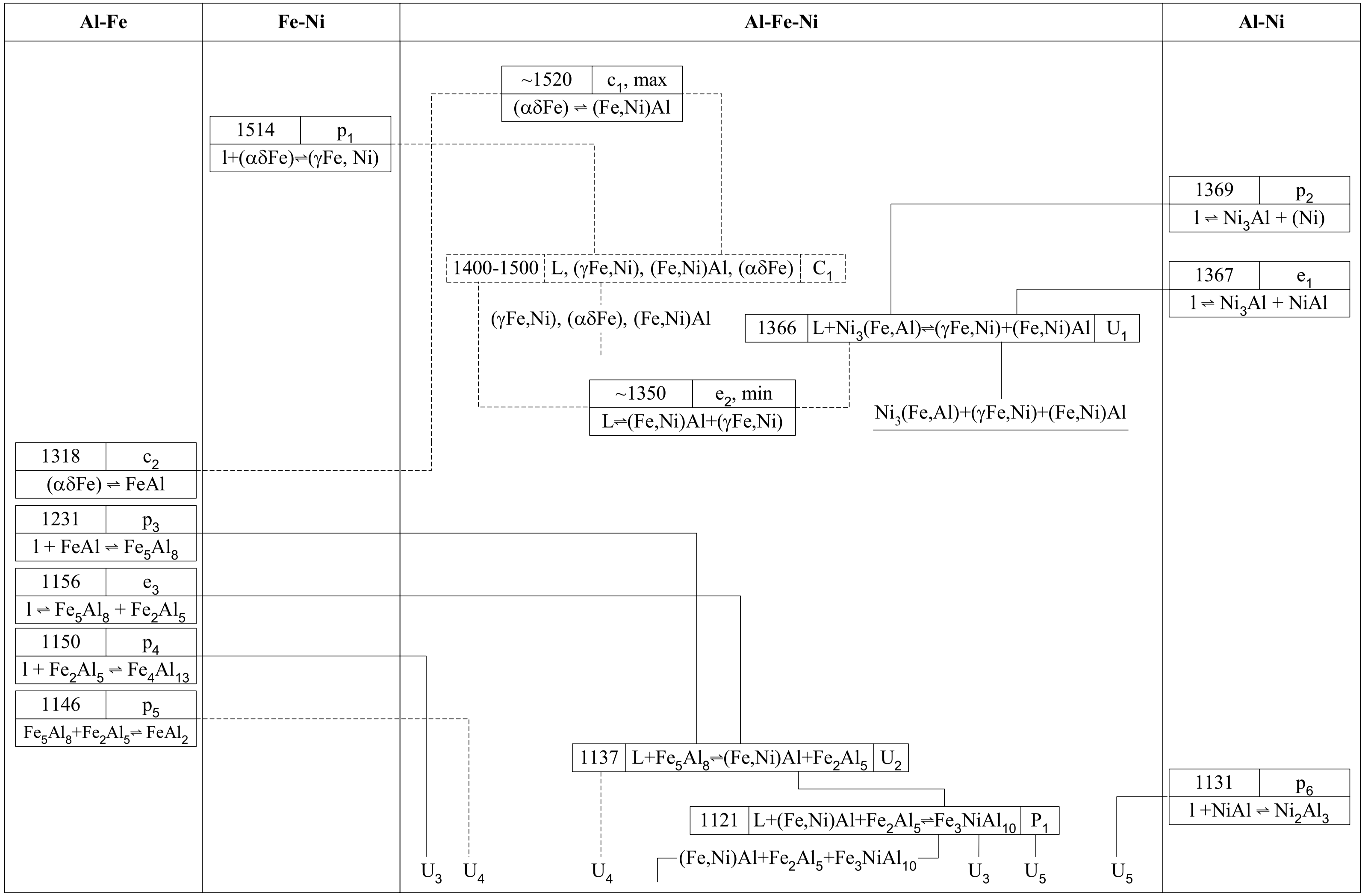

Fig. 2a: Al-Fe-Ni. Reaction scheme

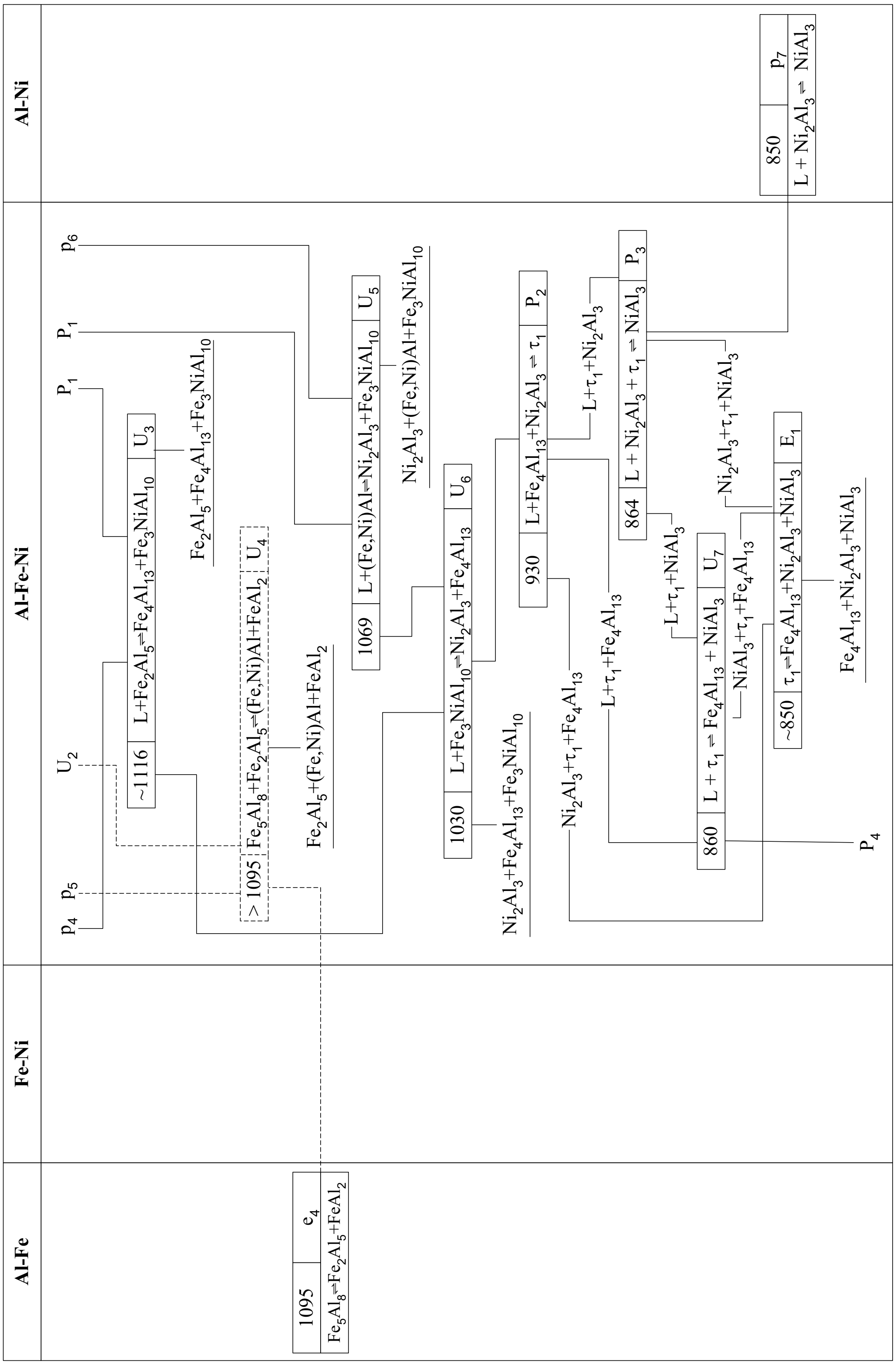

Fig. 2b: Al-Fe-Ni. Reaction scheme

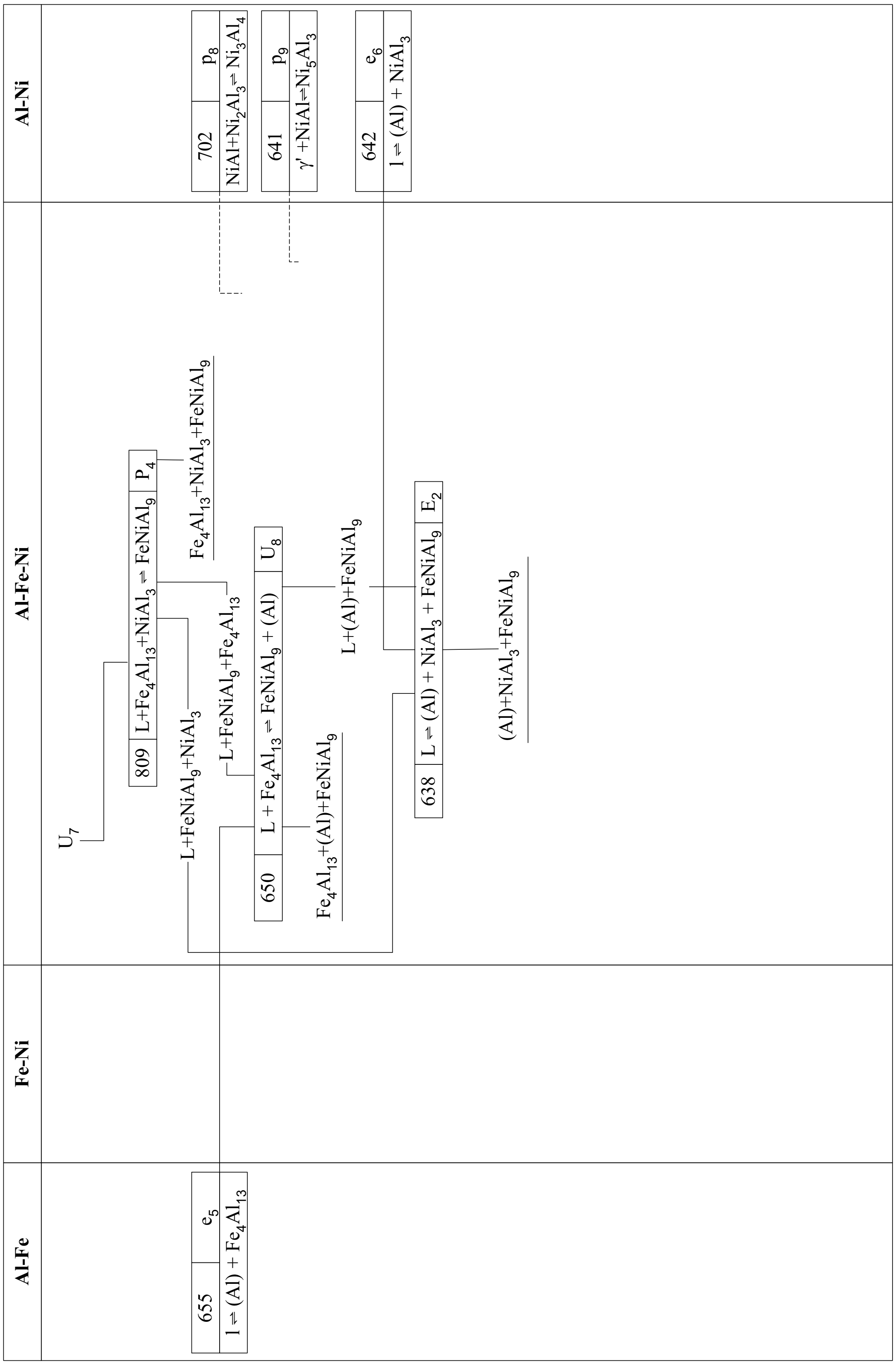

Fig. 2c: Al-Fe-Ni. Reaction scheme

Fig. 3a: Al-Fe-Ni. Projection of the liquidus surface

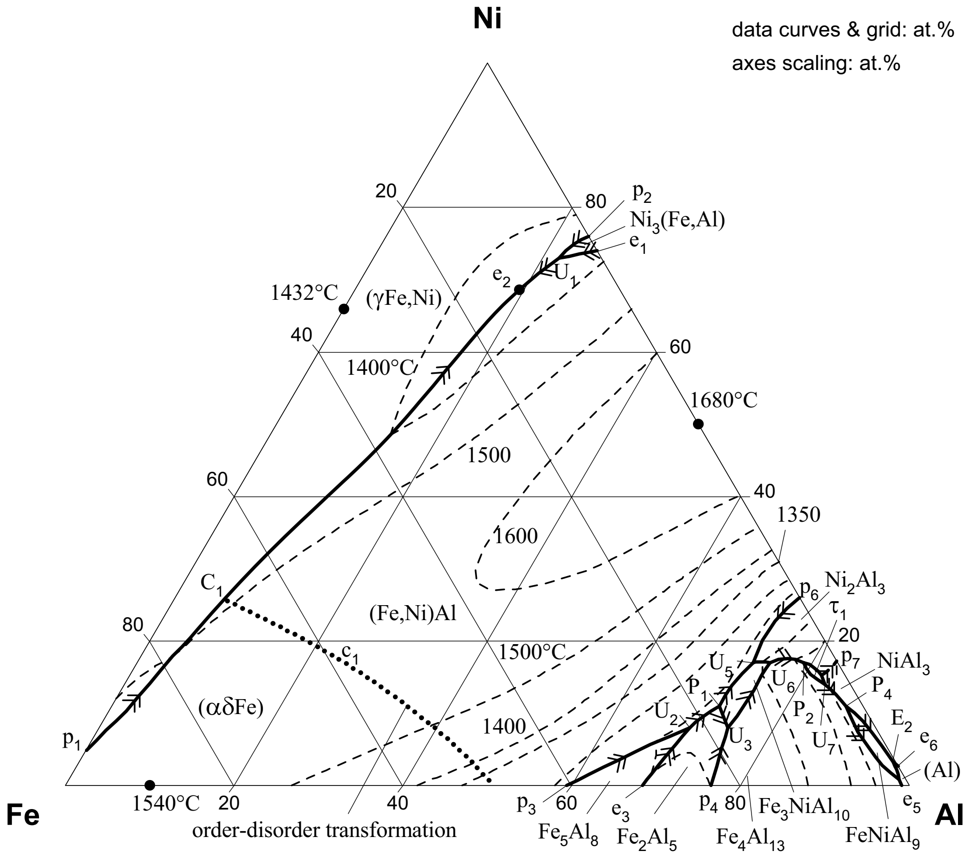

Fig. 3b: Al-Fe-Ni. Enlarged portion of the liquidus projection in Al corner

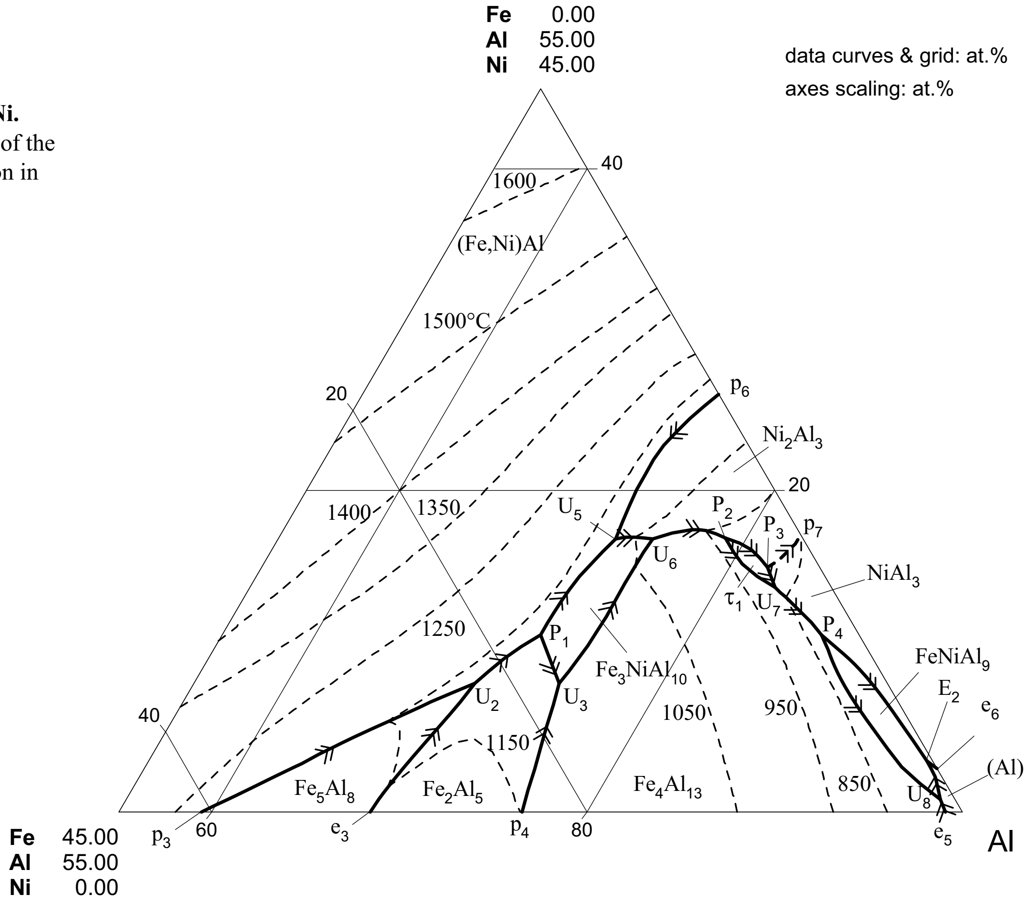

Fig. 4: Al-Fe-Ni. Solvus of the (γFe, Ni) phase

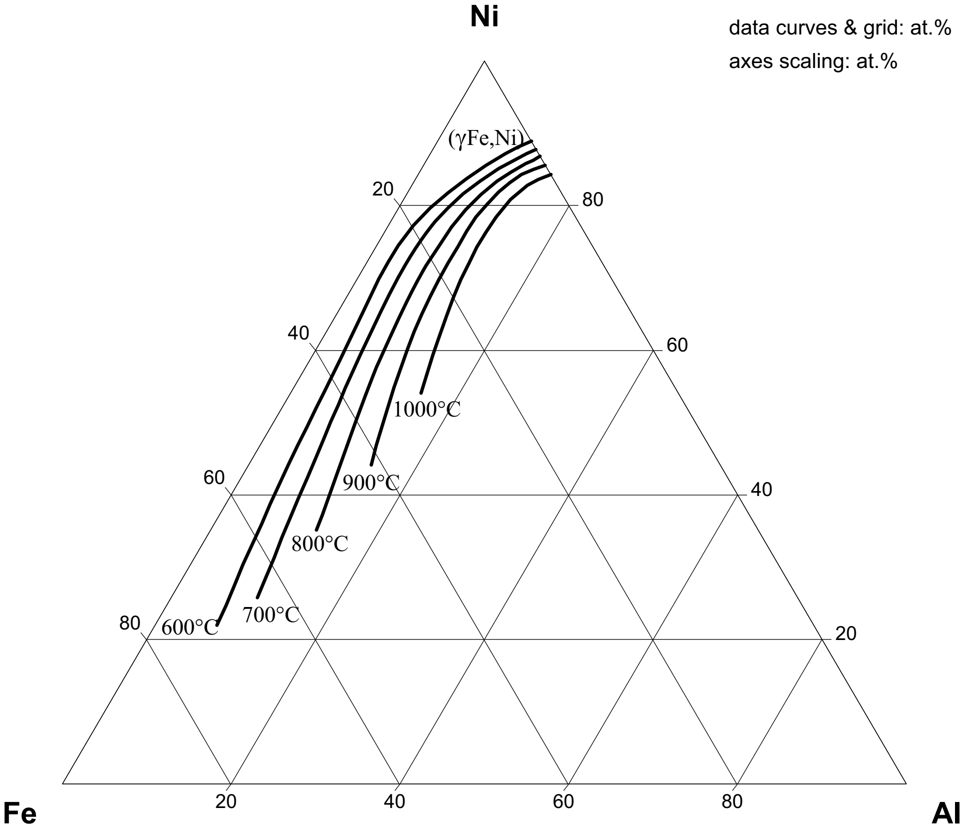

Fig. 5: Al-Fe-Ni. Isothermal section at 1350°C. The order-disorder transformation is not shown.

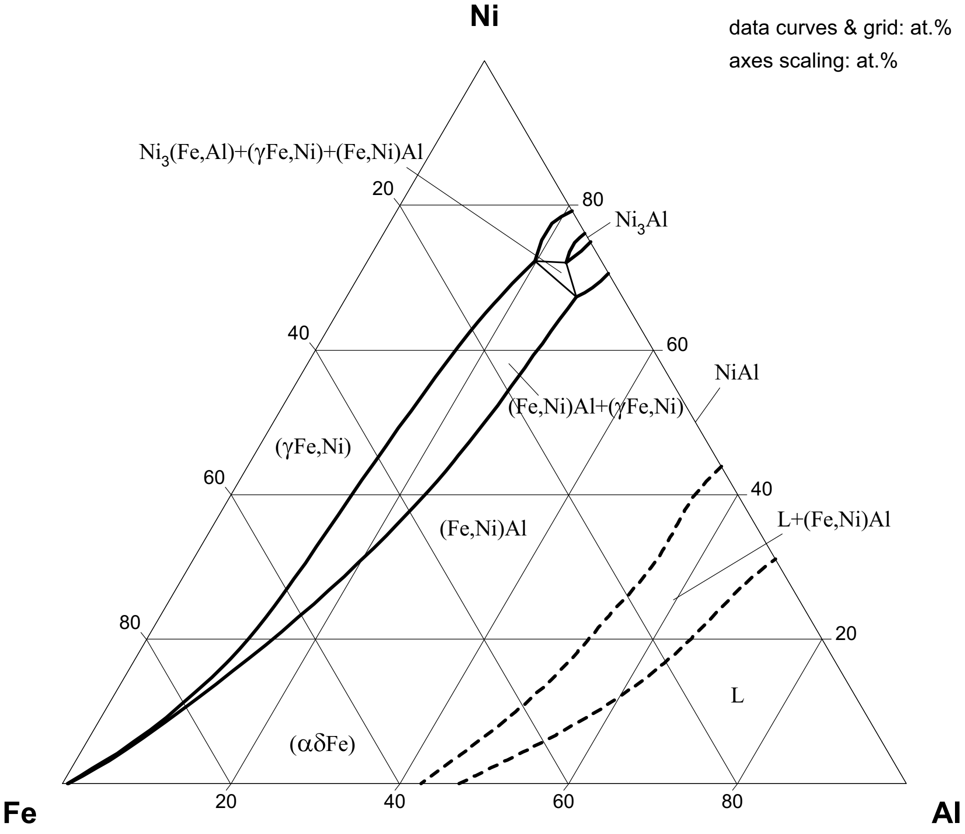

Fig. 6: Al-Fe-Ni. Isothermal section at 1250°C

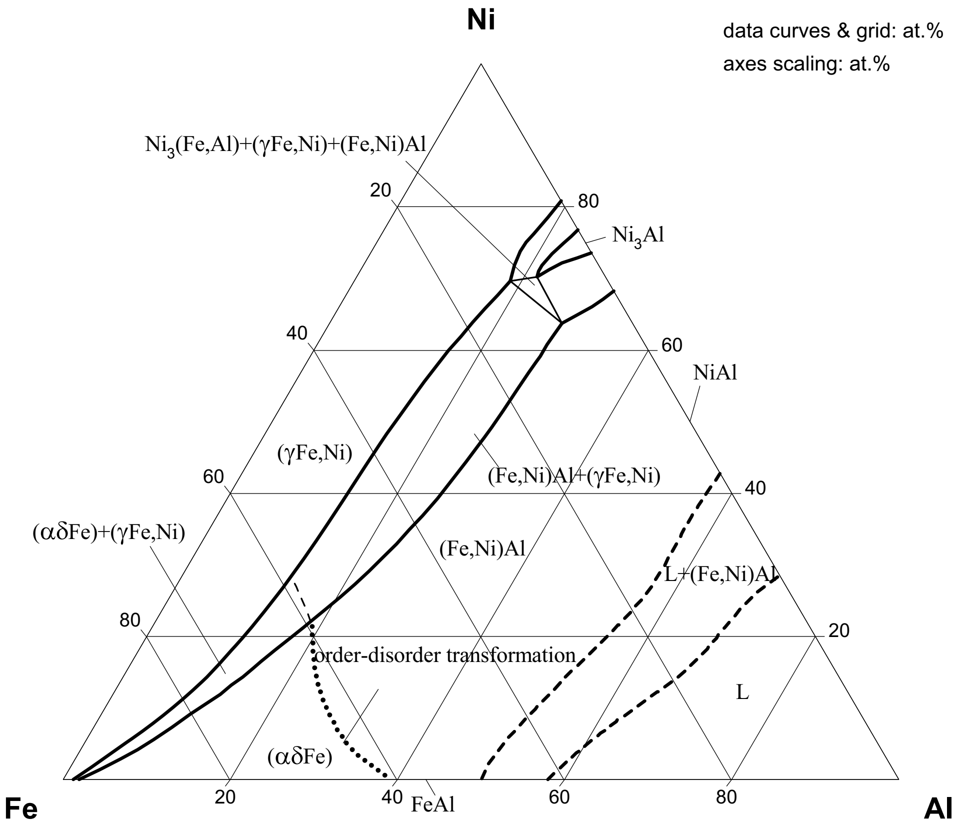

Fig. 7: Al-Fe-Ni. Partial isothermal section at 1150°C

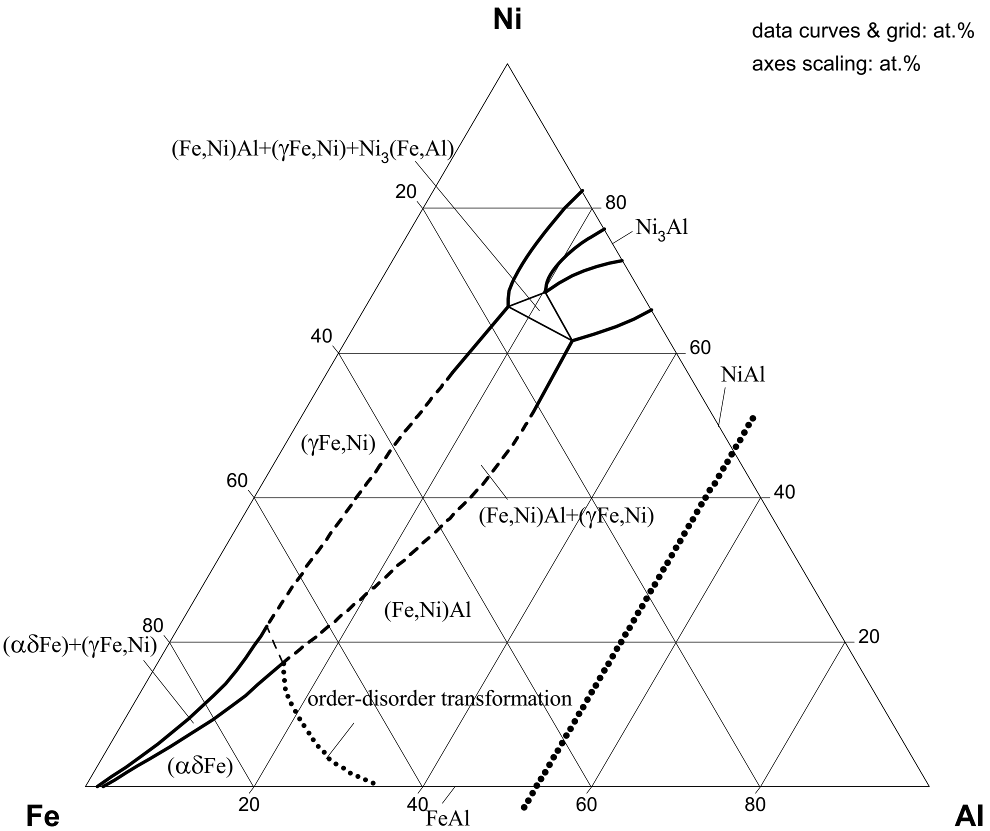

Fig. 8: Al-Fe-Ni.
Isothermal section at 1050°C

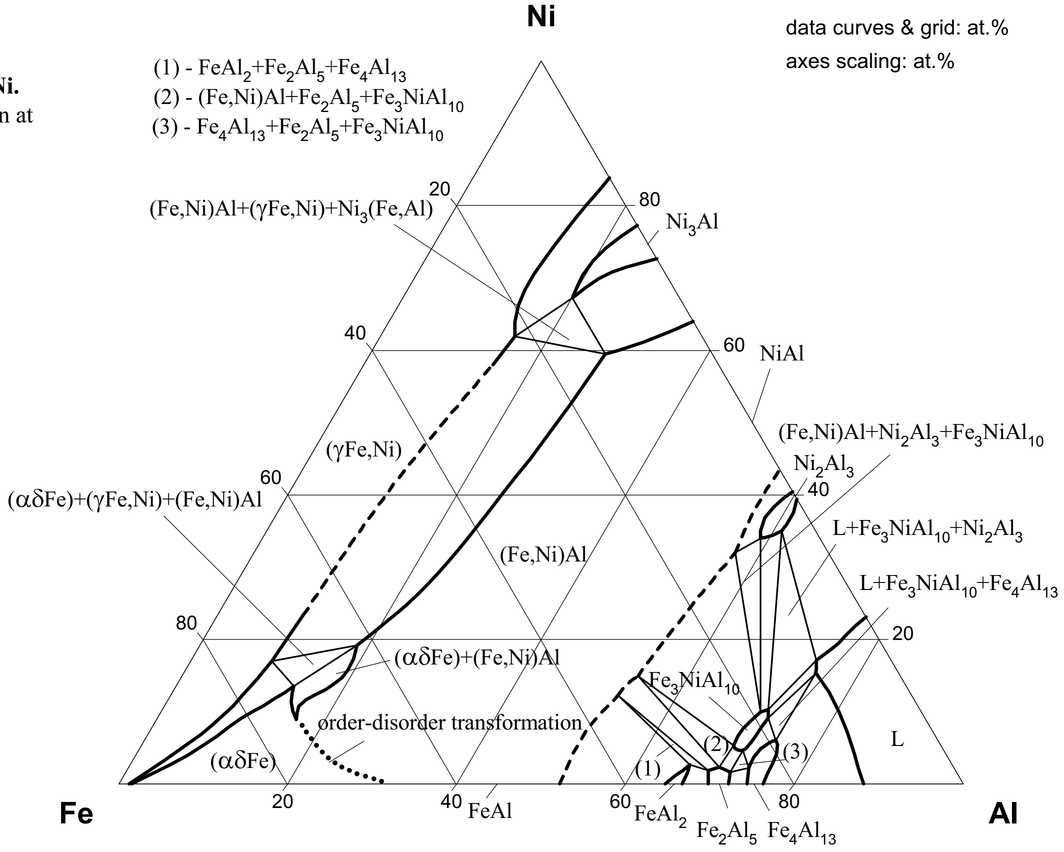

Fig. 9: Al-Fe-Ni.
Isothermal section at 950°C

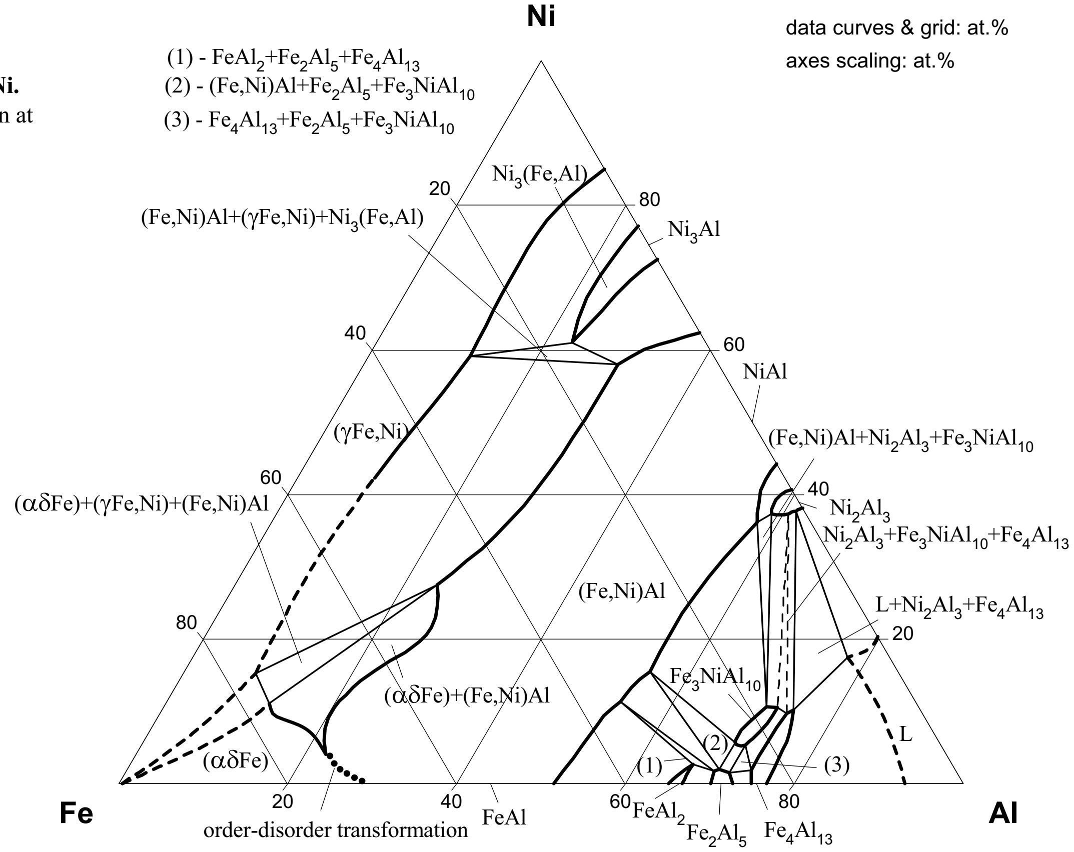

Fig. 10: Al-Fe-Ni. Isothermal section at 850°C

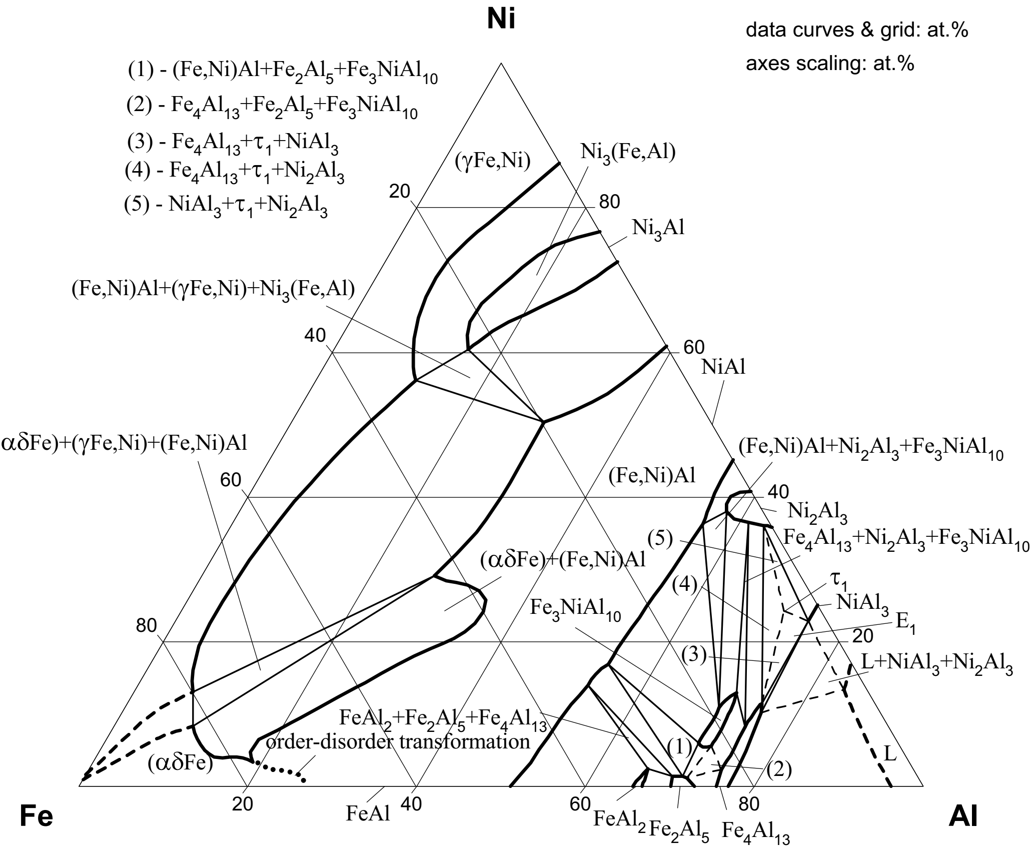

Fig. 11: Al-Fe-Ni. Partial isothermal section at 750°C

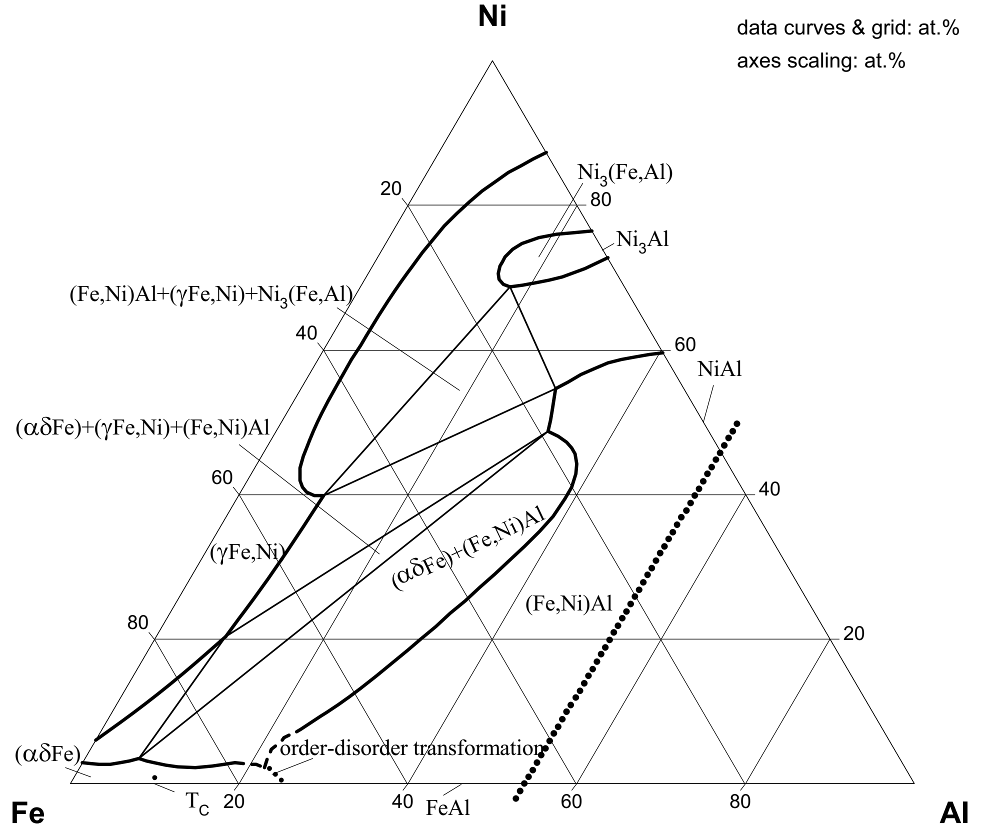

Fig. 12: Al-Fe-Ni. Partial isothermal section at 627°C

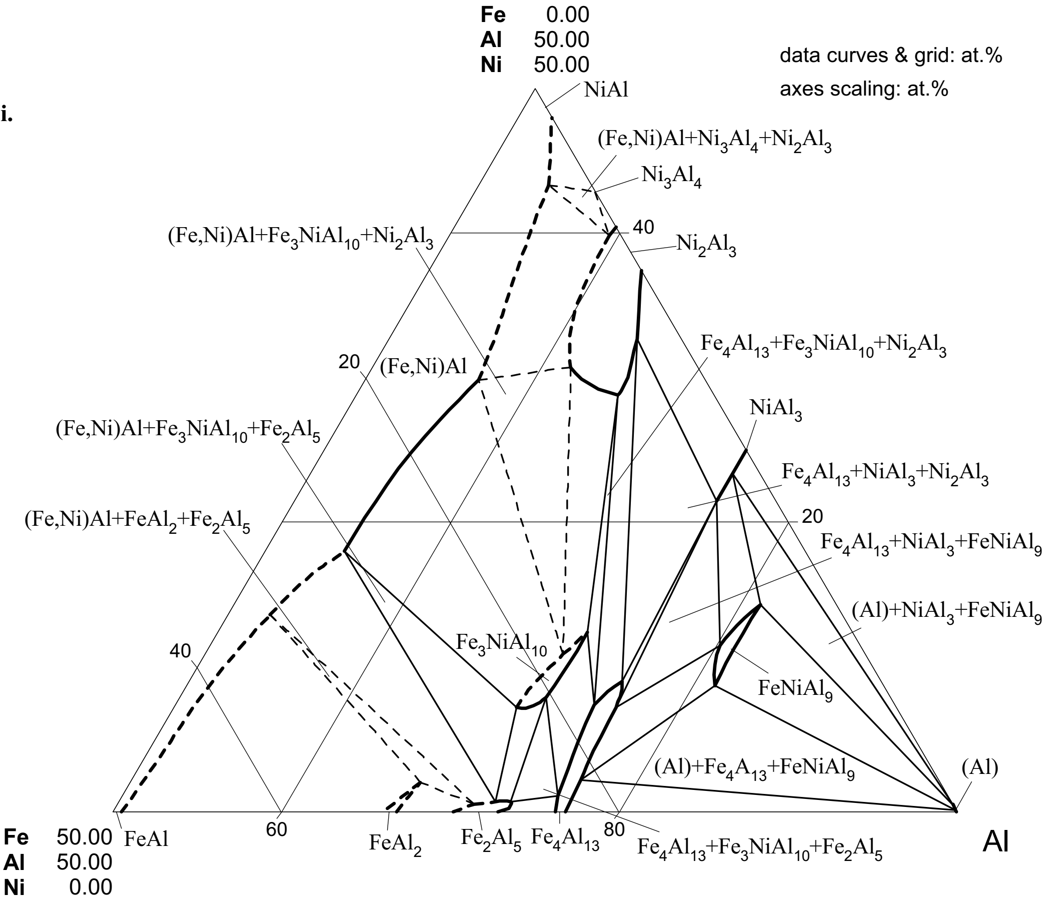

Fig. 13: Al-Fe-Ni. Solid phases in alloys cooled at 10 K/h [1938Bra, 1940Bra1, 1940Bra2]

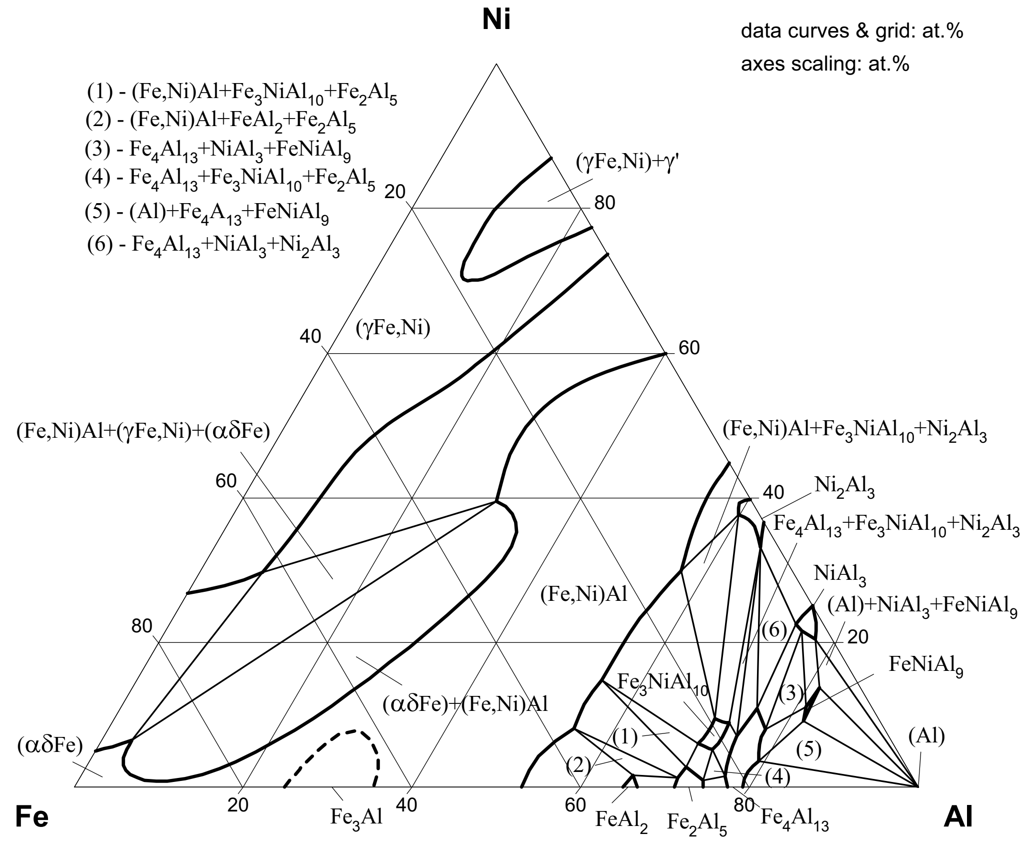

Fig. 14: Al-Fe-Ni. Vertical section at molar ratio of Ni:Al as 1:1

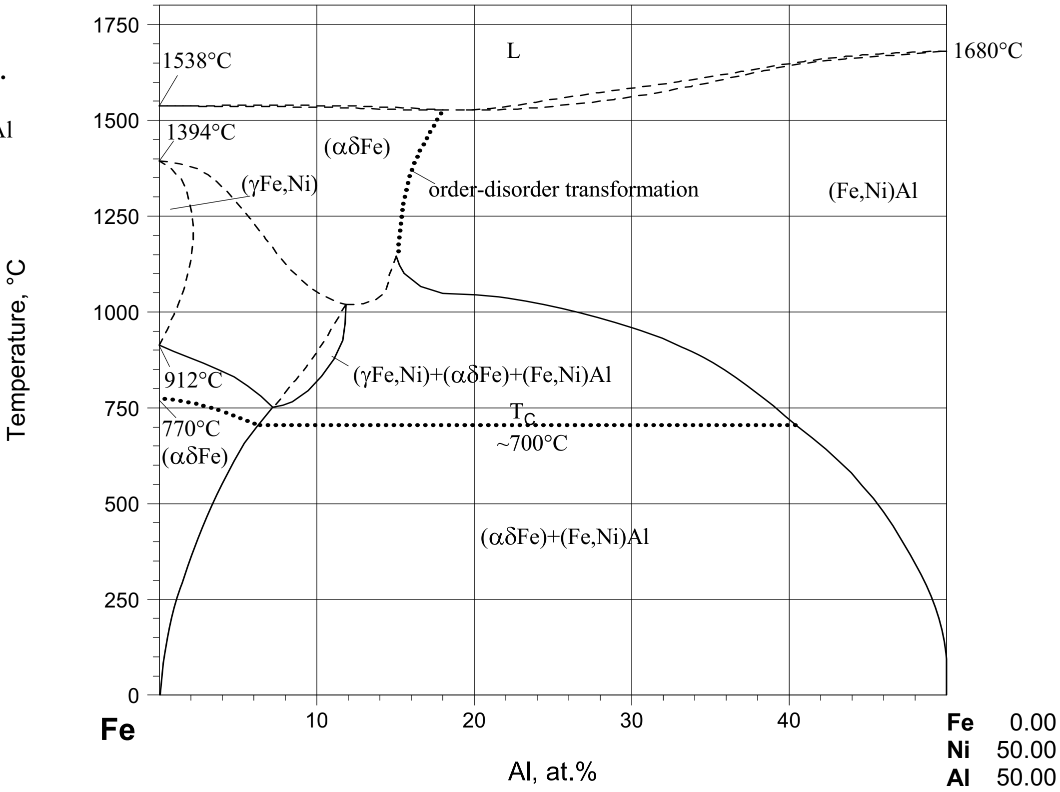

Fig. 15a: Al-Fe-Ni. Isopleth at 75 at.% Ni

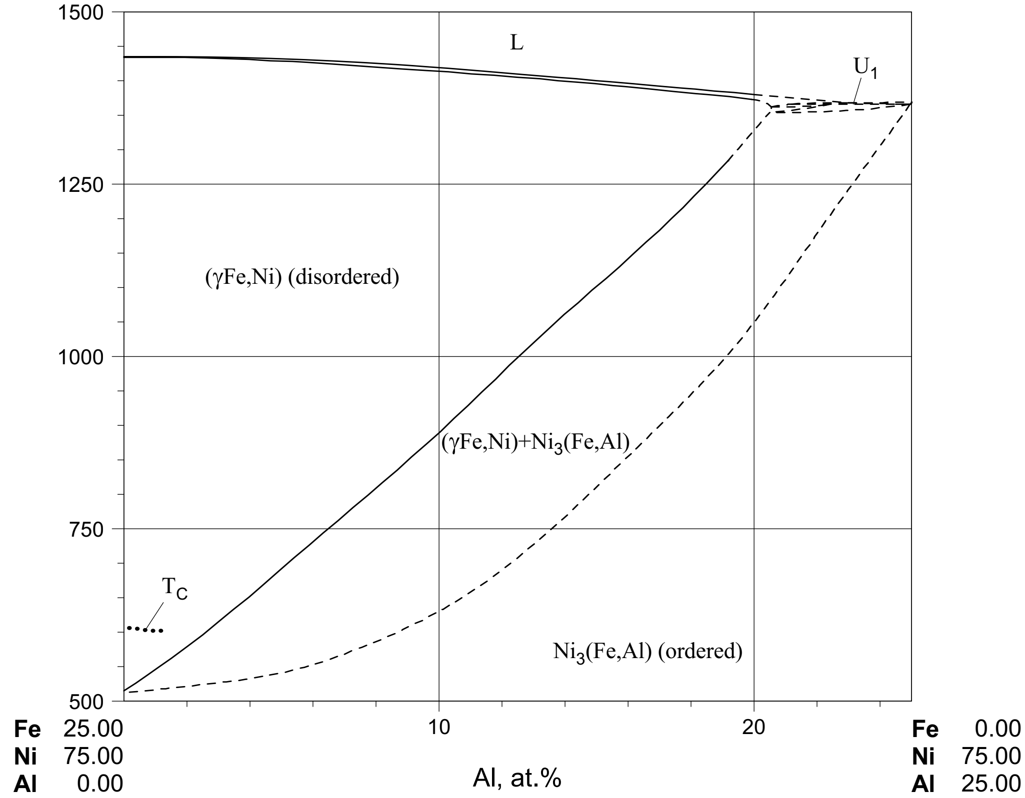

Fig. 15b: Al-Fe-Ni. Enlarged portion of isopleth at 75 at.% Ni

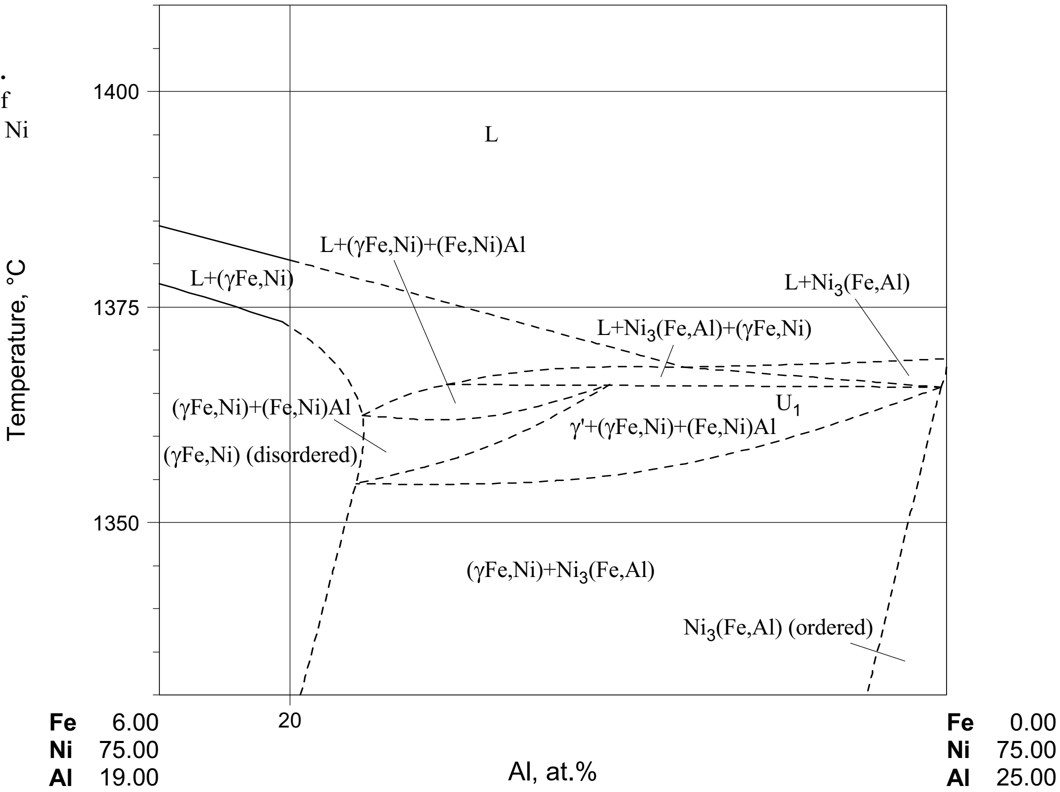

Fig. 16: Al-Fe-Ni. Isopleth at 50 at.% Al. Order-disorder transformation is not shown

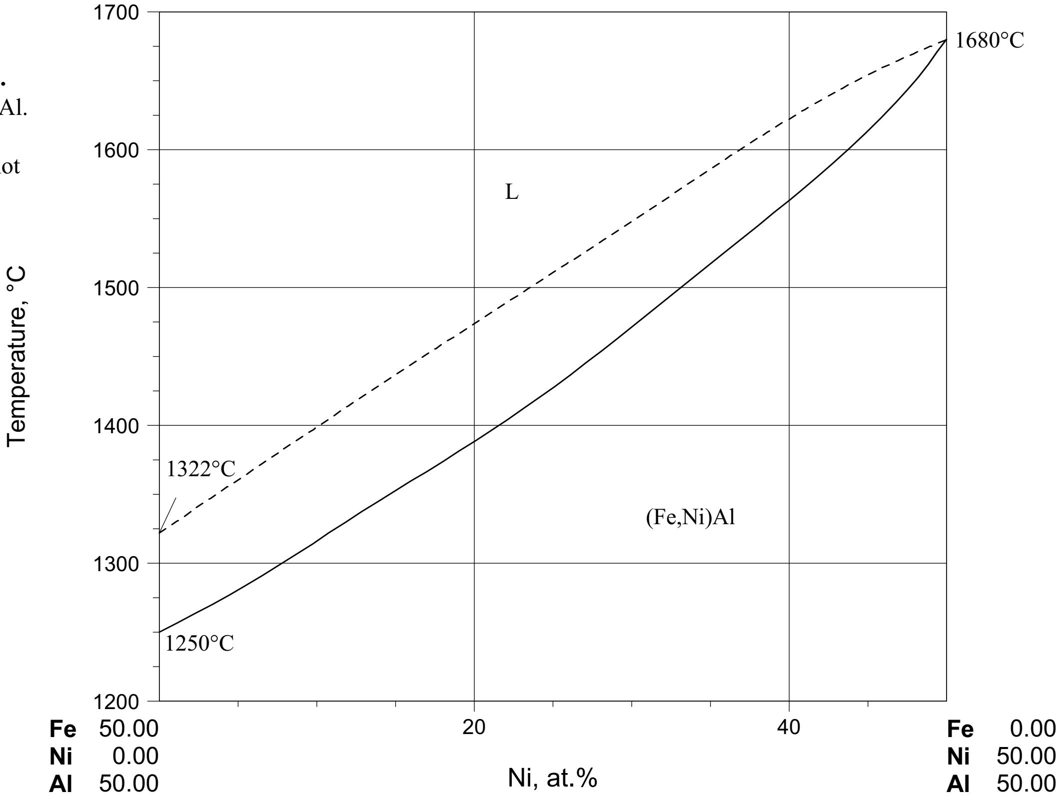

Fig. 17: Al-Fe-Ni.
Isopleth at 60 at.% Al

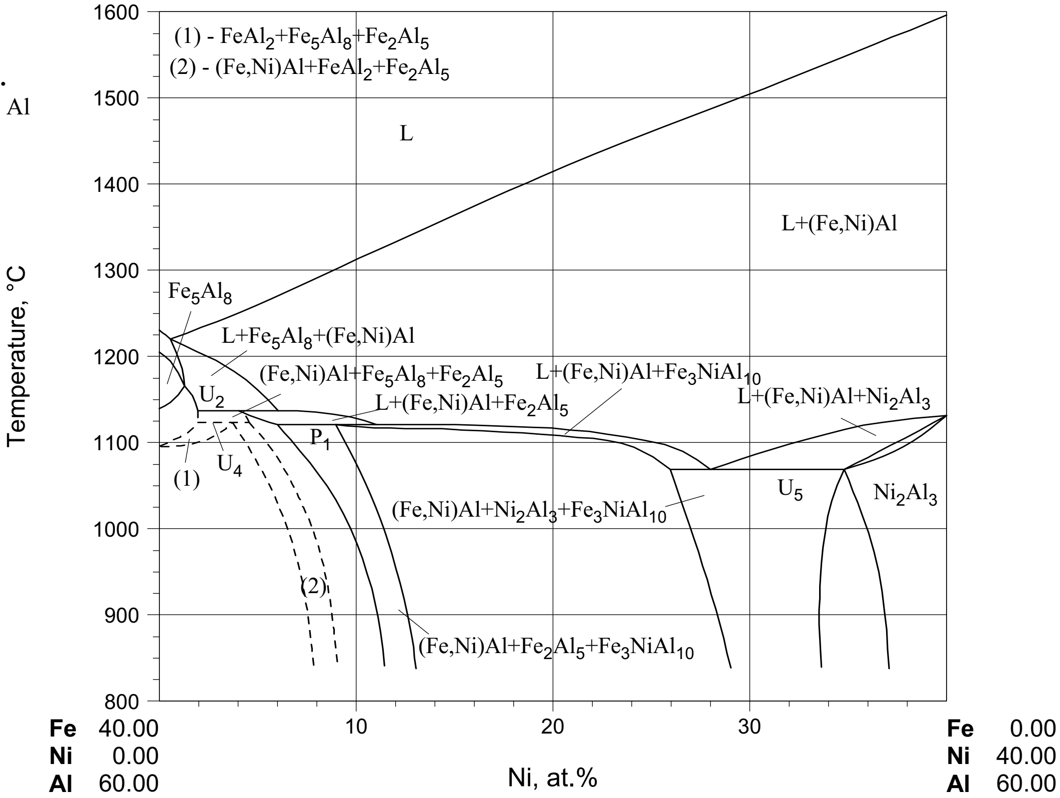

Fig. 18: Al-Fe-Ni.
Isopleth at 67 at.% Al

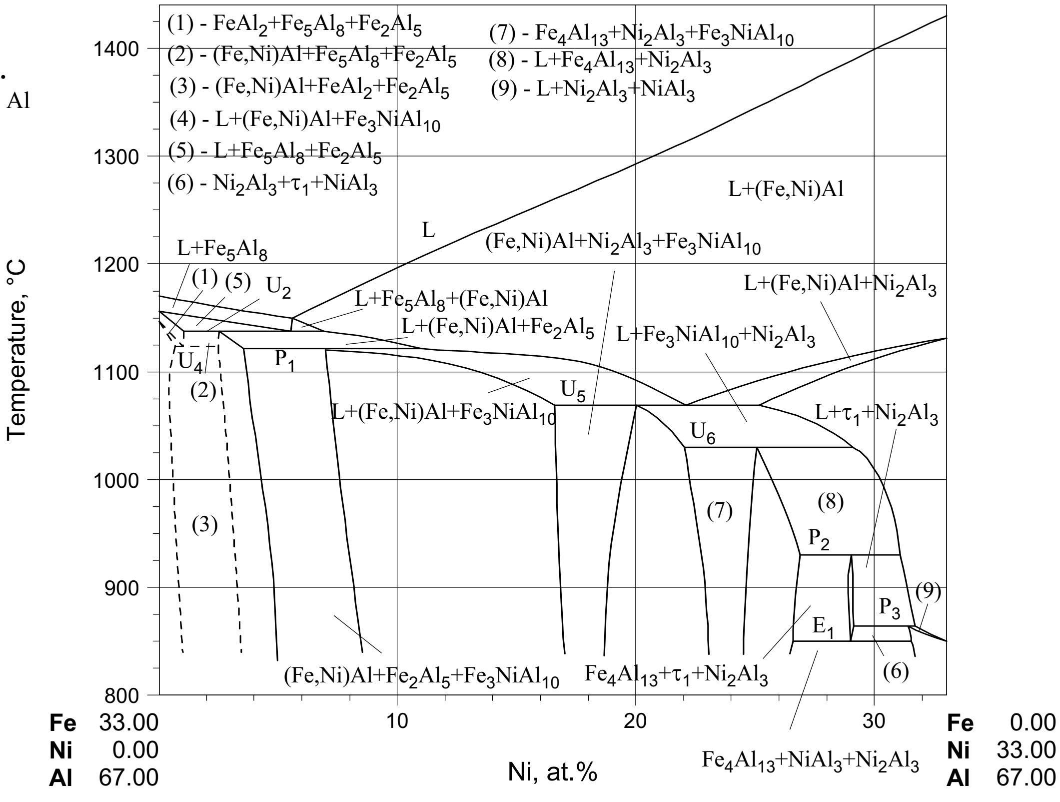

Fig. 19: Al-Fe-Ni.
Isopleth at 71.5 at.% Al

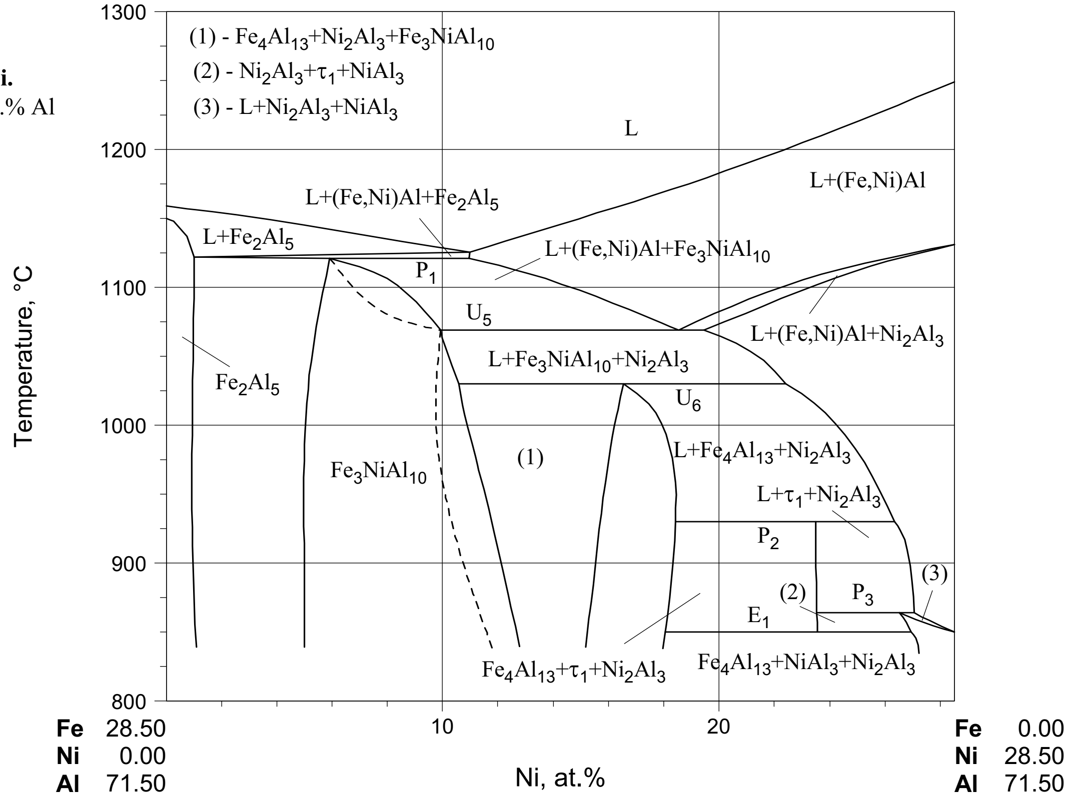

Fig. 20: Al-Fe-Ni.
Isopleth at 75 at.% Al

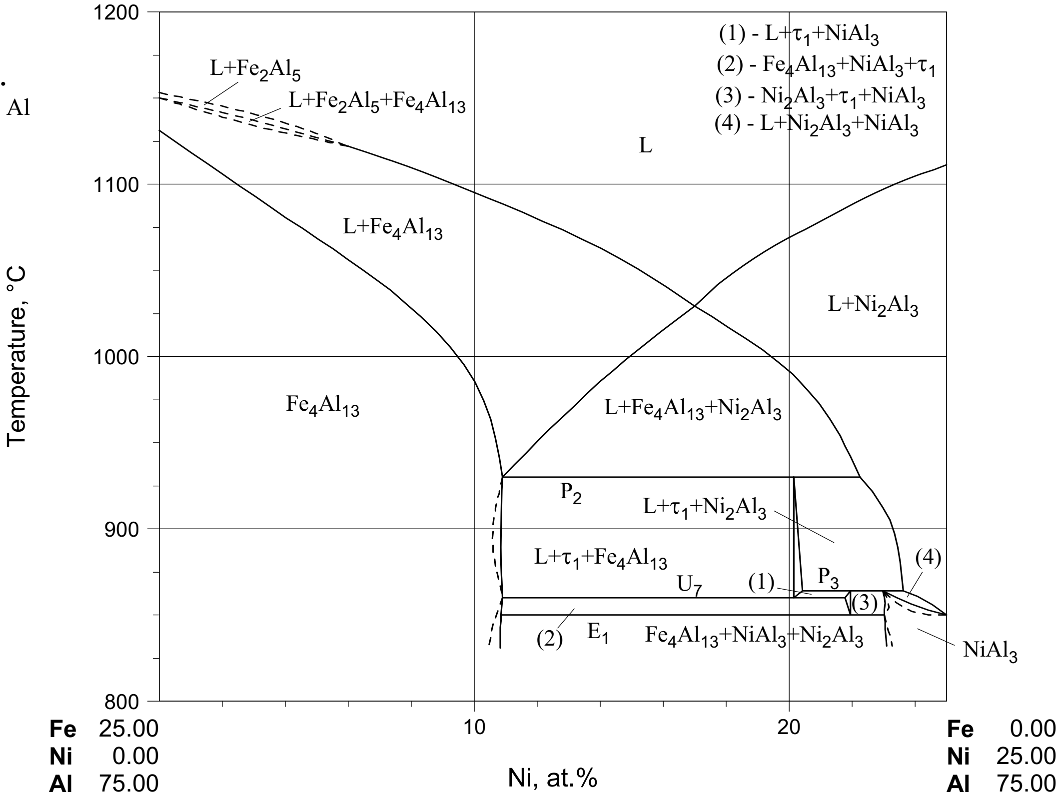

Fig. 21: Al-Fe-Ni.
Isopleth at 80 at.% Al

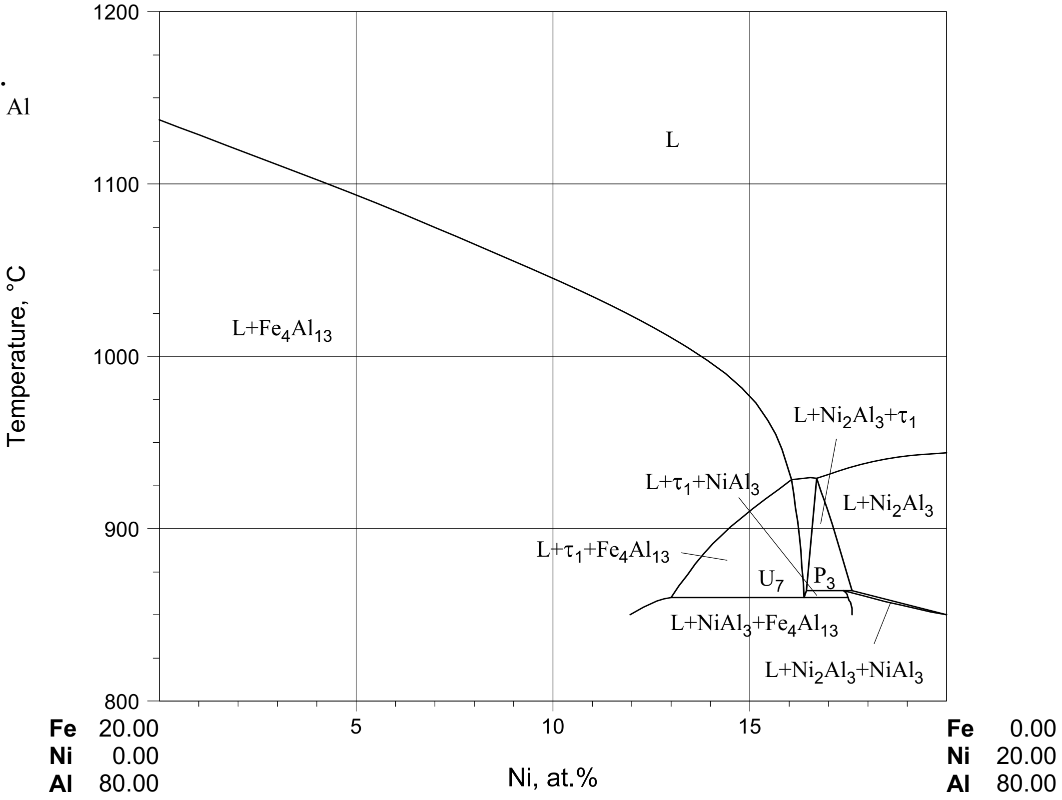

Fig. 22: Al-Fe-Ni.
Lattice heat capacity of τ$_1$ decagonal phase (at 71 at.% Al, 24 at.% Fe, 5 at.% Ni) according to [2010Pan]